Evaluation of substituent-bioactivity and anion impact of linear and T-shaped Silver(I) pyridinyl complexes as potential antiproliferative, antioxidant, antimicrobial agents and DNA- and BSA- binders

Adesola A. Adeleke,[1,2] Md. Shahidul Islam,[3] Kolawole Olofinsan,[3] Veronica F. Salau,[3] Chunderika Mocktar[4] and Bernard Omondi*[1]

[1] School of Chemistry and Physics, University of Kwazulu-Natal, Pietermaritzburg Campus, Private Bag X01, Scottsville 3209, South Africa

[2] Department of Chemical Sciences, Olabisi Onabanjo University, Ago-Iwoye, P. M. B. 2002, Nigeria

[3] Discipline of Biochemistry, School of Life Sciences, University of Kwazulu-Natal, Westville Campus, Private Bag X54001, Durban 4000, South Africa

[4] Discipline of Pharmaceutical Sciences, School of Health Sciences, University of Kwazulu-Natal, Westville Campus, Private Bag X54001, Durban 4000, South Africa

***Corresponding author.**

E-mail address: owaga@ukzn.ac.za http://orcid.org/0000-0002-3003-6712.

Supplementary information

Table of Contents

Table S1: ^{1}H-NMR chemical shifts of some protons in $\mathbf{E_{a-d}}$ complexes **1–12** and the IR band of (C=N) and pyridinyl N for $\mathbf{E_{a-d}}$ complexes **1–12**

Ligands (Complex)	δC(H=N)ppm	Δδ	Hb-py	Δδ	ν(C=N) cm^{-1}	Δν	ν(py—N) cm^{-1}	Δν
1 (Ea)	8.78 (9.20)	0.42	8.74 (8.78)	0.04	1627 (1627)	0	1584 (1580)	4
2 (Eb)	-	-	8.81 (8.78)	0.03	-	-	1606 (1586)	20
3 (Ec)	8.76 (8.74)	0.02	8.78 (8.78)	0.00	1610 (1612)	2	1552 (1585)	33
4 (Ed)	8.74 (8.68)	0.06	8.75 (8.74)	0.01	1608 (-)	-	1586 (1589)	3
5 (Ea)	8.78 (9.20)	0.42	8.74 (8.78)	0.04	1624 (1627)	3	1585 (1580)	5
6 (Eb)	-	-	8.79 (8.78)	0.01		-	1611 (1586)	25
7 (Ec)	8.76 (8.74)	0.02	8.79 (8.78)	0.01	1613 (1612)	1	1557 (1585)	28
8 (Ed)	8.74 (8.68)	0.06	8.76 (8.74)	0.02	1610 (-)	-	- (1589)	-

9 (Ea)	8.79 (9.20)	0.41	8.74 (8.78)	0.04	1625 (1627)	2	1585 (1580)	5
10 (Eb)	-	-	8.79 (8.78)	0.01		-	1609 (1586)	23
11 (Ec)	8.76 (8.74)	0.02	8.78 (8.78)	0.00	1609 (1612)	3	1552 (1585)	33
12 (Ed)	8.74 (8.68)	0.06	8.76 (8.74)	0.02	1609 (-)	-	- (1589)	-

Table S2: ^{15}N NMR chemical shifts of $\mathbf{E_{a-d}}$ and selected complexes (**2**, **7**, **8** and **9**)

Ligand (Complex)	$\delta^{15}N_{py}$ (ppm)	$\Delta\delta^{15}N_{py}$ (ppm)	$\delta^{15}N{=}C$(ppm)	$\Delta\delta^{15}N_{im}$ (ppm)
2 (Eb)	323 (314)	9	-	-
7 (Ec)	303 (327)	24	326 (327)	1
8 (Ed)	324 (317)	7	339 (339)	0
9 (Ea)	329 (333)	4	-	-

Table S3: Physical and chemical data of Silver(I) complexes **1–12**

Comp.	Anal. Calcd. (Anal. found)			M.pt.	MS		MC
	C	H	N	(°C)	Calcd.	Found	(Λ_m/ S m^2 mol^{-1}) X 10^{-4}
1	50.90 (50.62)	3.56 (3.23)	12.37 (12.39)	157-158	504.32	504	22.5
2	48.50 (48.49)	2.71 (2.54)	11.78 (11.58)	186-187	532.41	532	19.8
3	50.55 (50.49)	3.18 (3.13)	12.28 (12.06)	146-147	508.30	508	13.4
4	55.53 (55.80)	4.30 (4.00)	12.45 (12.24)	164-165	500.37	501	20.4
5	47.74 (47.52)	3.34 (3.11)	9.28 (9.09)	169-170	504.32	504	26.3
6	45.62 (45.38)	2.55 (2.55)	8.87 (8.61)	168-169	532.41	532	15.7
7	47.43 (47.40)	2.99 (2.74)	9.22 (9.00)	209-210	508.30	508	24.4
8	52.06 (52.05)	4.03 (3.89)	9.34 (9.27)	227-228	500.37	501	19.2
9	45.96 (45.82)	3.09 (2.85)	8.58 (8.52)	165-166	504.32	504	29.0
10	44.06 (43.93)	2.37 (2.27)	8.22 (8.04)	183-184	532.41	532	23.3
11	45.68 (45.68)	2.76 (2.74)	8.52 (8.38)	171-172	508.30	508	27.8
12	49.94 (49.73)	3.73 (3.41)	8.63 (8.60)	220-221	500.37	501	20.8

DNA Binding Studies

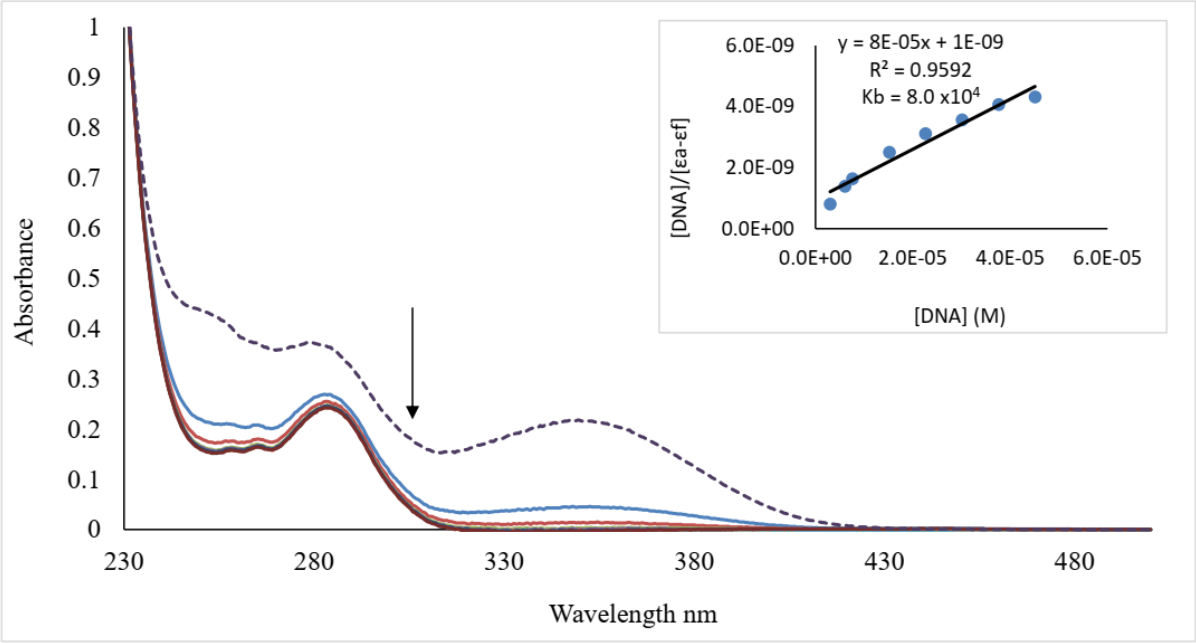

Figure S1: Electronic Absorption Spectra of Ligand $\mathbf{E_a}$ at 2.0 x 10^{-5} M in the absence (dashed line) and the presence of different concentrations of CT-DNA (0 – 3.0 x 10^5 M) at 285 nm λ_{max}. (inset) A stern-volmer plot of $\mathbf{E_a}$ interaction with CT-DNA

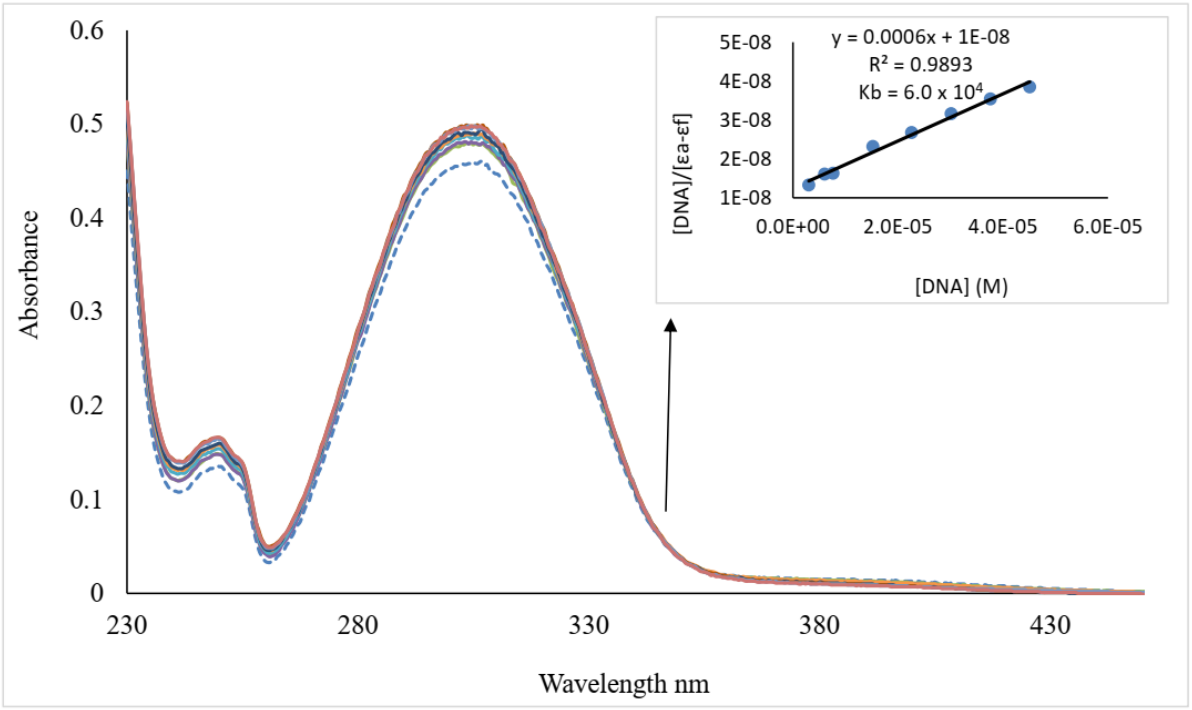

Figure S2: Electronic Absorption Spectra of Ligand $\mathbf{E_b}$ at 2.0 x 10^{-5} M in the absence (dashed line) and the presence of different concentrations of CT-DNA (0 – 3.0 x 10^5 M) at 302 nm λ_{max}. (inset) A stern-volmer plot of $\mathbf{E_b}$ interaction with CT-DNA

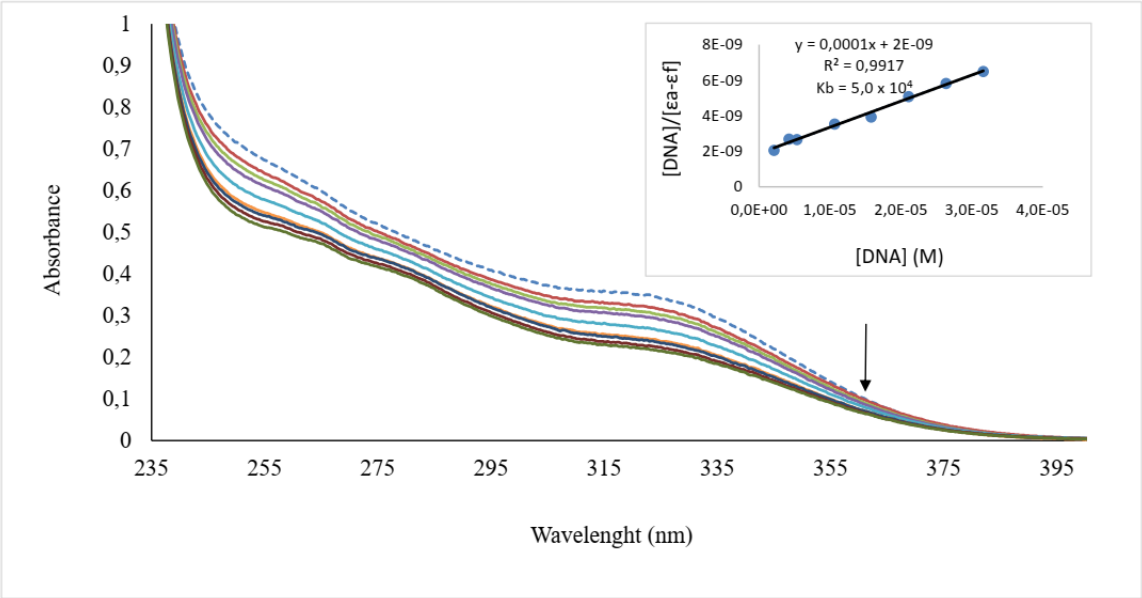

Figure S3: Electronic Absorption Spectra of Ligand $\mathbf{E_c}$ at 2.0 x 10^{-5} M in the absence (dashed line) and the presence of different concentrations of CT-DNA (0 – 3.0 x 10^5 M) at 327 nm λ_{max}. (inset) A stern-volmer plot of $\mathbf{E_c}$ interaction with CT-DNA

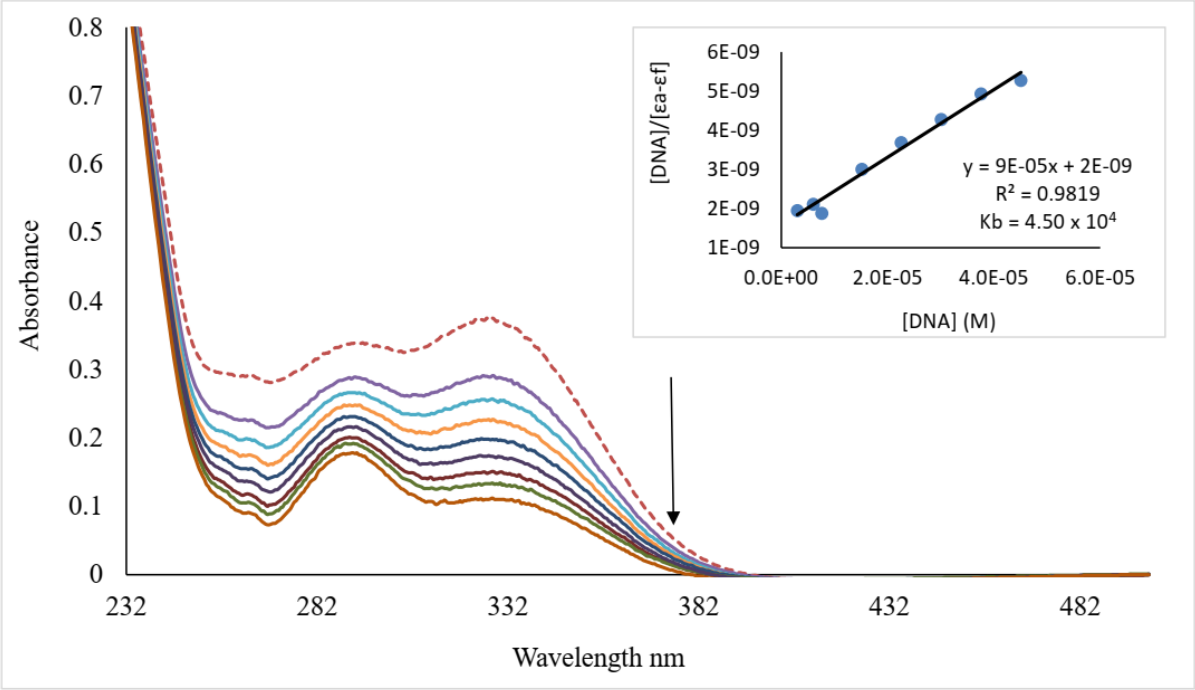

Figure S4: Electronic Absorption Spectra of Ligand $\mathbf{E_d}$ at 2.0 x 10^{-5} M in the absence (dashed line) and the presence of different concentrations of CT-DNA (0 – 3.0 x 10^5 M) at 333 nm λ_{max}. (inset) A stern-volmer plot of $\mathbf{E_d}$ interaction with CT-DNA

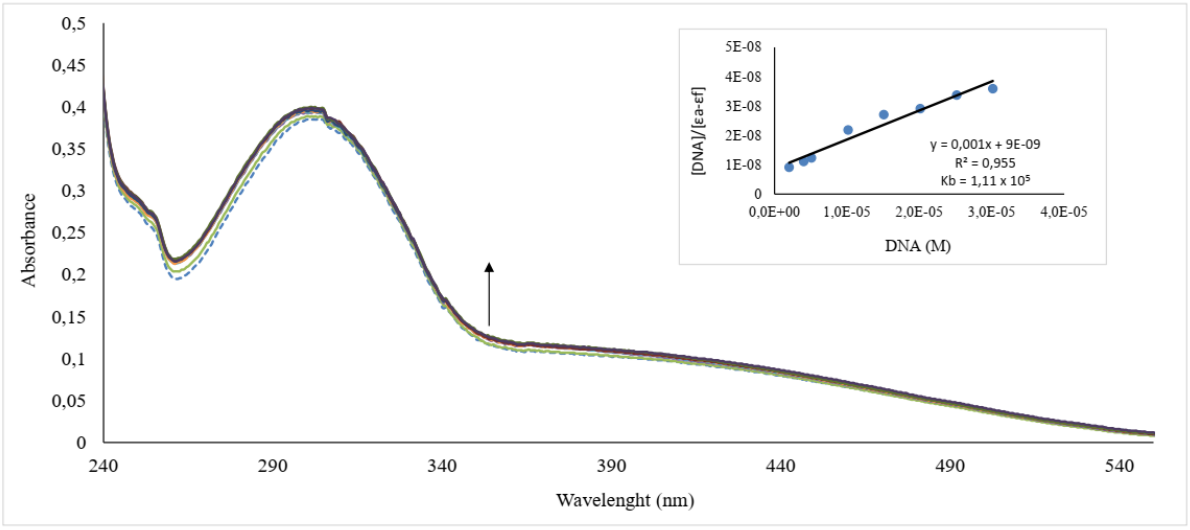

Figure S5: Electronic Absorption Spectra of complex **2** at 2.0 x 10^{-5} M in the absence (dashed line) and the presence of different concentrations of CT-DNA (0 – 3.0 x 10^5 M) at 306 nm λ_{max}. (inset) A stern-volmer plot of **2** interaction with CT-DNA

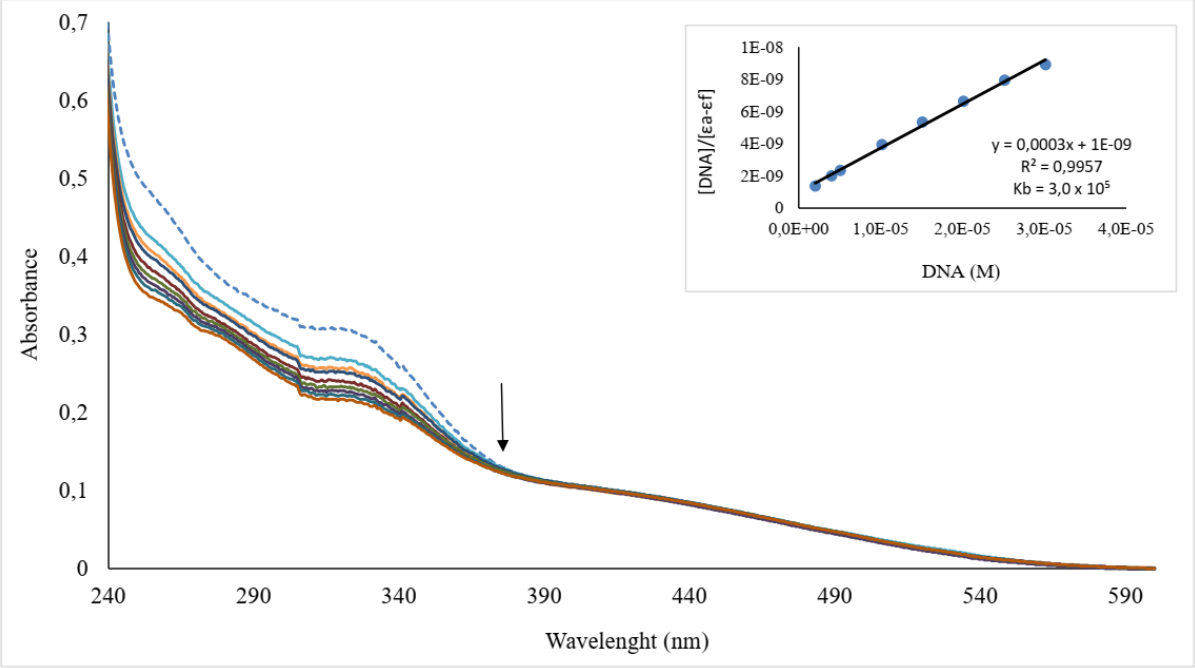

Figure S6: Electronic Absorption Spectra of complex **3** at 2.0 x 10^{-5} M in the absence (dashed line) and the presence of different concentrations of CT-DNA (0 – 3.0 x 10^5 M) at 330 nm λ_{max}. (inset) A stern-volmer plot of **3** interaction with CT-DNA

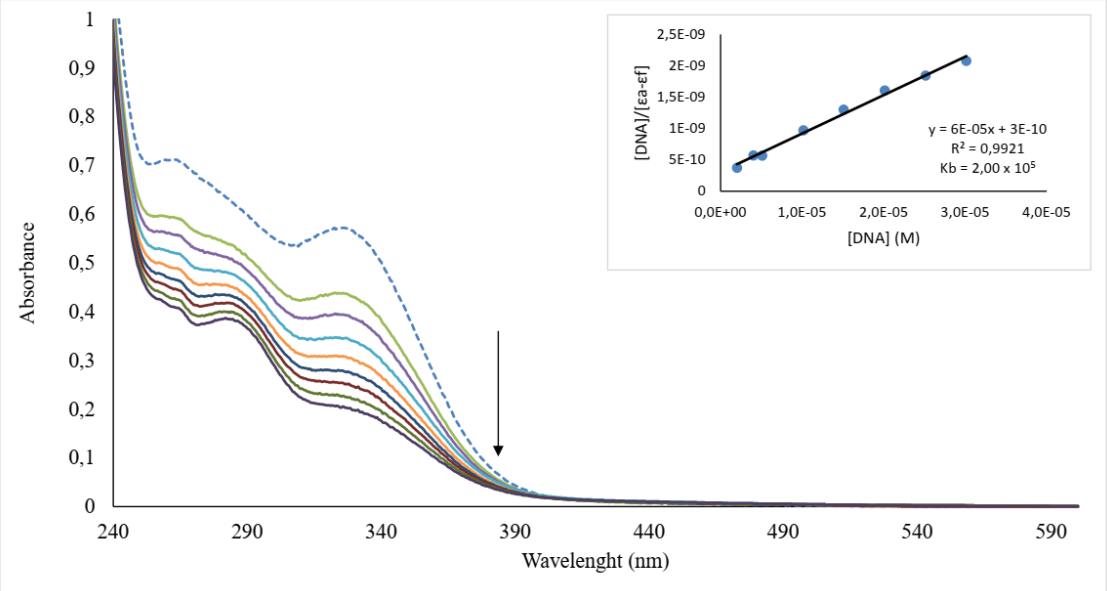

Figure S7: Electronic Absorption Spectra of complex **4** at 2.0 x 10^{-5} M in the absence (dashed line) and the presence of different concentrations of CT-DNA (0 – 3.0 x 10^5 M) at 332 nm λ_{max}. (inset) A stern-volmer plot of **4** interaction with CT-DNA

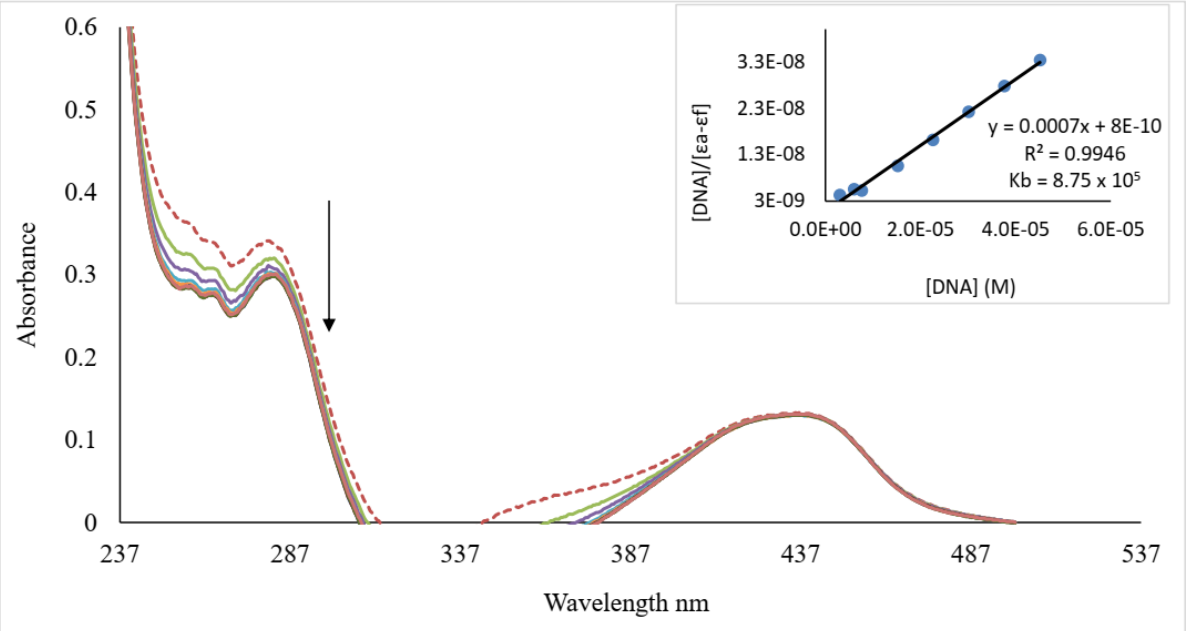

Figure S8: Electronic Absorption Spectra of complex **5** at 2.0 x 10^{-5} M in the absence (dashed line) and the presence of different concentrations of CT-DNA (0 – 3.0 x 10^5 M) at 285 nm λ_{max}. (inset) A stern-volmer plot of **5** interaction with CT-DNA

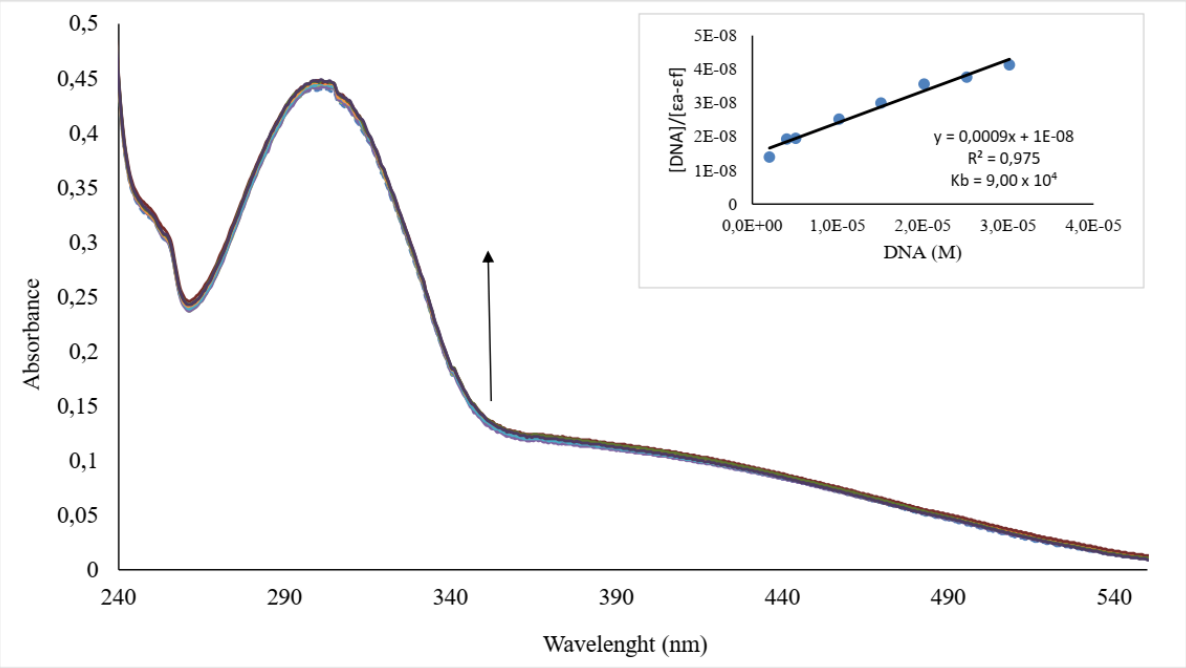

Figure S9: Electronic Absorption Spectra of complex **6** at 2.0 x 10^{-5} M in the absence (dashed line) and the presence of different concentrations of CT-DNA (0 – 3.0 x 10^5 M) at 306 nm λ_{max}. (inset) A stern-volmer plot of **6** interaction with CT-DNA

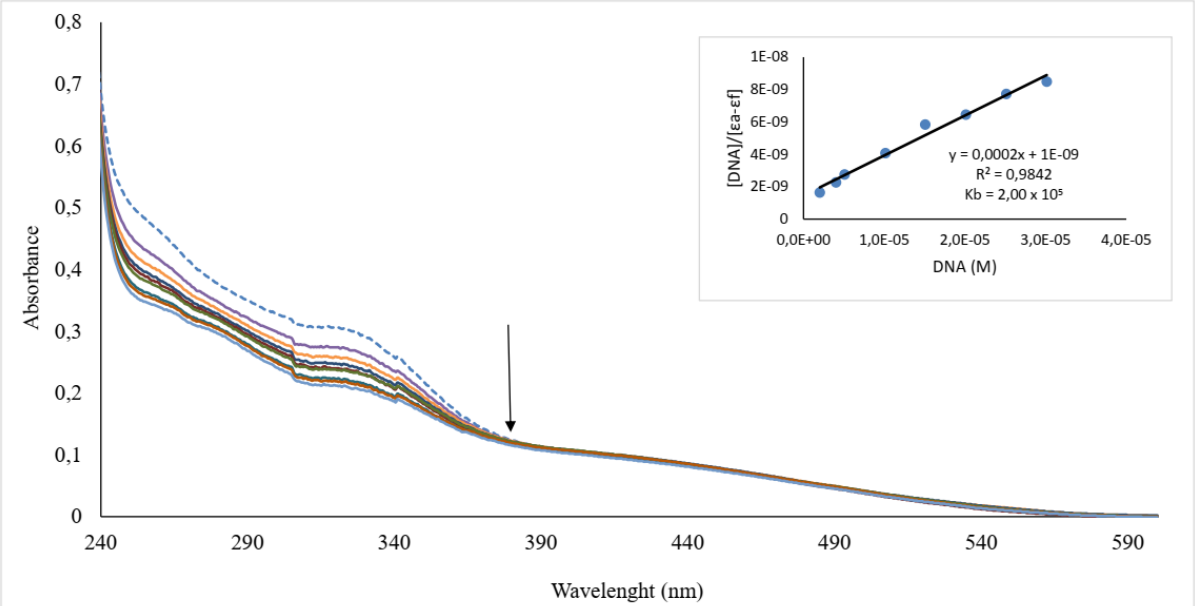

Figure S10: Electronic Absorption Spectra of complex **7** at 2.0 x 10^{-5} M in the absence (dashed line) and the presence of different concentrations of CT-DNA (0 – 3.0 x 10^5 M) at 328 nm λ_{max}. (inset) A stern-volmer plot of **7** interaction with CT-DNA

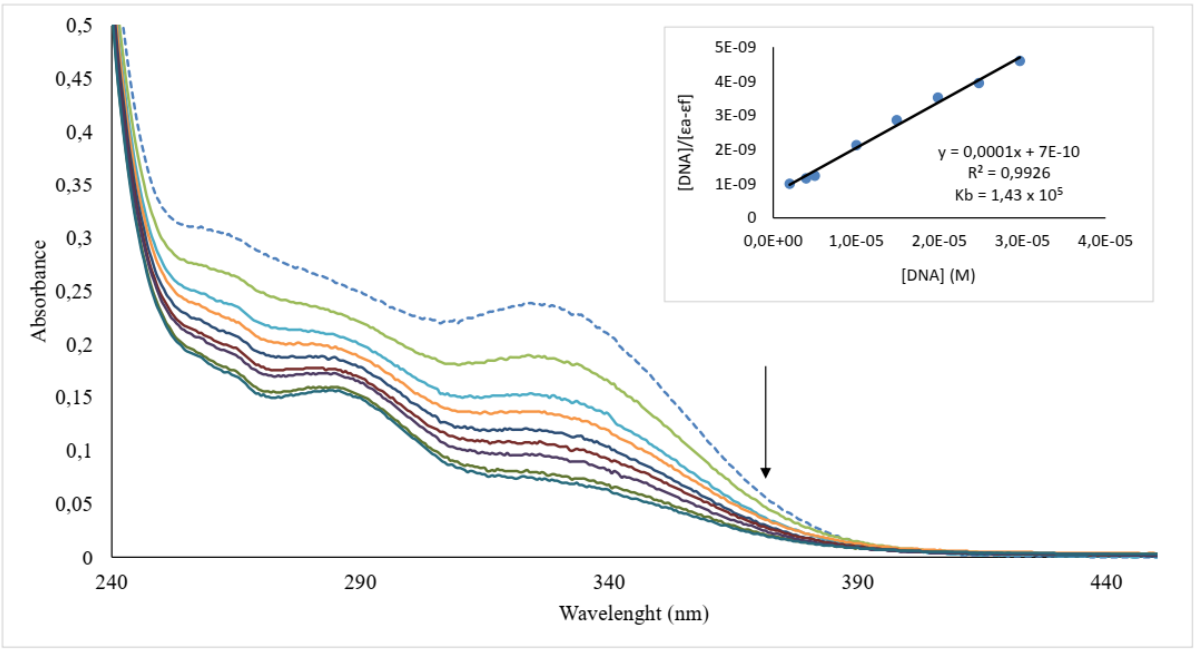

Figure S11: Electronic Absorption Spectra of complex **8** at 2.0 x 10^{-5} M in the absence (dashed line) and the presence of different concentrations of CT-DNA (0 – 3.0 x 10^5 M) at 332 nm λ_{max}. (inset) A stern-volmer plot of **8** interaction with CT-DNA

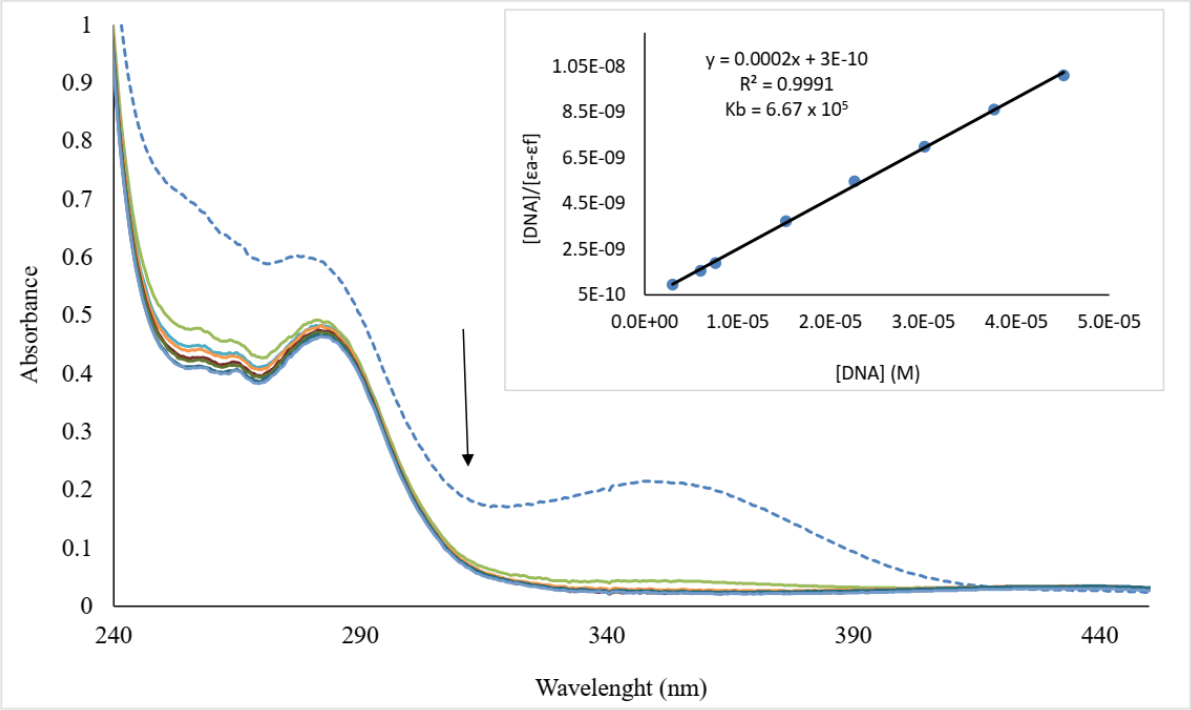

Figure S12: Electronic Absorption Spectra of complex **9** at 2.0 x 10^{-5} M in the absence (dashed line) and the presence of different concentrations of CT-DNA (0 – 3.0 x 10^5 M) at 282 nm λ_{max}. (inset) A stern-volmer plot of **9** interaction with CT-DNA

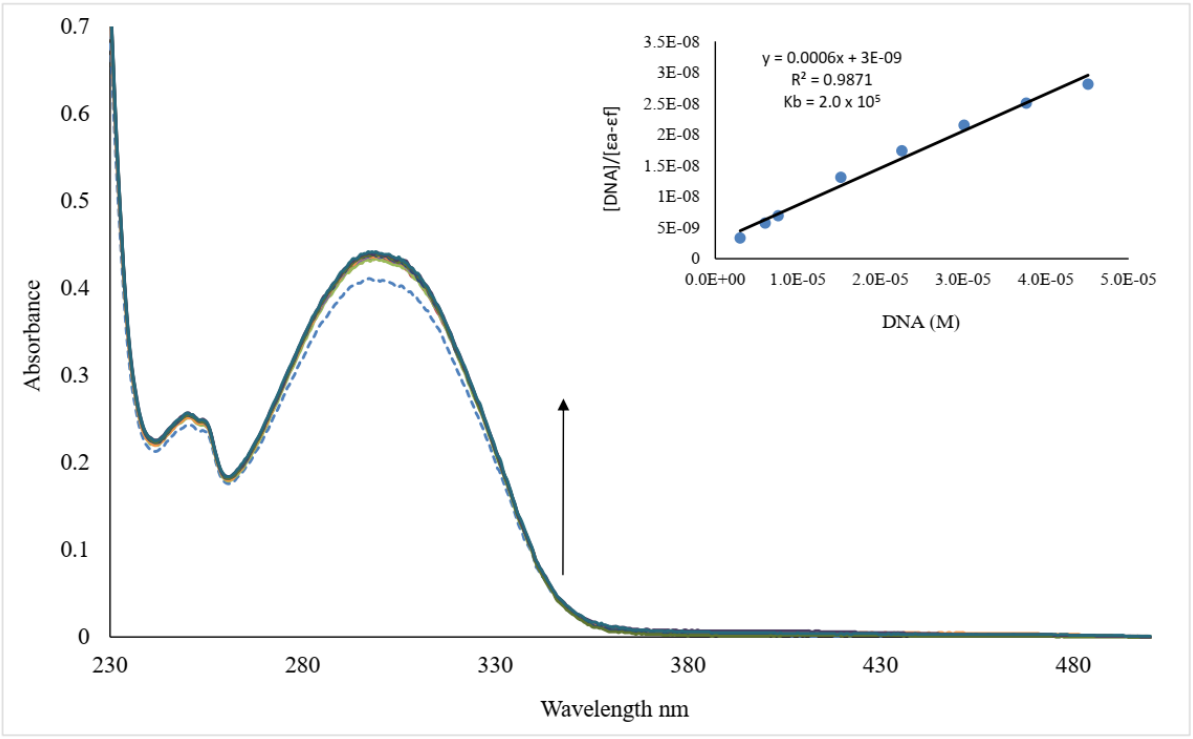

Figure S13: Electronic Absorption Spectra of complex **10** at 2.0 x 10^{-5} M in the absence (dashed line) and the presence of different concentrations of CT-DNA (0 – 3.0 x 10^5 M) at 300 nm λ_{max}. (inset) A stern-volmer plot of **10** interaction with CT-DNA

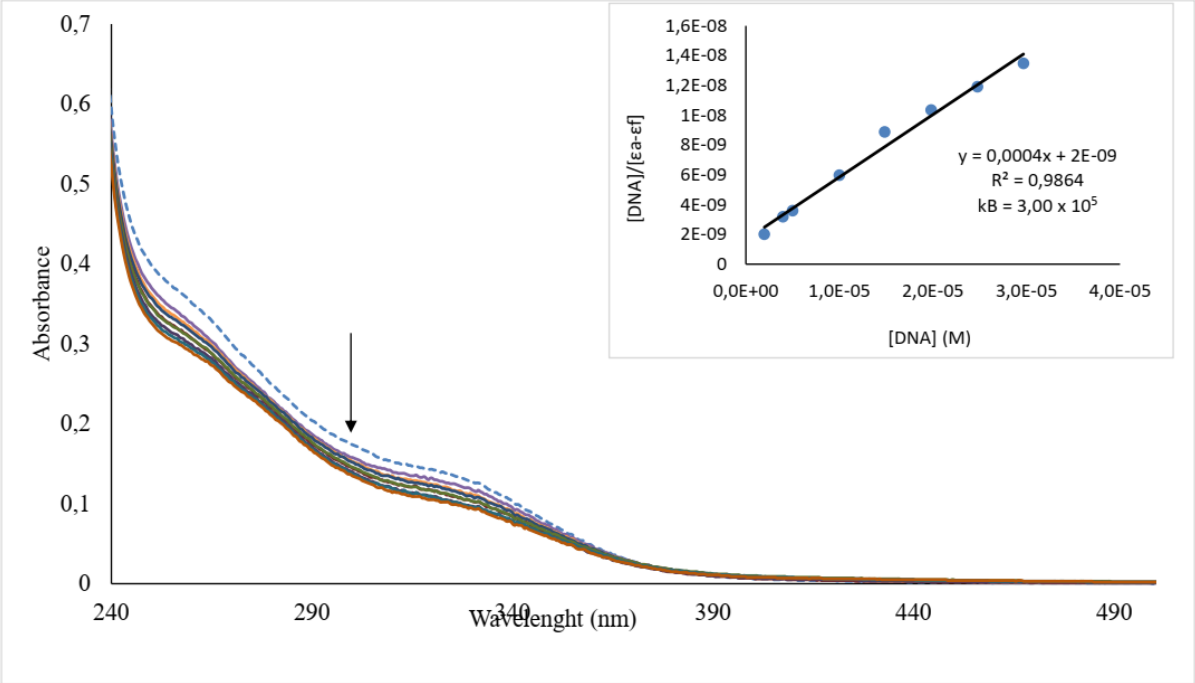

Figure S14: Electronic Absorption Spectra of complex **11** at 2.0 x 10^{-5} M in the absence (dashed line) and the presence of different concentrations of CT-DNA (0 – 3.0 x 10^5 M) at 331 nm λ_{max}. (inset) A stern-volmer plot of **11** interaction with CT-DNA

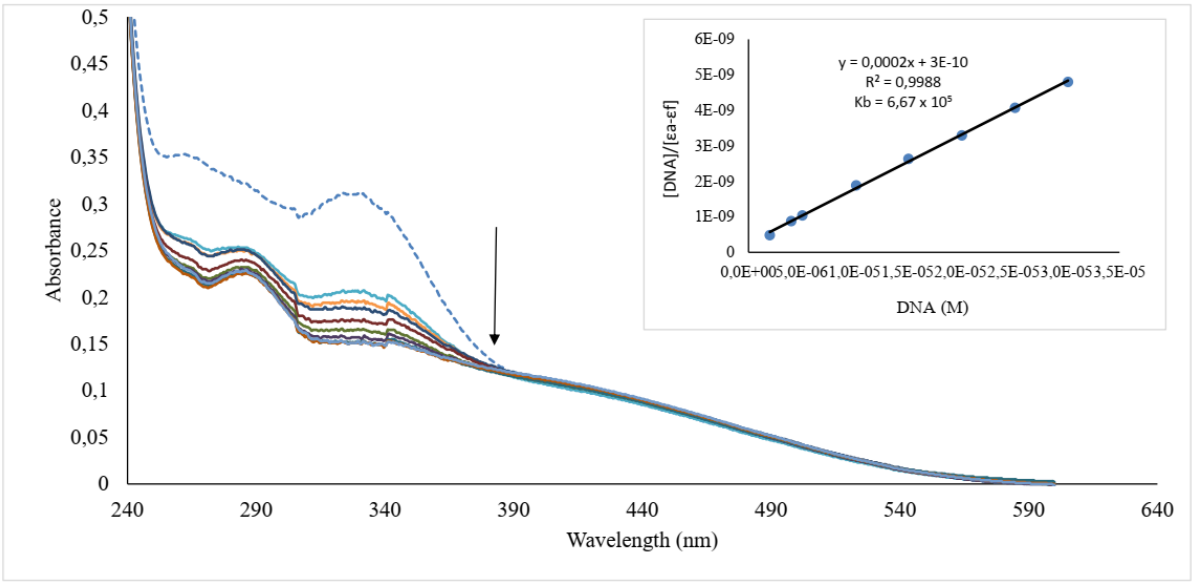

Figure S15: Electronic Absorption Spectra of complex **12** at 2.0 x 10-5 M in the absence (dashed line) and the presence of different concentrations of CT-DNA (0 – 3.0 x 10^5 M) at 340 nm λ_{max}. (inset) A stern-volmer plot of **12** interaction with CT-DNA

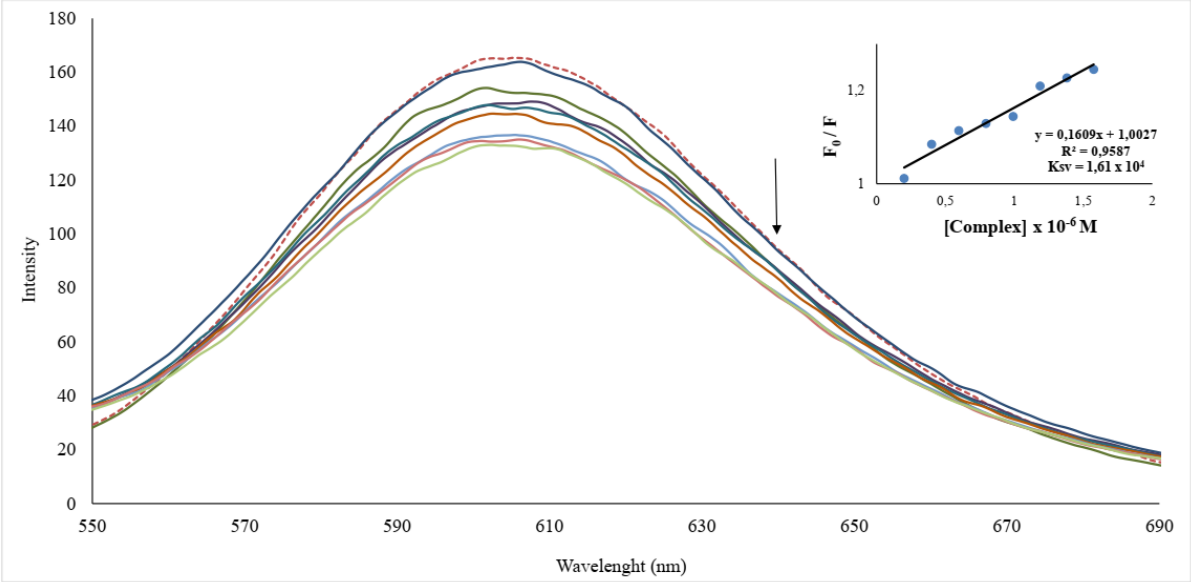

Figure S16: The Fluorescence spectra of EB-CT-DNA in the absence (dashed line) and the presence of different concentration of complex **3**. (inset) Stern-Volmer plot of **3** interactions with EB-CT- DNA

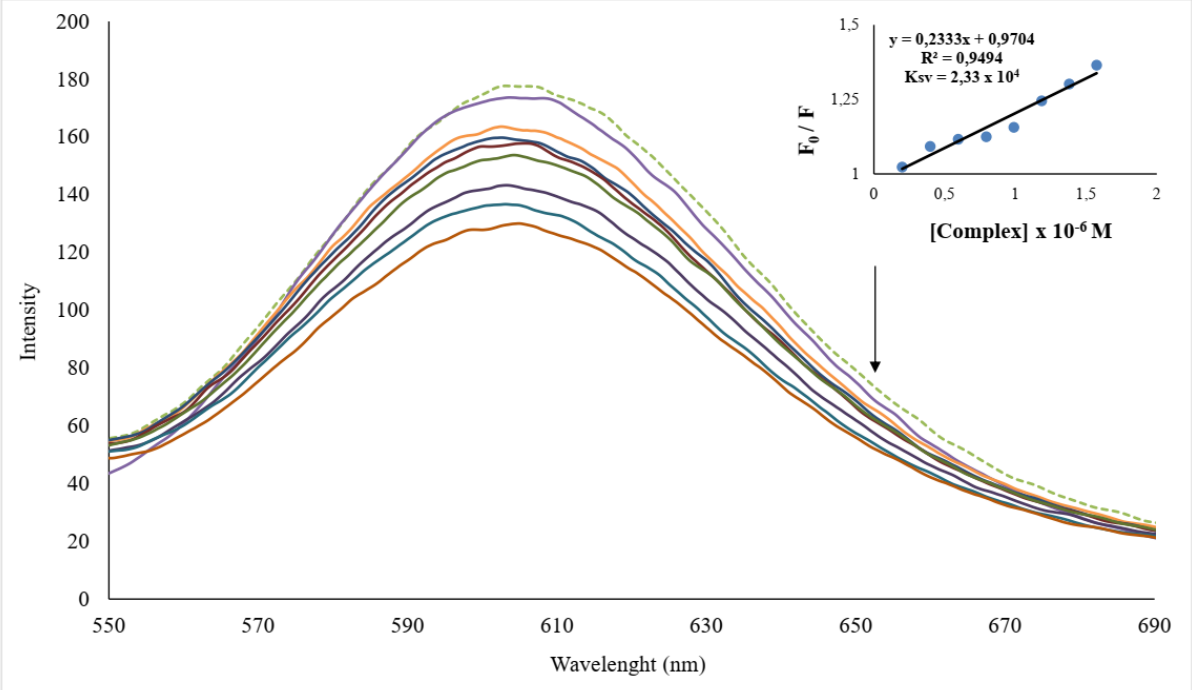

Figure S17: The Fluorescence spectra of EB-CT-DNA in the absence (dashed line) and the presence of different concentration of complex **4**. (inset) Stern-Volmer plot of **4** interaction with EB-CT- DNA

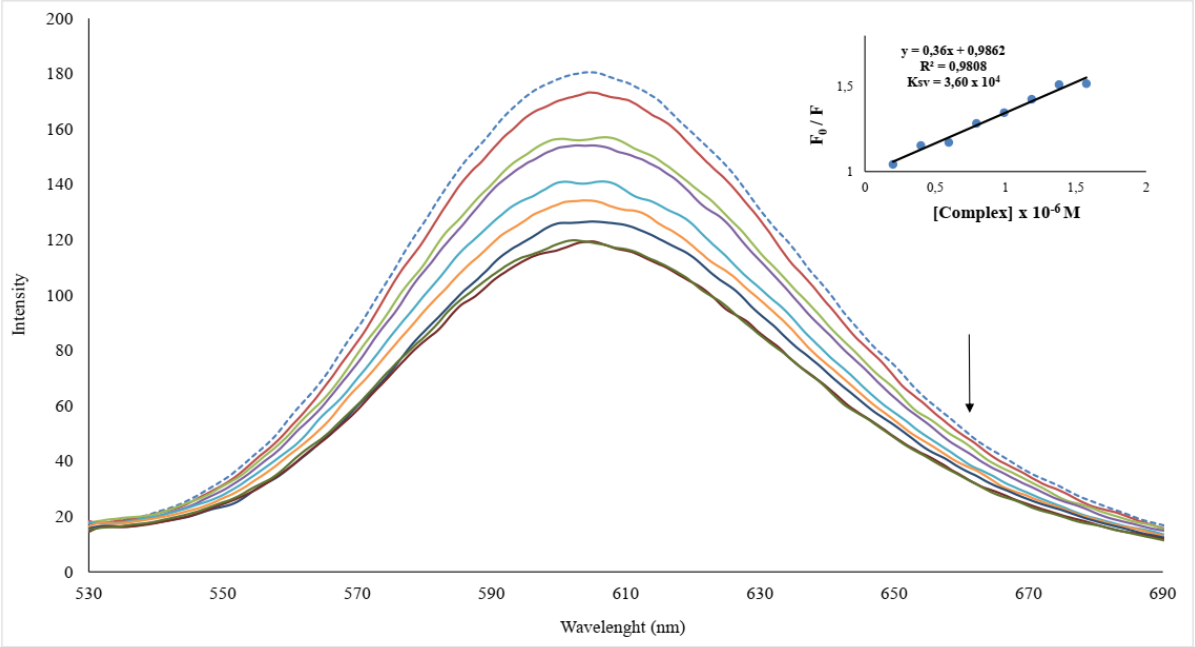

Figure S18: The Fluorescence spectra of EB-CT-DNA in the absence (dashed line) and the presence of different concentrations s of complex **5**. (inset) Stern-Volmer plot of **5** interaction with EB-CT- DNA

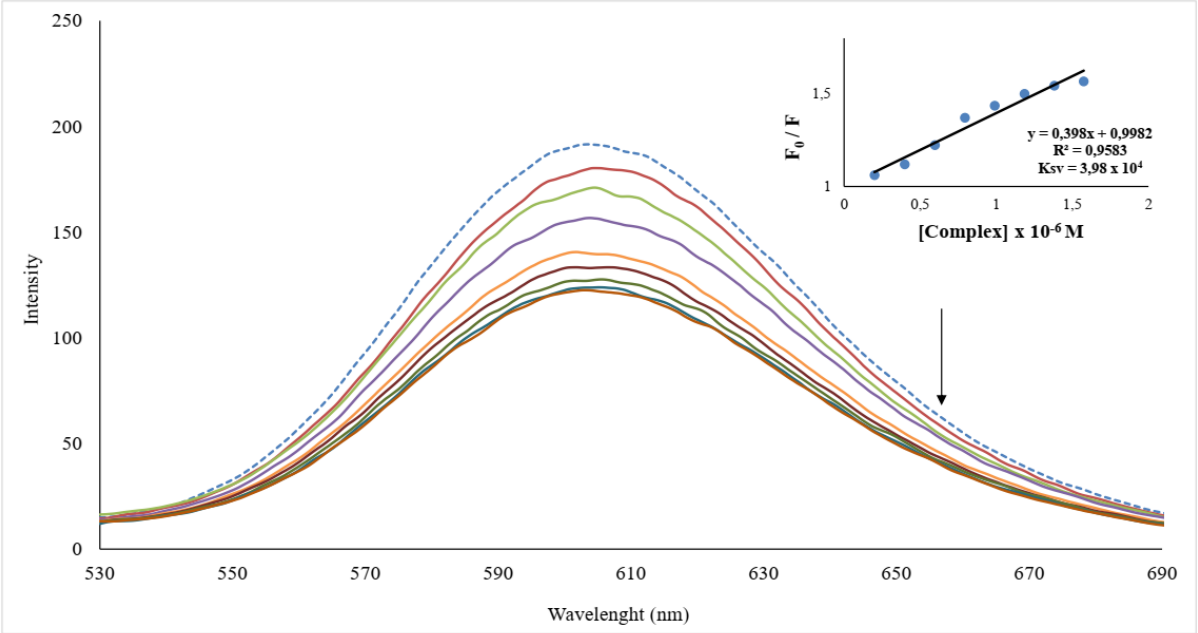

Figure S19: The Fluorescence spectra of EB-CT-DNA in the absence (dashed line) and the presence of different concentrations of complex **7**. (inset) Stern-Volmer plot of **7** interaction with EB-CT- DNA

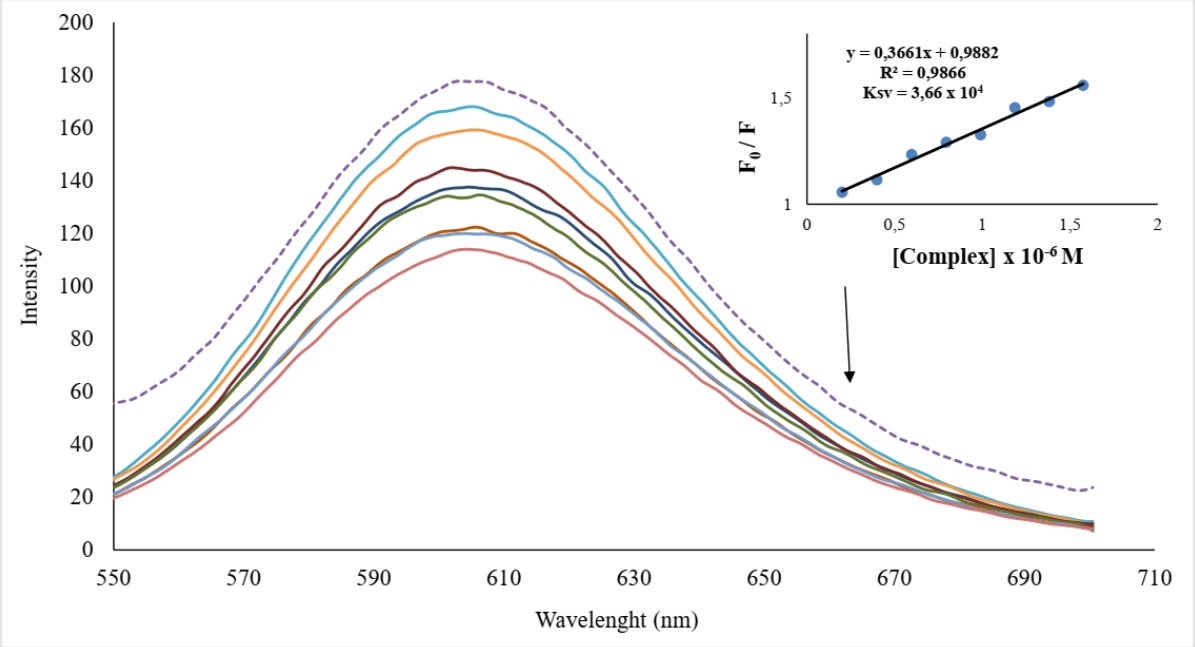

Figure S20: The Fluorescence spectra of EB-CT-DNA in the absence (dashed line) and the presence of different concentration of complex **8**. (inset) Stern-Volmer plot of **8** interaction with EB-CT- DNA

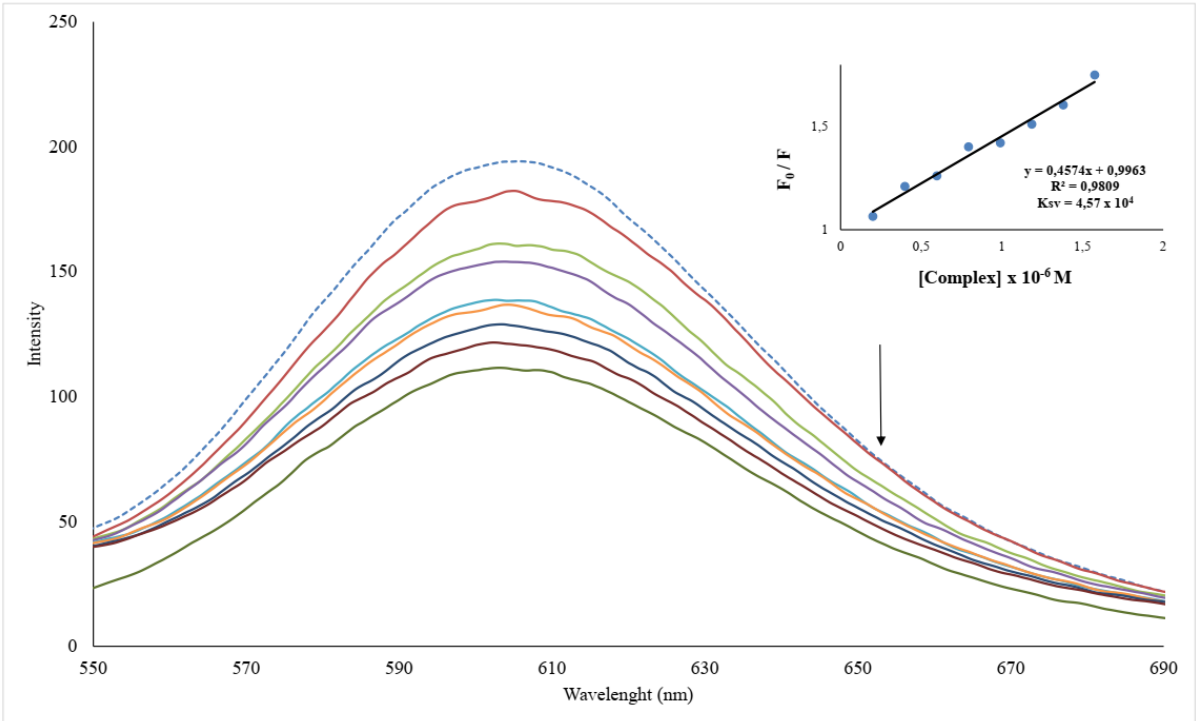

Figure S21: The Fluorescence spectra of EB-CT-DNA in the absence (dashed line) and the presence of different concentrations of complex **9**. (inset) Stern-Volmer plot of **9** interaction with EB-CT- DNA

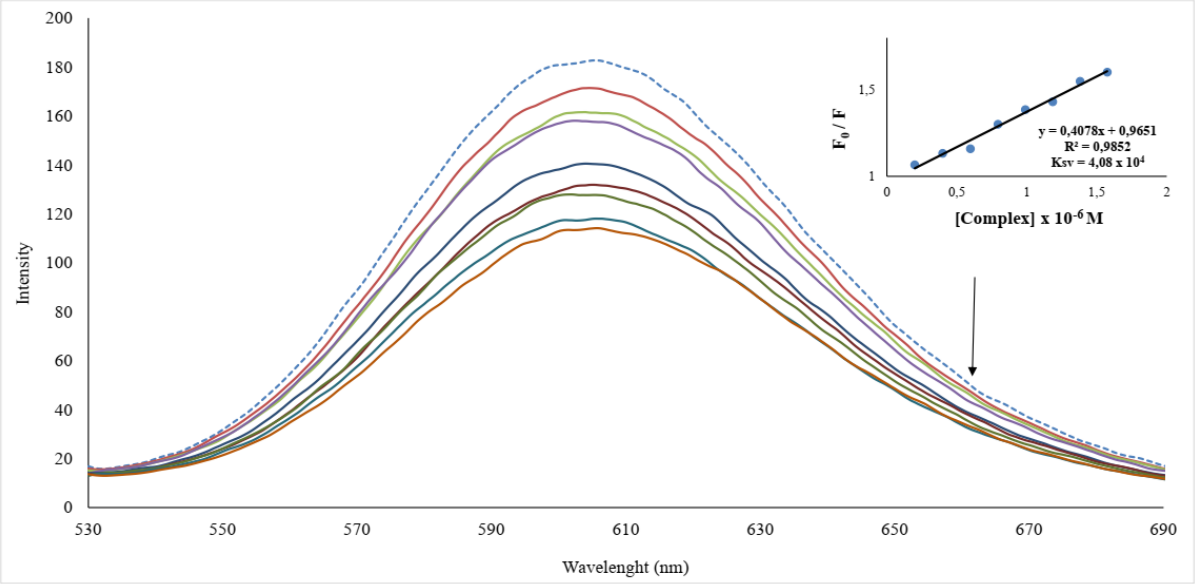

Figure S22: The Fluorescence spectra of EB-CT-DNA in the absence (dashed line) and the presence of different concentrations of complex **11**. (inset) Stern-Volmer plot of **11** interaction with EB-CT- DNA

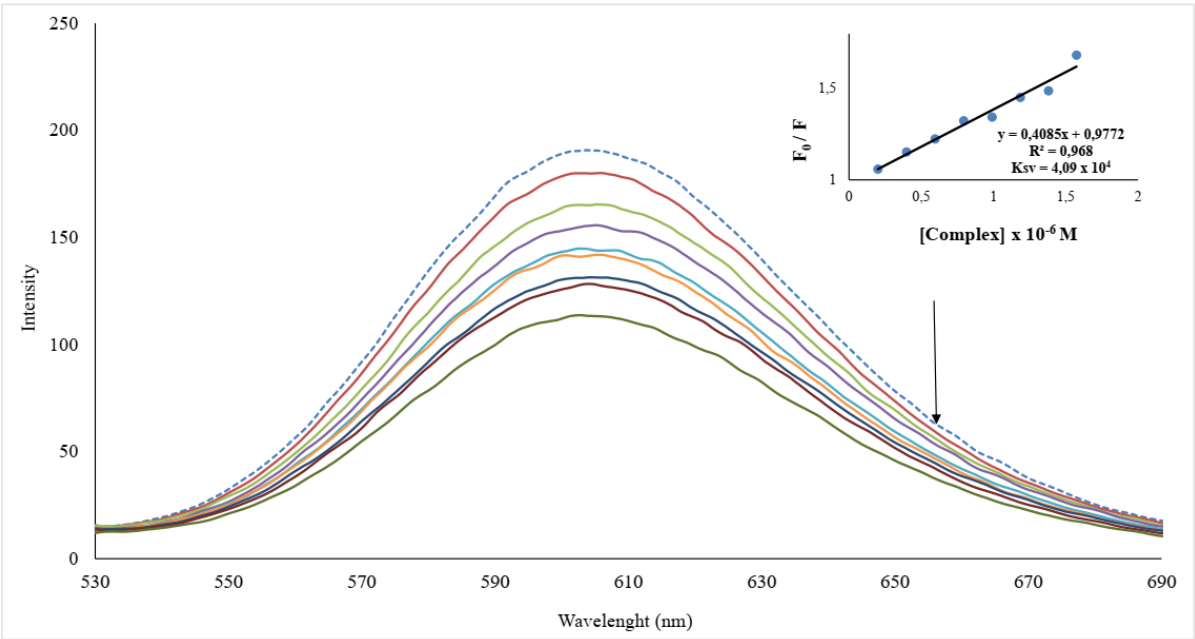

Figure S23: The Fluorescence spectra of EB-CT-DNA in the absence (dashed line) and the presence of different concentrations of complex **12**. (inset) Stern-Volmer plot of **12** interaction with EB-CT- DNA

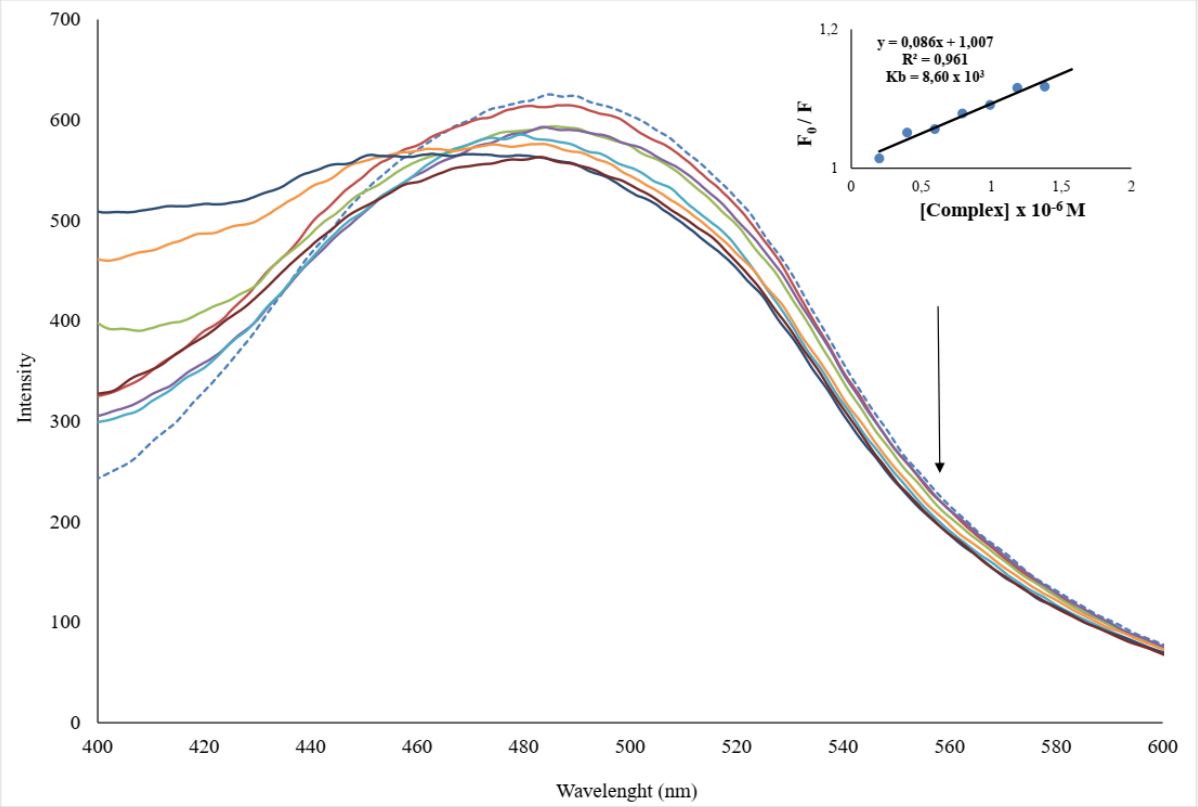

Figure S24: The Fluorescence spectra of Hoechst 33342-CT-DNA in the absence (dashed line) and the presence of different concentrations of complex **6**. (inset) Stern-Volmer plot of **6** interaction with Hoechst 33342-CT-DNA

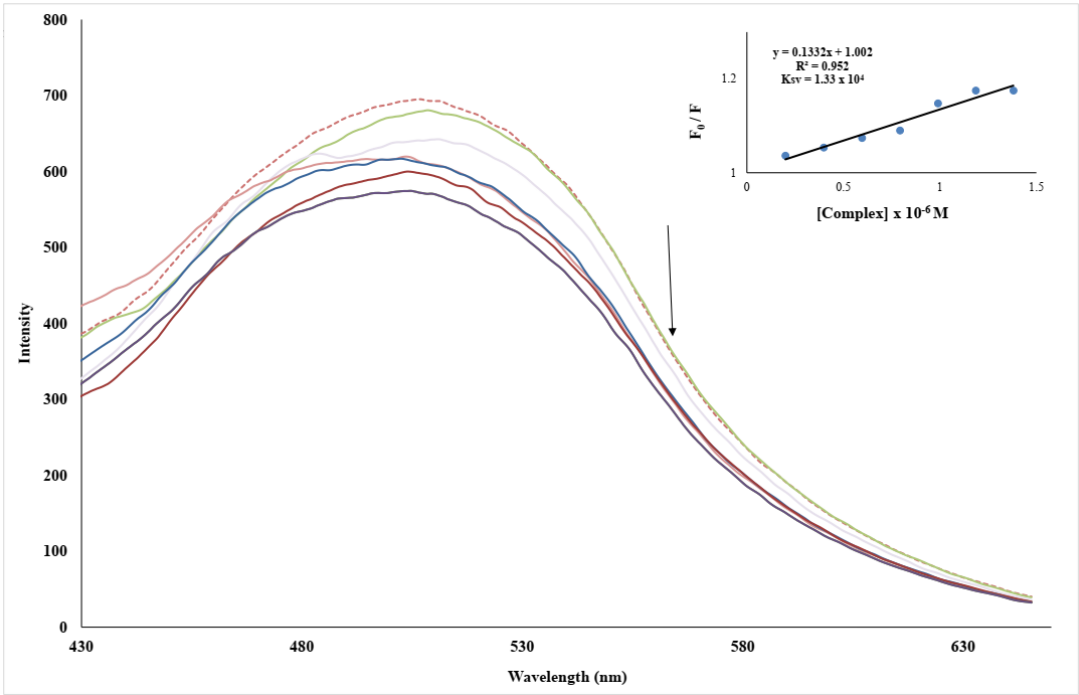

Figure S25: The Fluorescence spectra of Hoechst 33342-CT-DNA in the absence (dashed line) and the presence of different concentration of complex **10**. (inset) Stern-Volmer plot of **10** interaction with Hoechst 33342-CT-DNA

The double-logarithmic plot of EB-CT-DNA–Complexes interactions at room temperature.

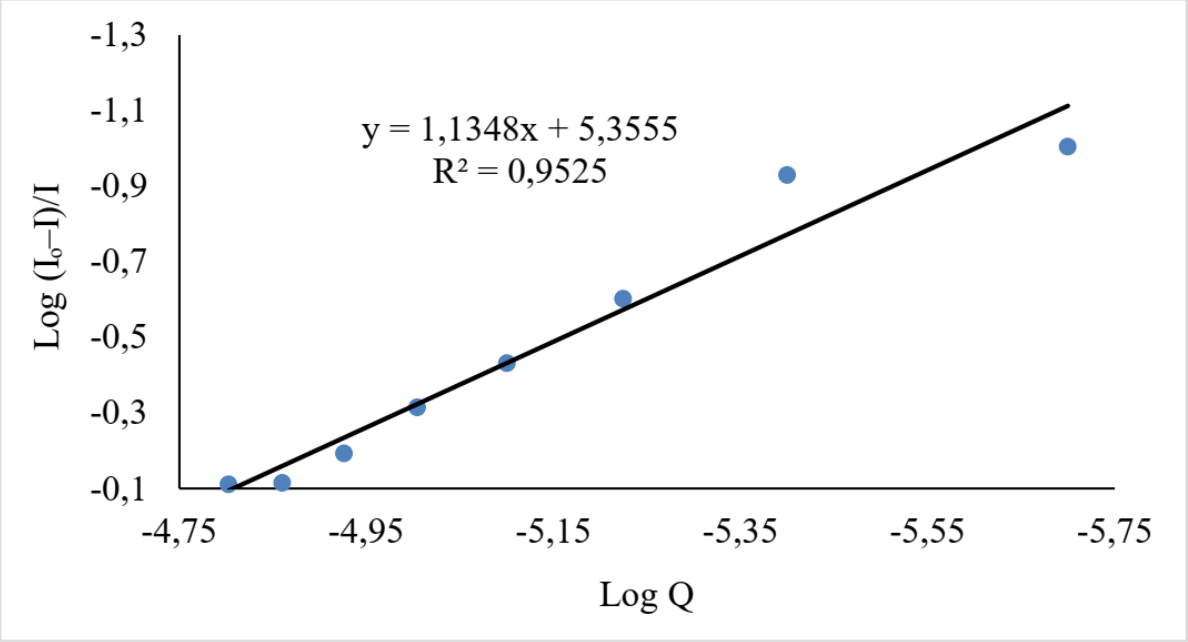

Figure S26: The double-logarithmic plot of EB-CT-DNA–Complex **1** interaction at room temperature.

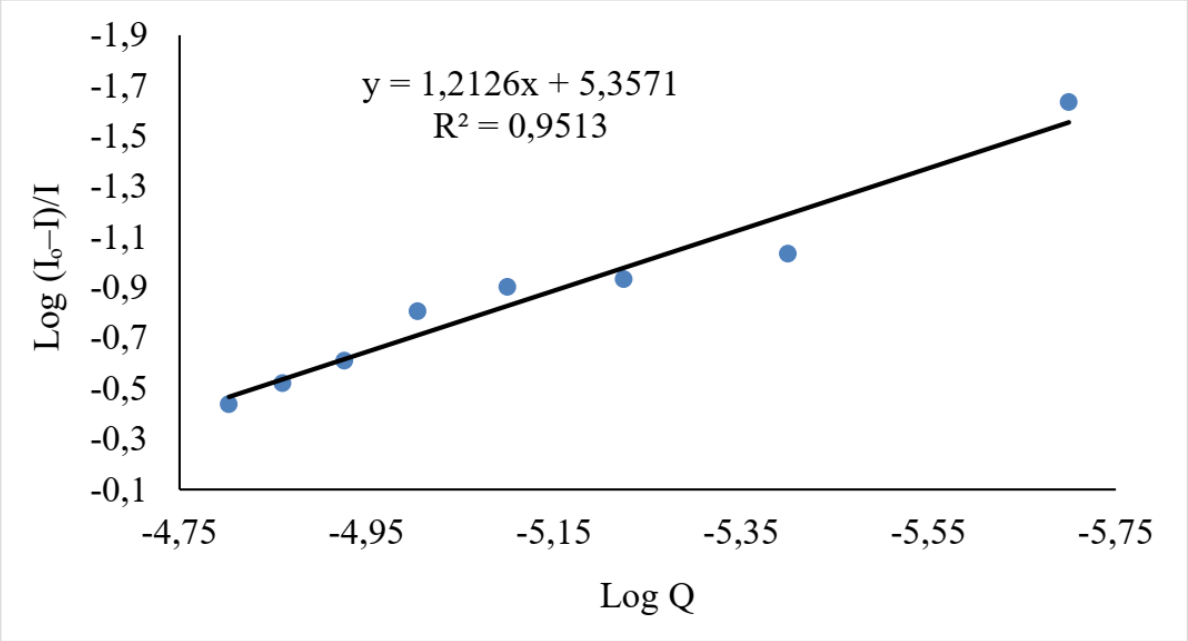

Figure S27: The double-logarithmic plot of EB-CT-DNA–Complex **4** interaction at room temperature.

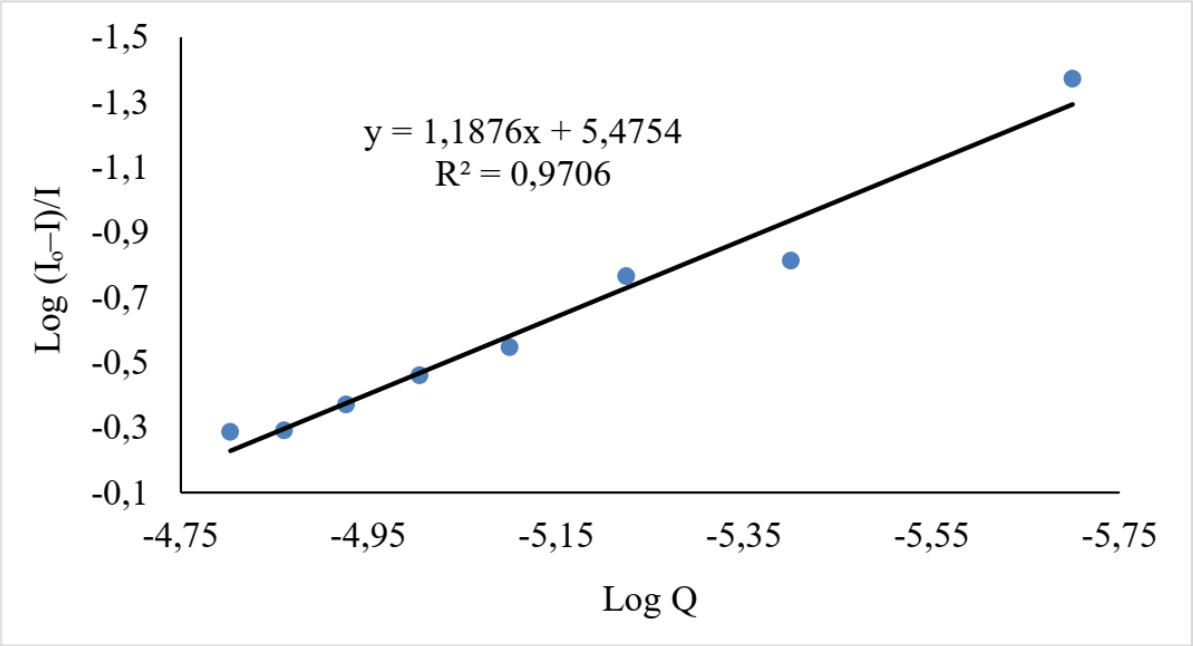

Figure S28: The double-logarithmic plot of EB-CT-DNA–Complex **5** interaction at room temperature.

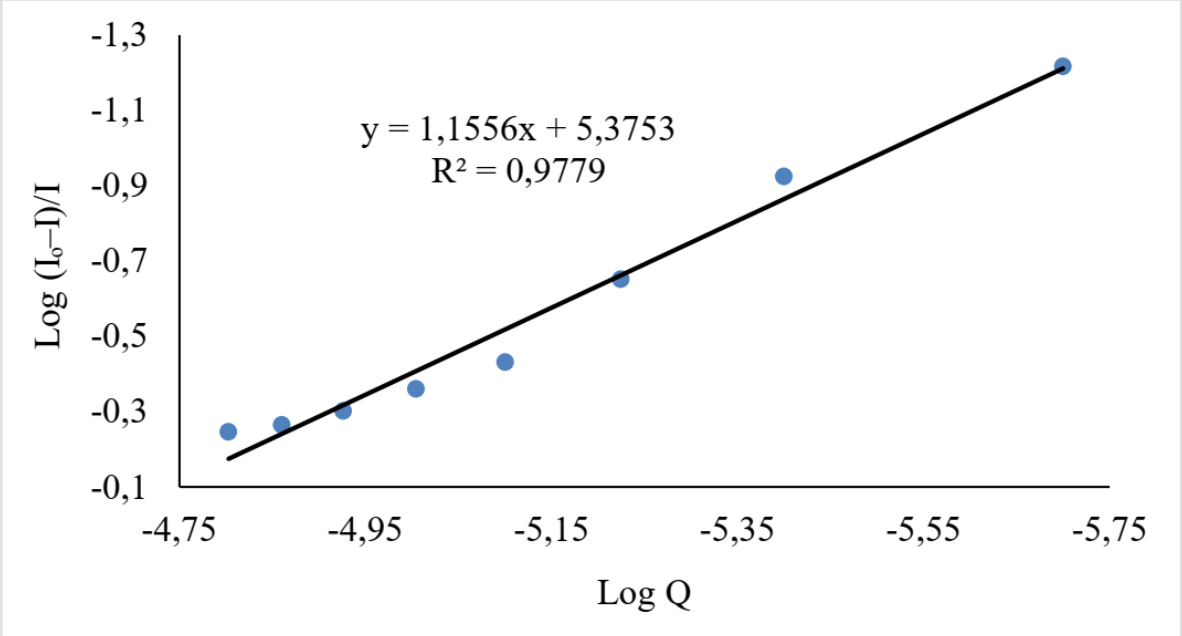

Figure S29: The double-logarithmic plot of EB-CT-DNA–Complex **7** interaction at room temperature.

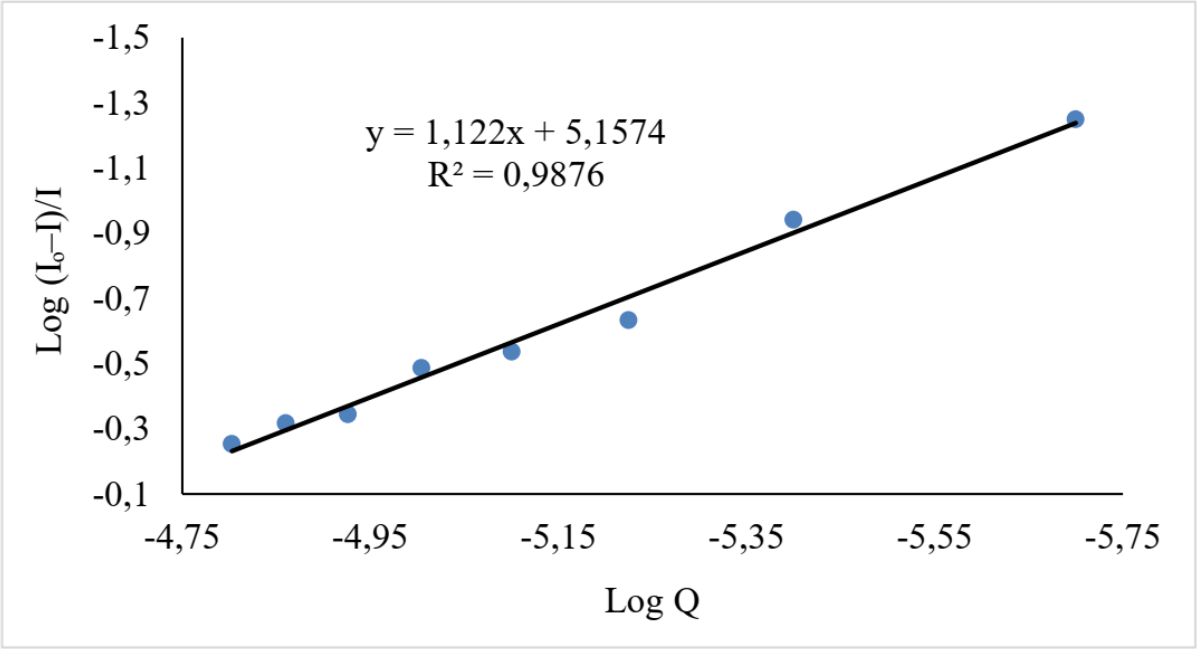

Figure S30: The double-logarithmic plot of EB-CT-DNA–Complex **8** interaction at room temperature.

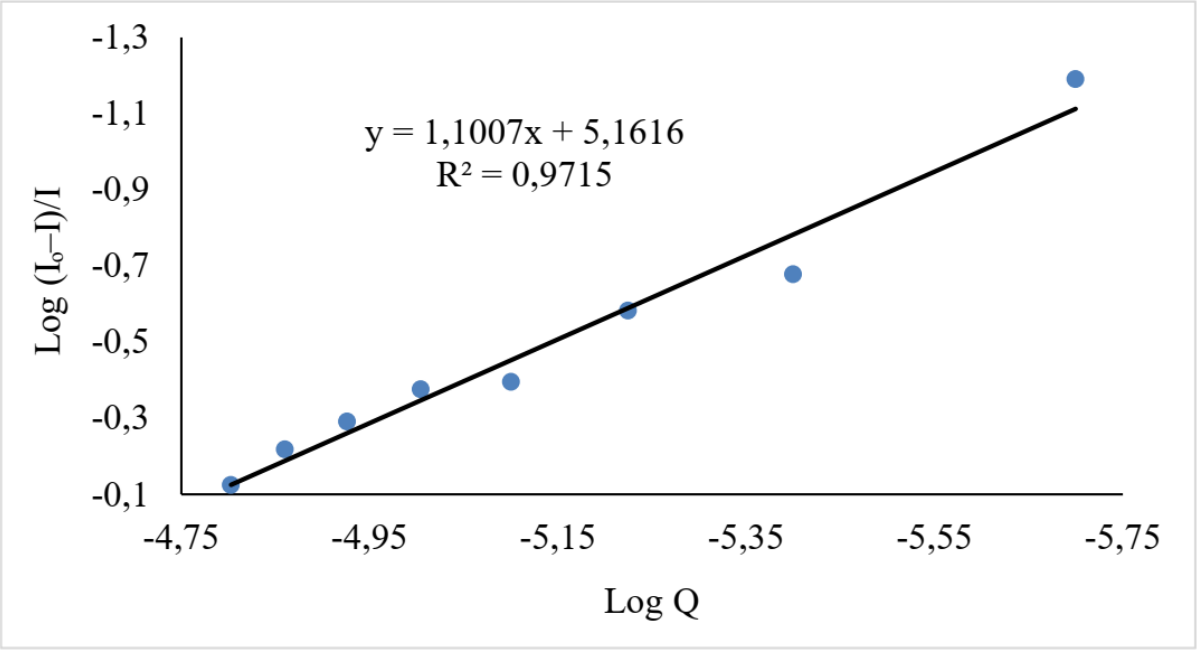

Figure S31: The double-logarithmic plot of EB-CT-DNA–Complex **9** interaction at room temperature.

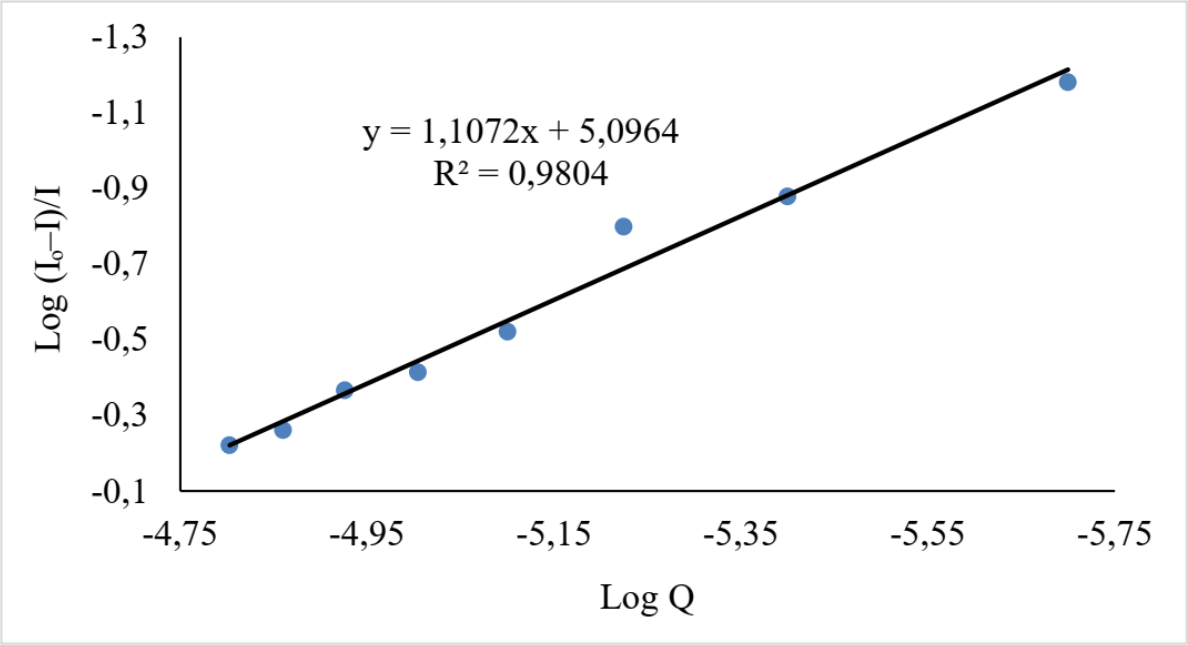

Figure S32: The double-logarithmic plot of EB-CT-DNA–Complex **11** interaction at room temperature.

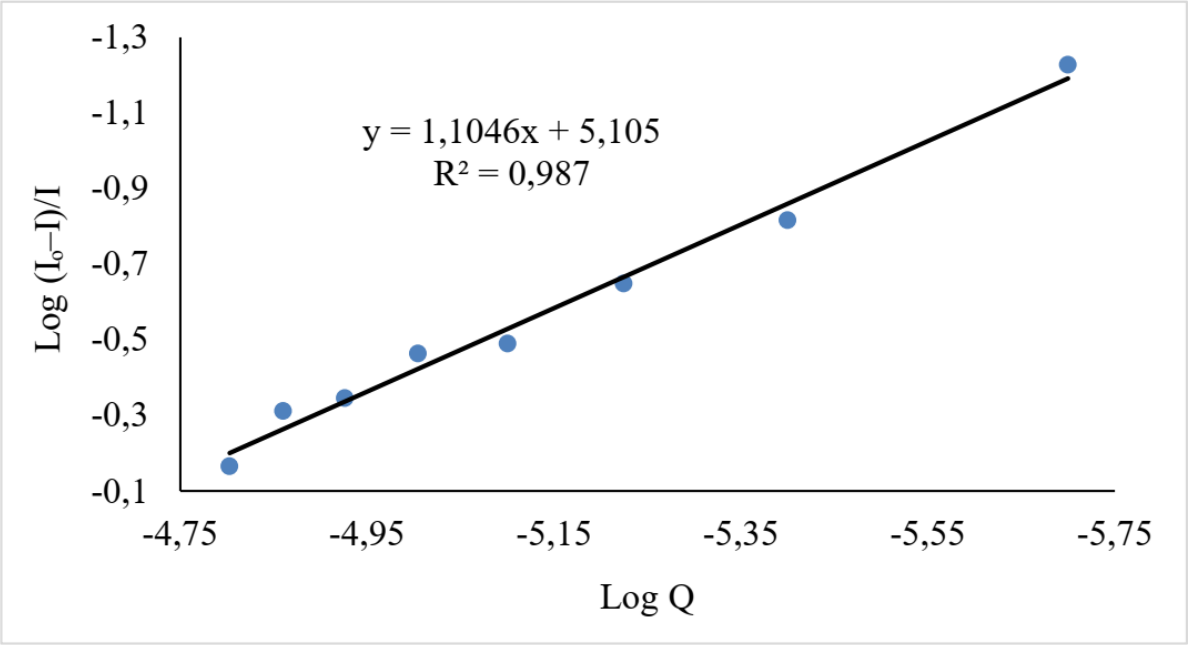

Figure S33: The double-logarithmic plot of EB-CT-DNA–Complex **12** interaction at room temperature.

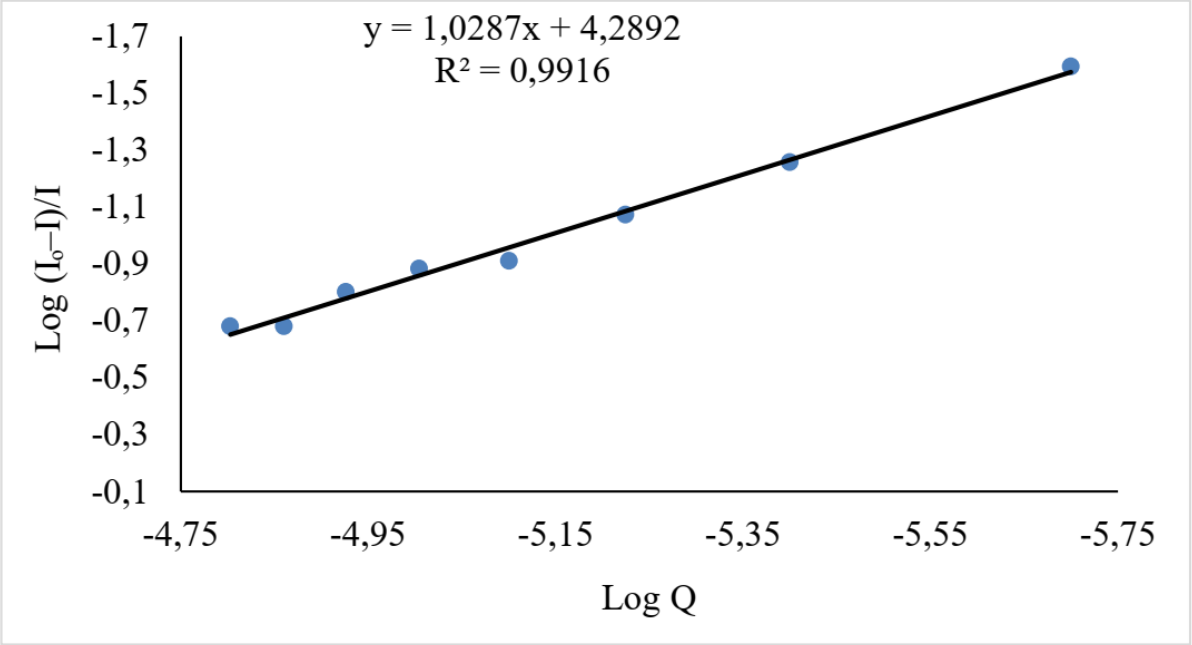

Figure S34: The double-logarithmic plot of Hoechst 33342-CT-DNA –Complex **2** interaction at room temperature.

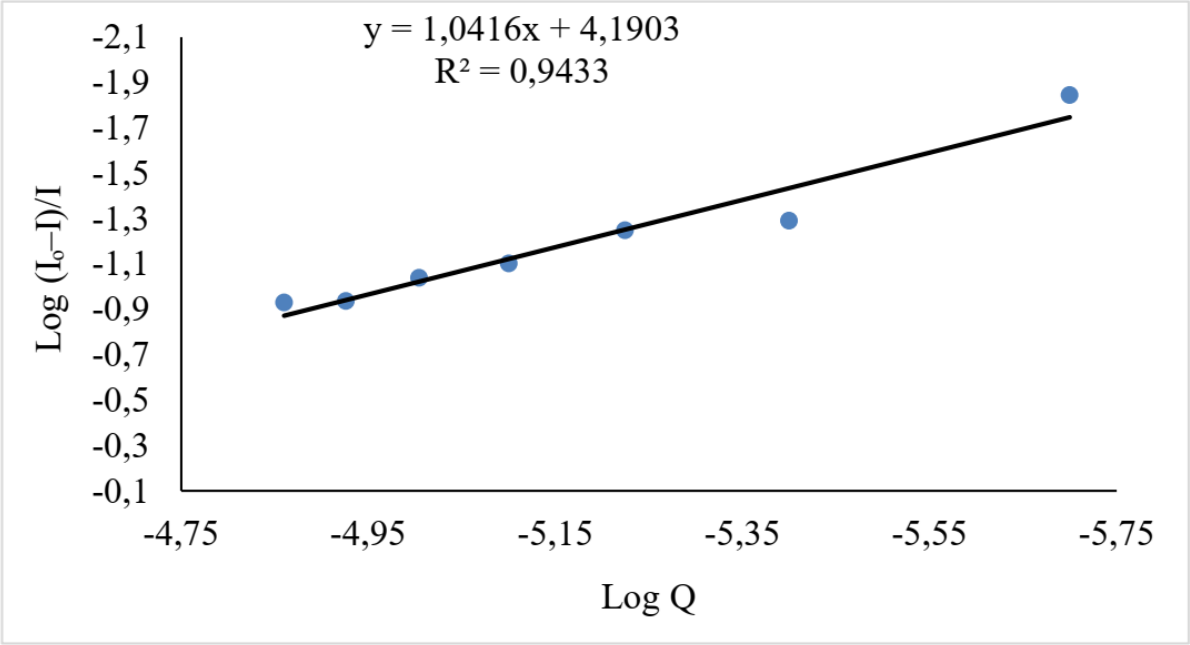

Figure S35: The double-logarithmic plot of Hoechst 33342-CT-DNA –Complex **6** interaction at room temperature.

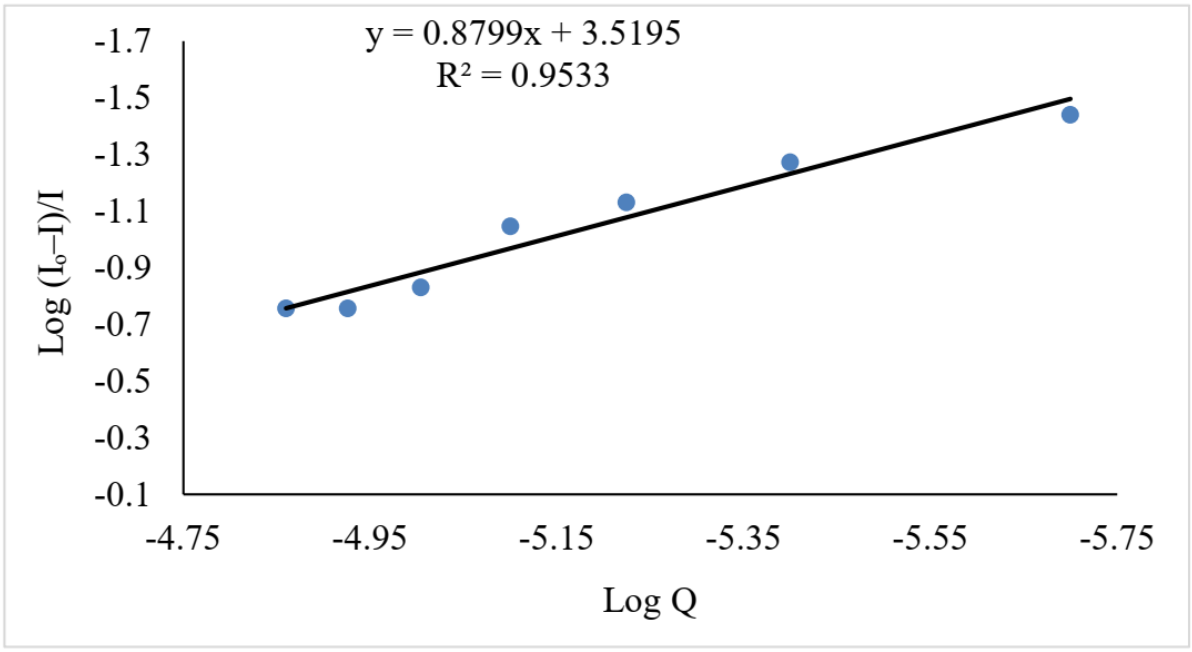

Figure S36: The double-logarithmic plot of Hoechst 33342-CT-DNA–Complex **10** interaction at room temperature.

BSA Binding studies using Electronic Absorption method

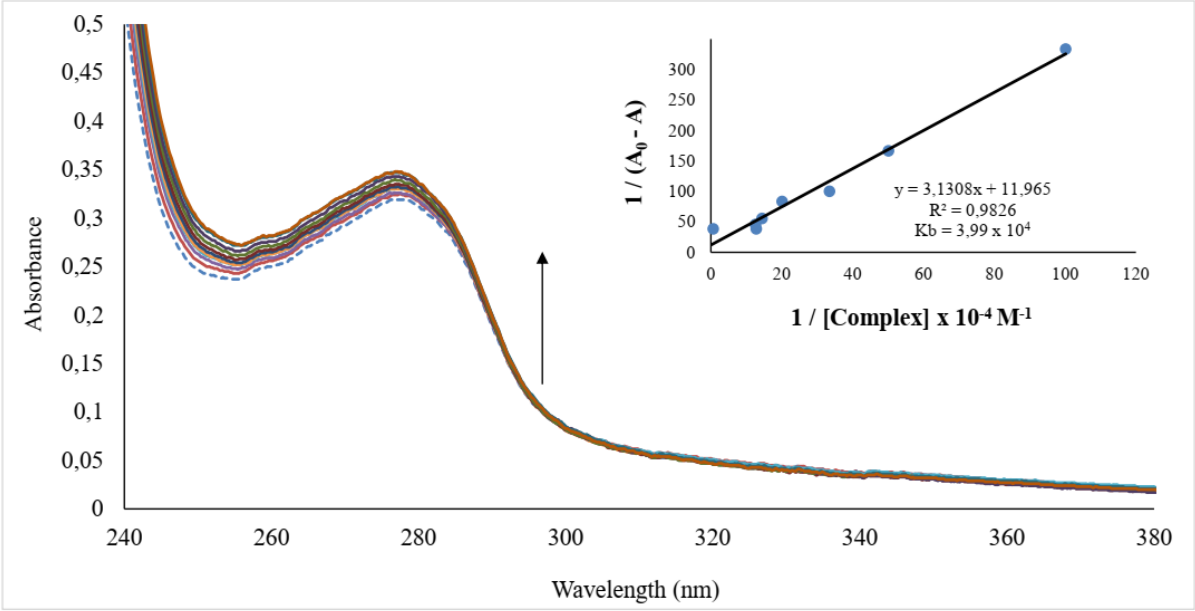

Figure S37: Electronic Absorption Spectra of BSA in the absence (dashed line) and the presence of different concentrations of complexes **1**. (inset) Plot of $1/(A_o - A)$ vs. $1/[Complex] \times 10^{-4}\ M^{-1}$

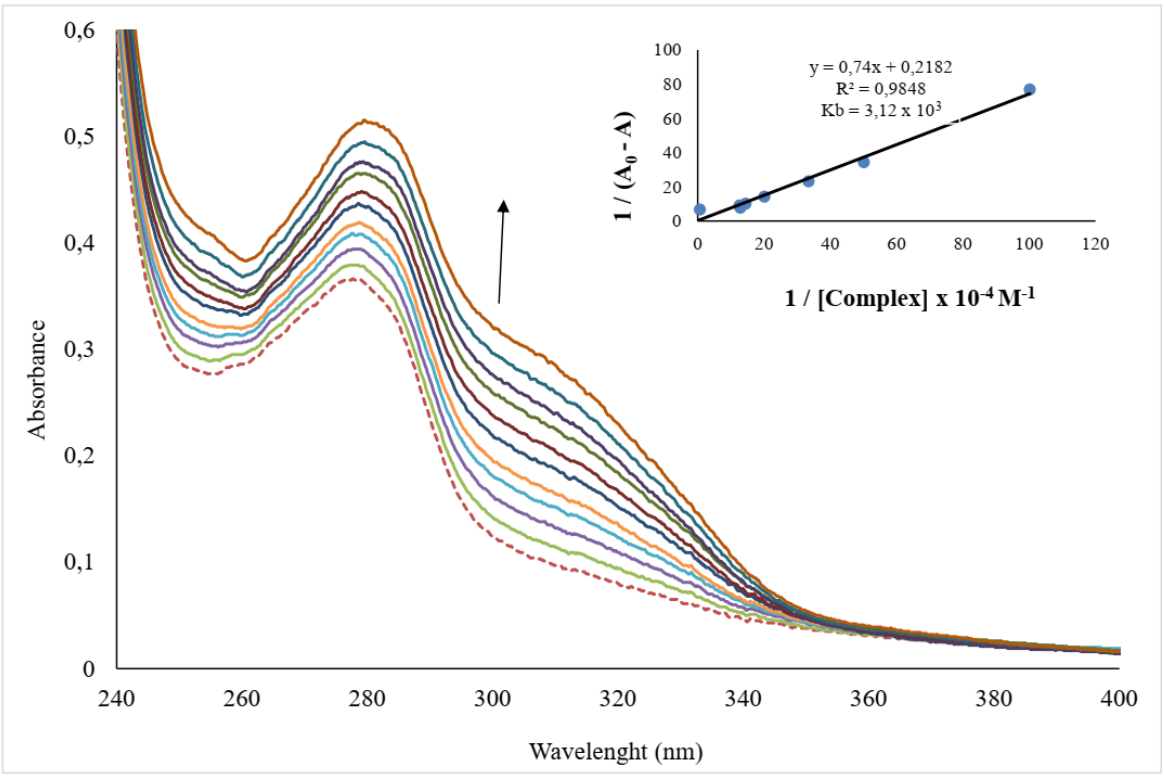

Figure S38: Electronic Absorption Spectra of BSA in the absence (dashed line) and the presence of different concentrations of complexes **2**. (inset) Plot of $1/(A_o - A)$ vs. $1/[Complex] \times 10^{-4}\ M^{-1}$

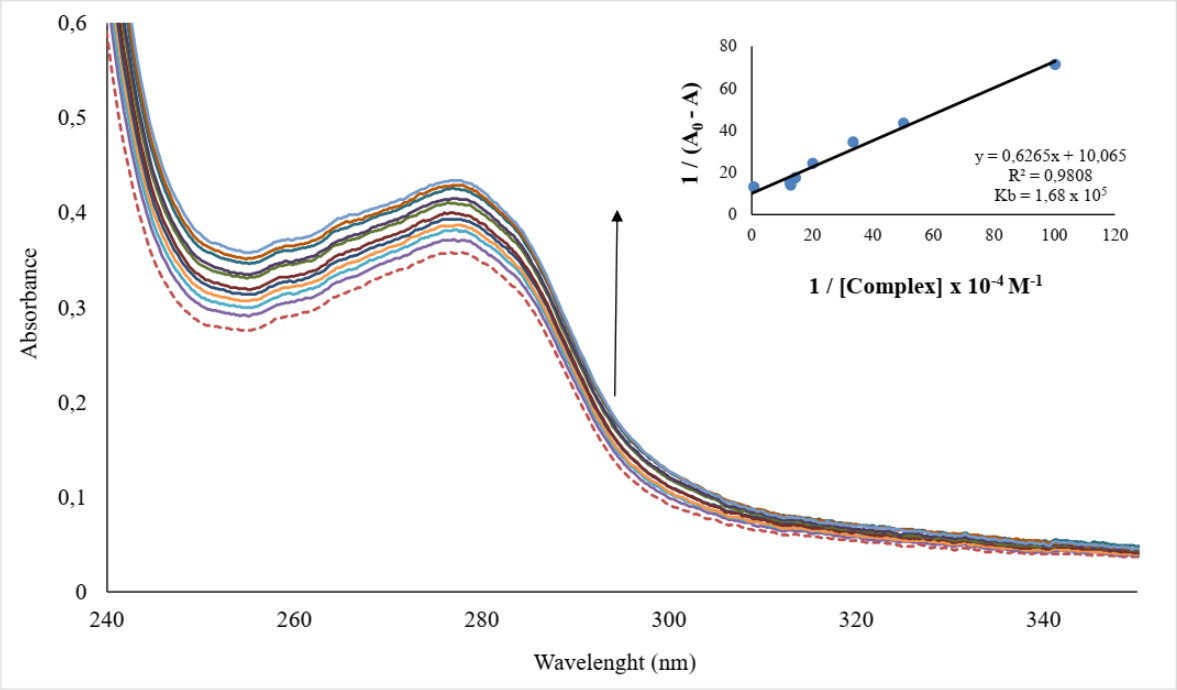

Figure S39: Electronic Absorption Spectra of BSA in the absence (dashed line) and the presence of different concentrations of complex **3**. (inset) plot of 3 $1/(A-A_0)$ vs. $1/[Complex] \times 10^{-4}\ M^{-1}$

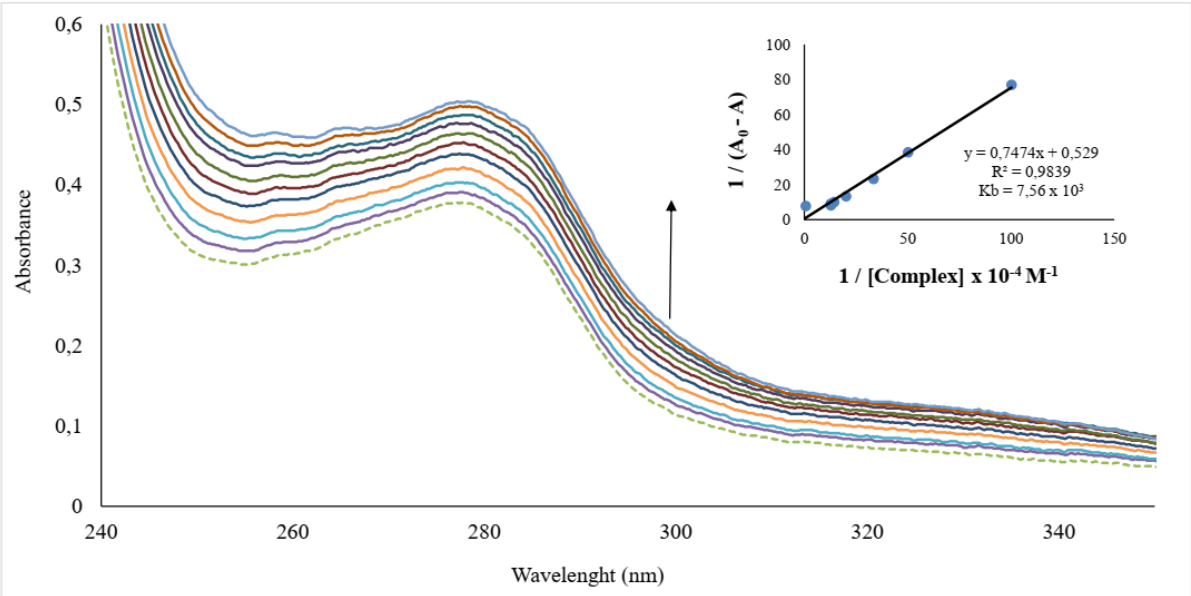

Figure S40: Electronic Absorption Spectra of BSA in the absence (dashed line) and the presence of different concentrations of complexes **4**. (inset) Plot of $1/(A_o - A)$ vs. $1/[Complex] \times 10^{-4}\ M^{-1}$

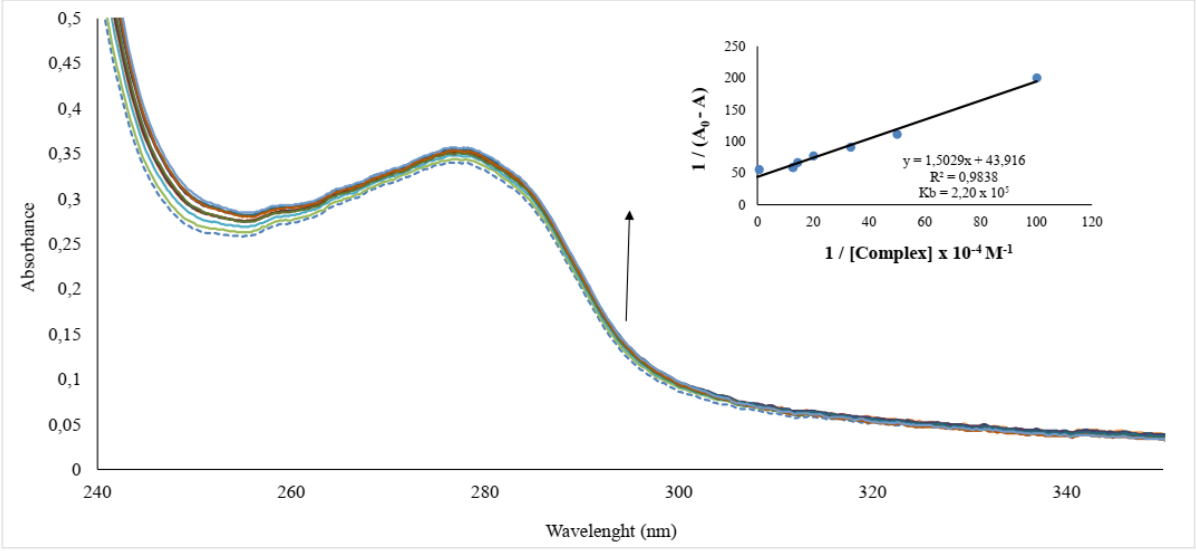

Figure S41: Electronic Absorption Spectra of BSA in the absence (dashed line) and the presence of different concentrations of complexes **5**. (inset) Plot of $1/(A_o - A)$ vs. $1/[Complex] \times 10^{-4}\ M^{-1}$

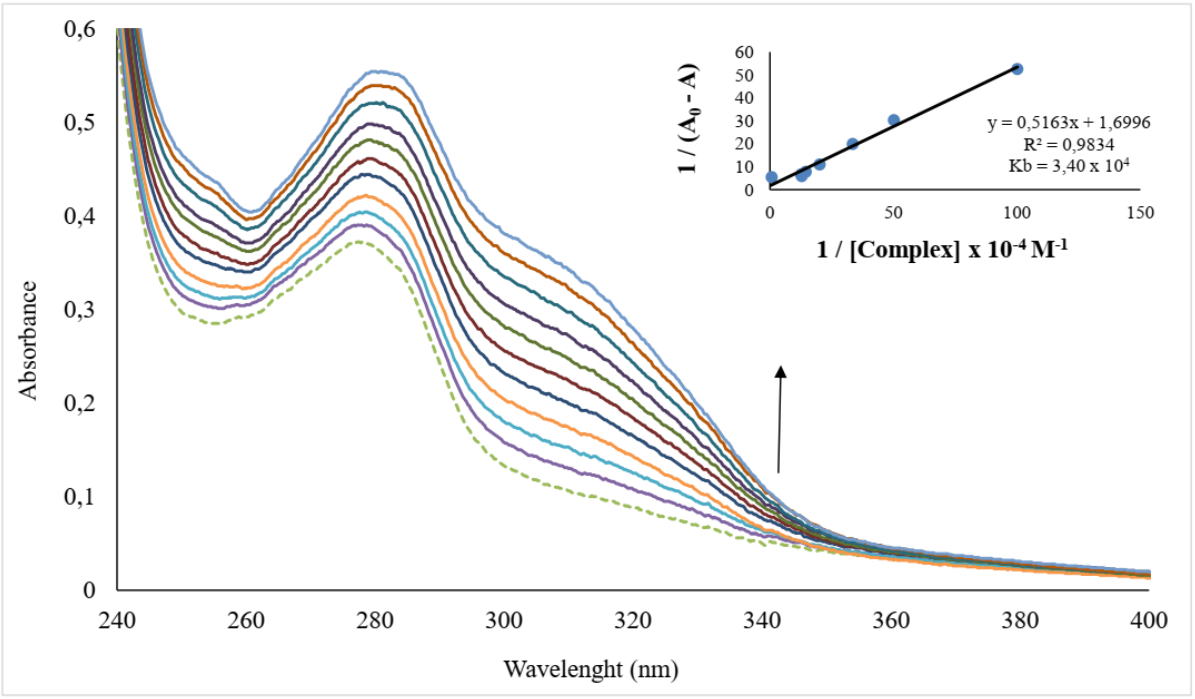

Figure S42: Electronic Absorption Spectra of BSA in the absence (dashed line) and the presence of different concentrations of complexes **6**. (inset) Plot of $1/(A_o - A)$ vs. $1/[Complex] \times 10^{-4}\ M^{-1}$

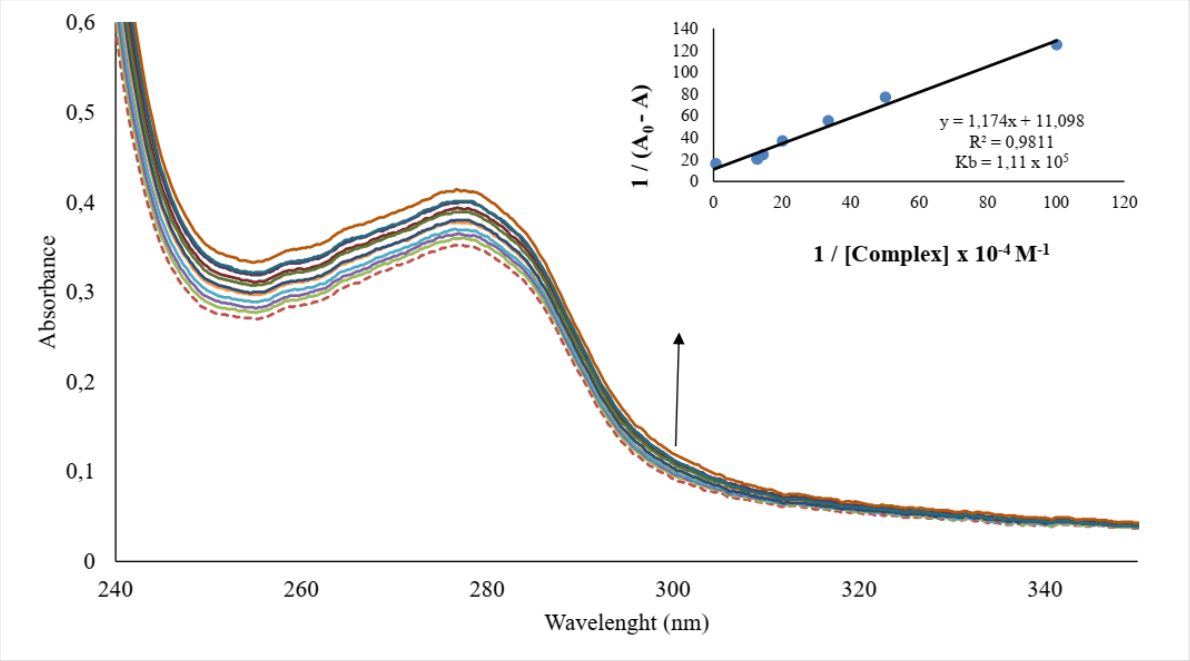

Figure S43: Electronic Absorption Spectra of BSA in the absence (dashed line) and the presence of different concentrations of complexes **7**. (inset) Plot of $1/(A_o - A)$ vs. $1/[Complex] \times 10^{-4}\ M^{-1}$

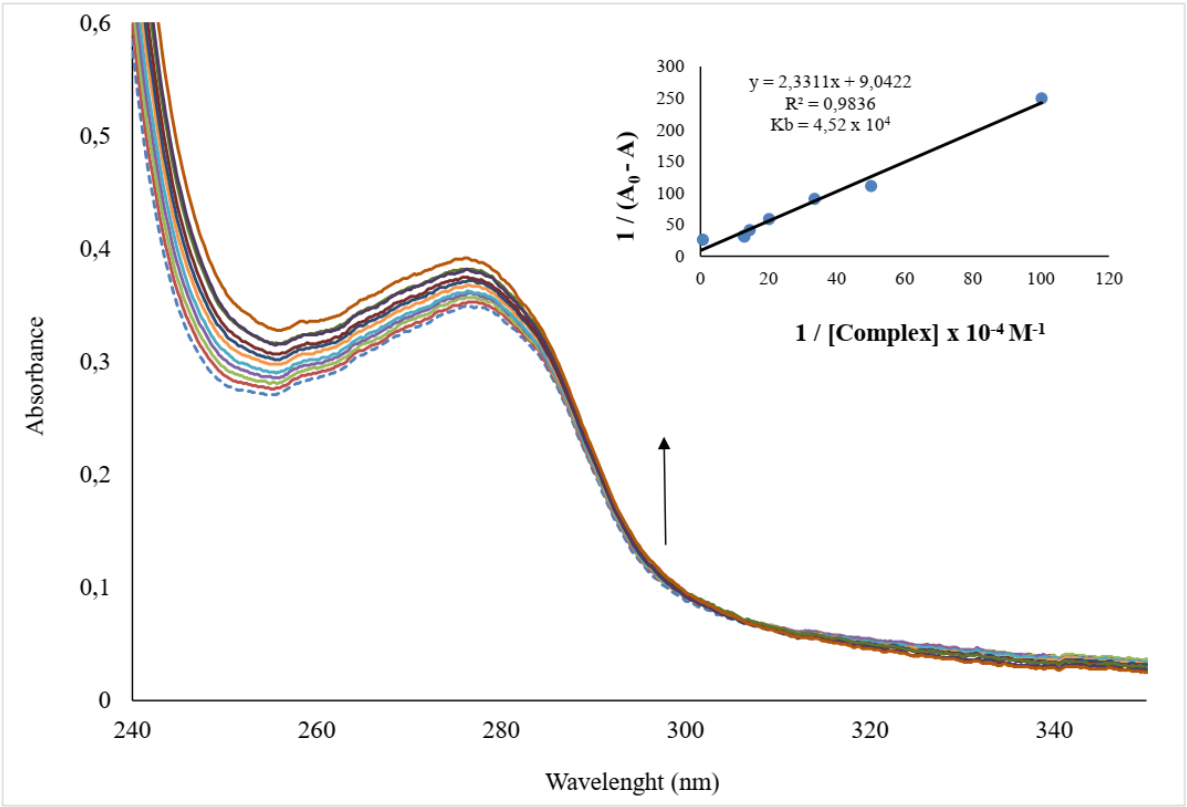

Figure S44: Electronic Absorption Spectra of BSA in the absence (dashed line) and the presence of different concentrations of complexes **8**. (inset) Plot of $1/(A_o - A)$ vs. $1/[Complex] \times 10^{-4}\ M^{-1}$

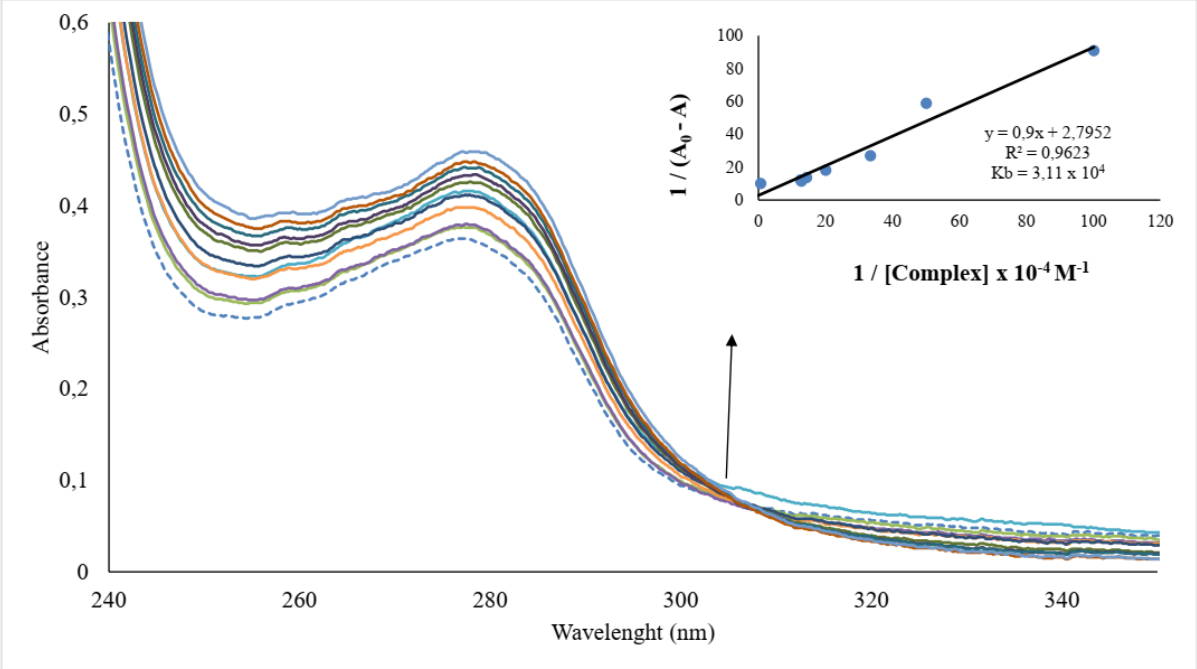

Figure S45: Electronic Absorption Spectra of BSA in the absence (dashed line) and the presence of different concentrations of complexes **9**. (inset) Plot of $1/(A_o - A)$ vs. $1/[Complex] \times 10^{-4}\ M^{-1}$

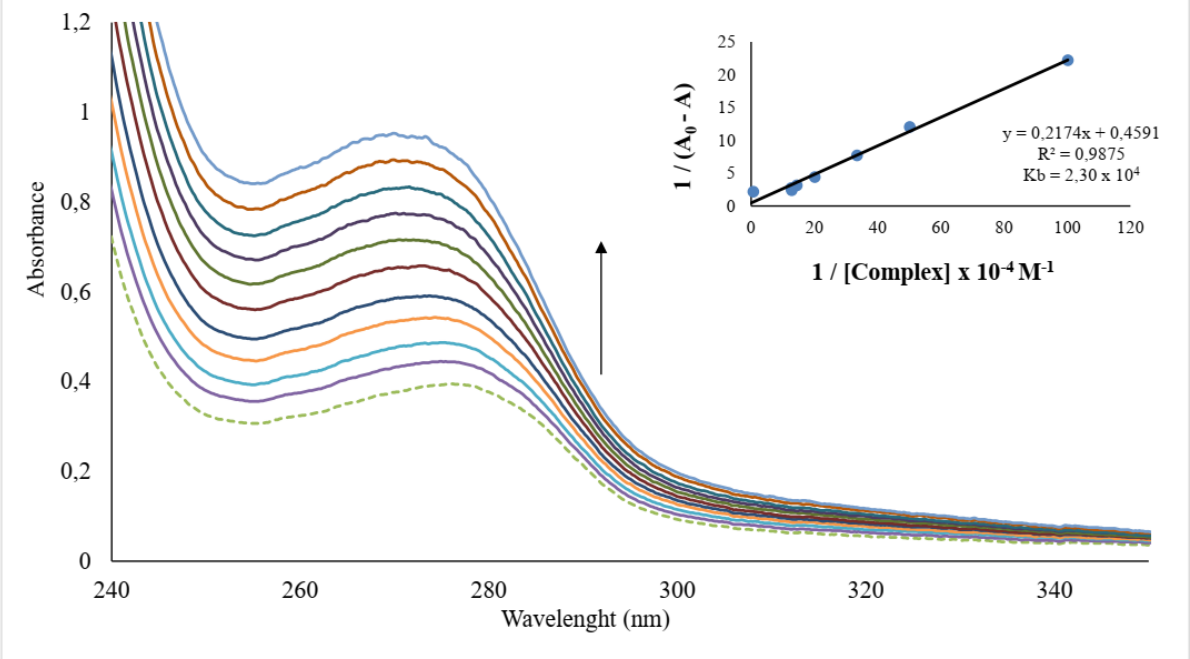

Figure S46: Electronic Absorption Spectra of BSA in the absence (dashed line) and the presence of different concentrations of complexes **11**. (inset) Plot of $1/(A_o - A)$ vs. $1/[Complex] \times 10^{-4}\ M^{-1}$

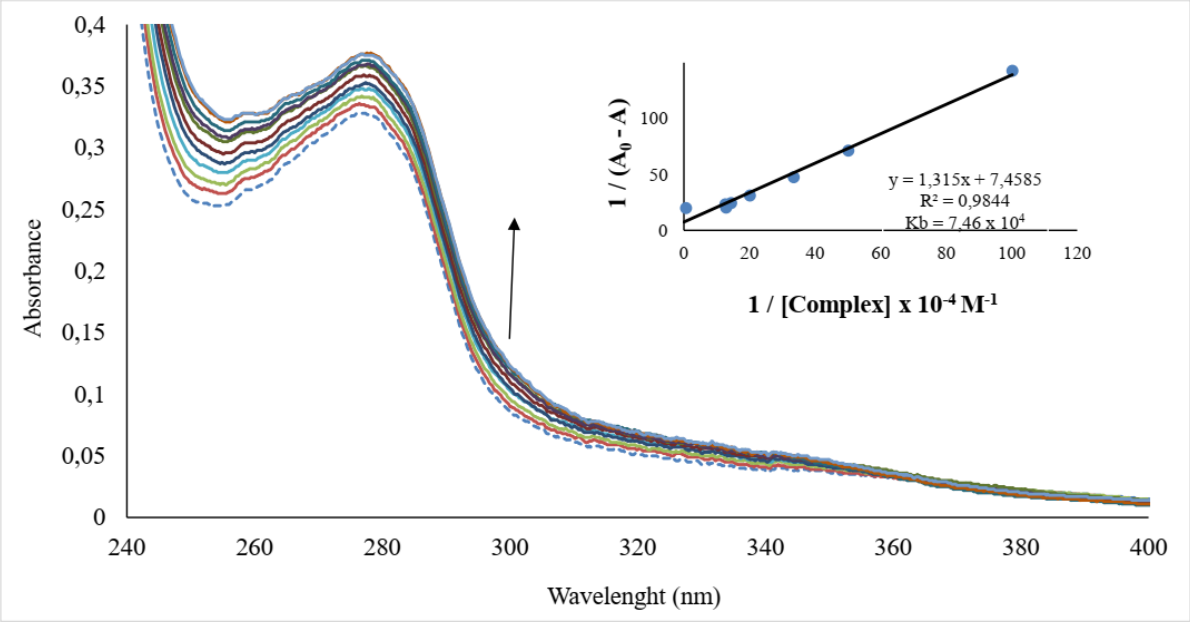

Figure S47: Electronic Absorption Spectra of BSA in the absence (dashed line) and the presence of different concentrations of complexes **12**. (inset) Plot of $1/(A_o - A)$ vs. $1/[Complex] \times 10^{-4}\ M^{-1}$

BSA Binding studies using the Fluorescence method

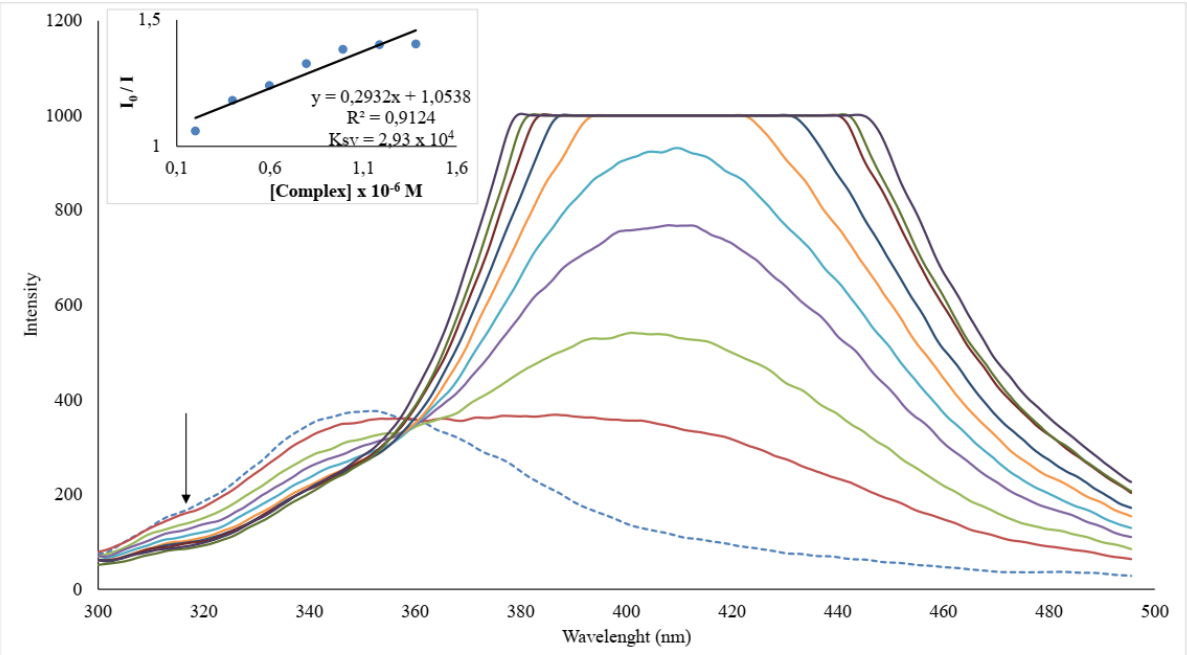

Figure S48: Fluorescence emission spectra of BSA in the absence(dashed line) and the presence of different concentration of complex **2**. (inset) Stern-Volmer plot of complex **2** interaction with BSA

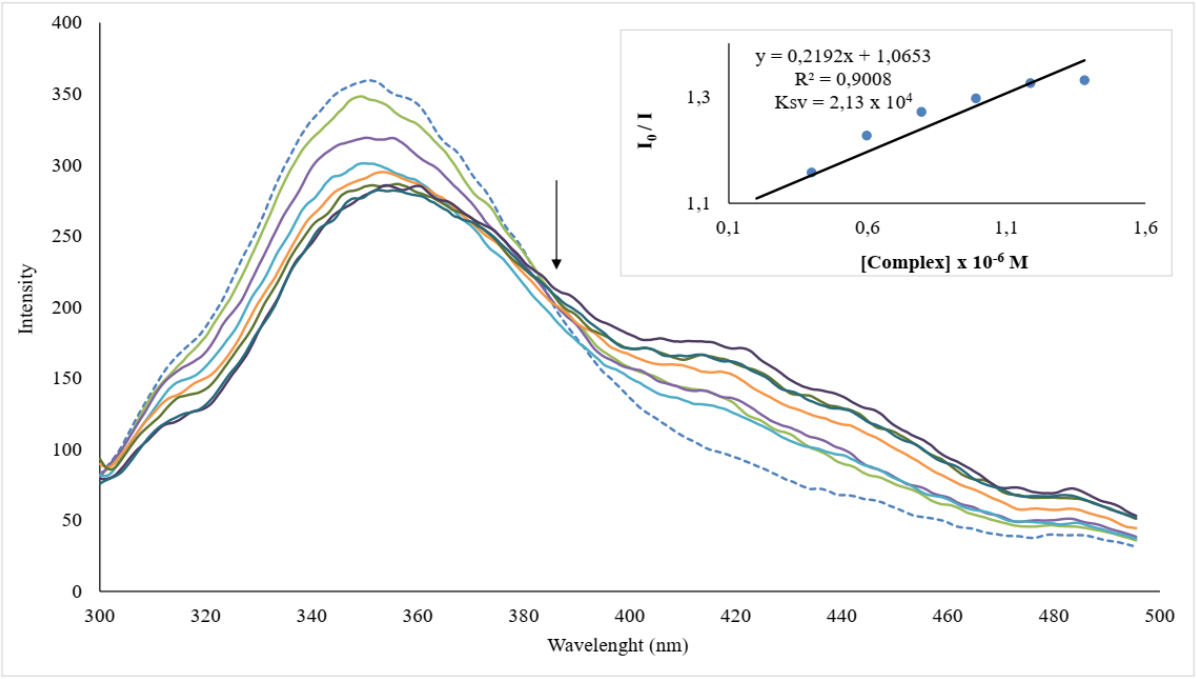

Figure S49: Fluorescence emission spectra of BSA in the absence(dashed line) and the presence of different concentrations of complex **3**. (inset) Stern-Volmer plot of complex **3** interaction with BSA.

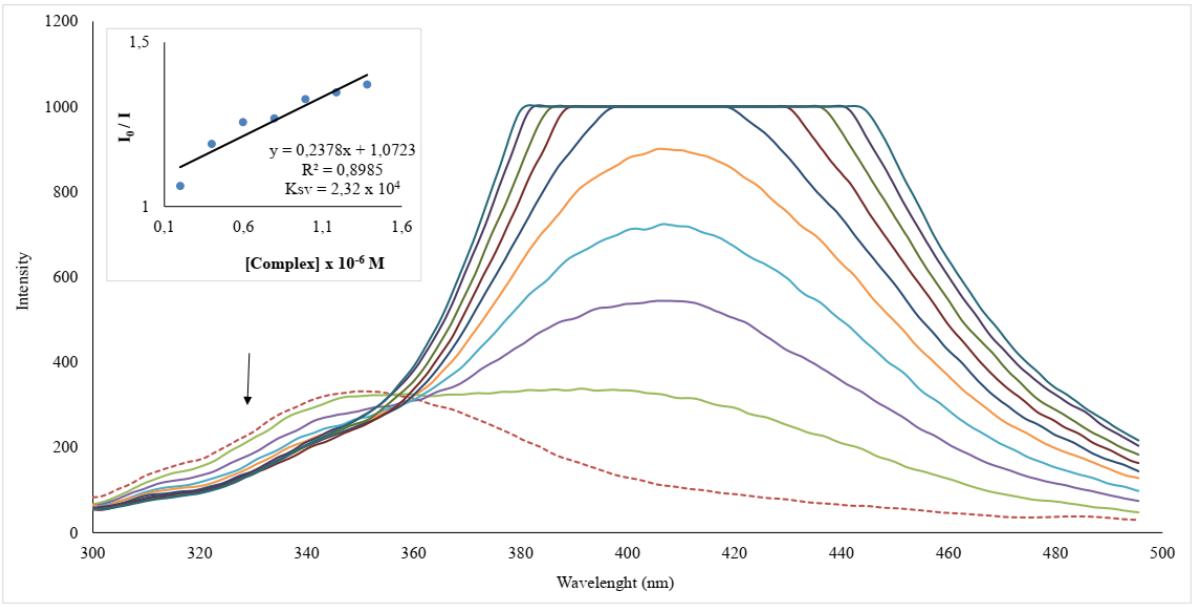

Figure S50: Fluorescence emission spectra of BSA in the absence(dashed line) and the presence of different concentrations of complex **6**. (inset) Stern-Volmer plot of complex **6** interaction with BSA

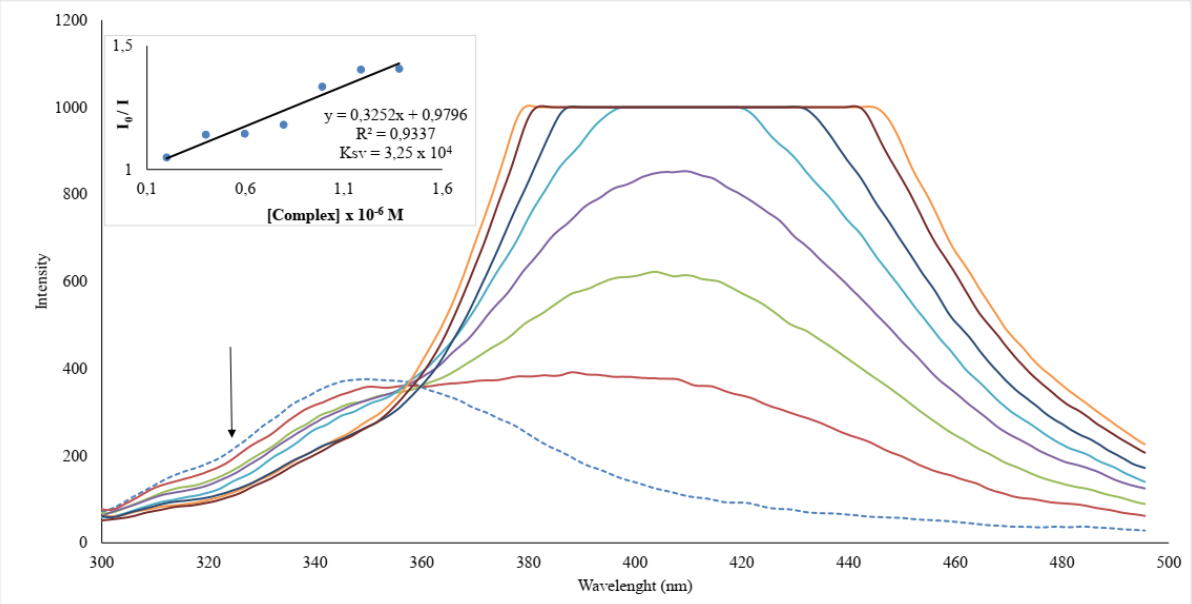

Figure S51: Fluorescence emission spectra of BSA in the absence(dashed line) and the presence of different concentrations of complex **10**. (inset) Stern-Volmer plot of complex **10** interaction with BSA

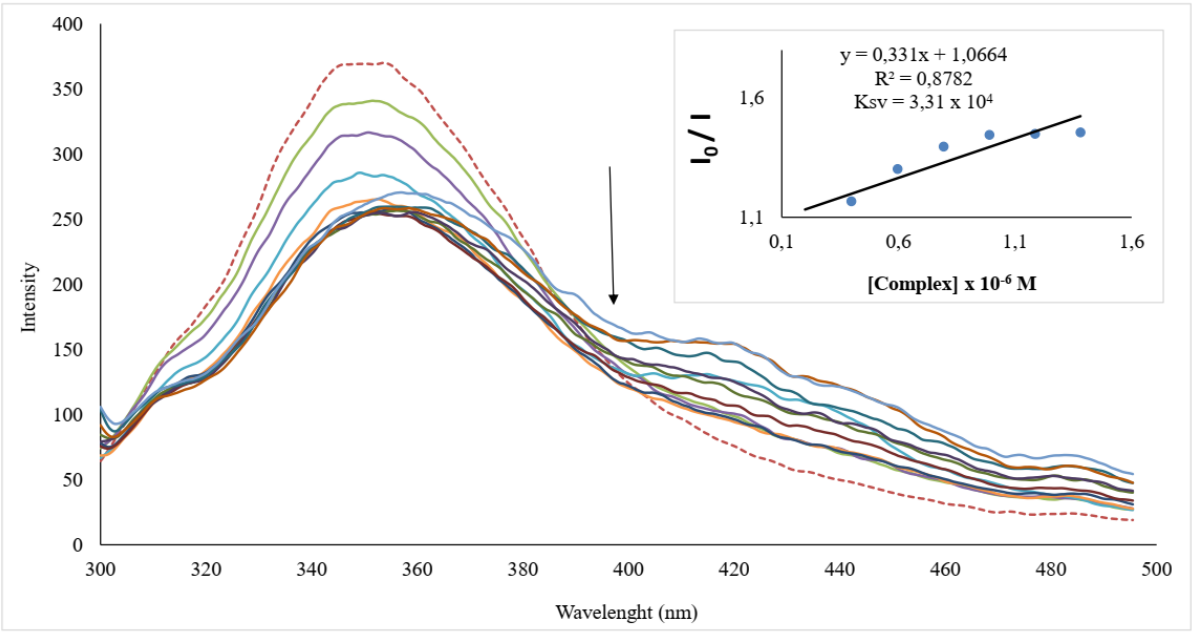

Figure S52: Fluorescence emission spectra of BSA in the absence(dashed line) and the presence of different concentrations of complex **11**. (inset) Stern-Volmer plot of complex **11** interaction with BSA

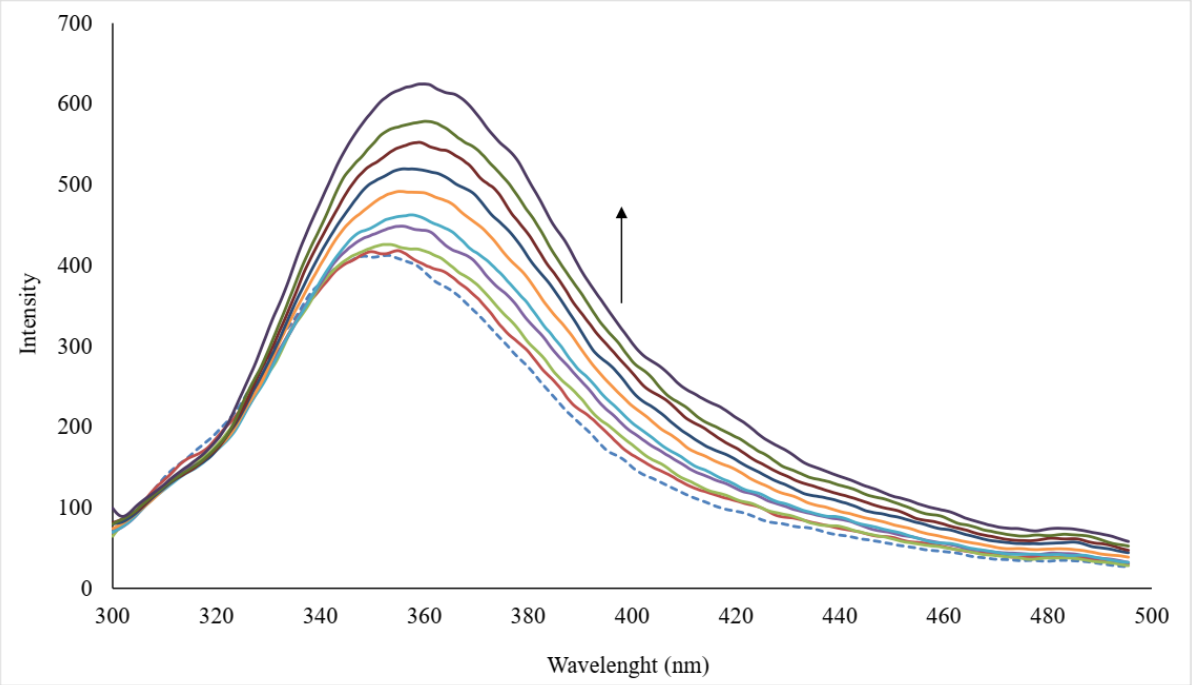

Figure S53: Fluorescence emission spectra of BSA in the absence(dashed line) and the presence of different concentration of complex **1**

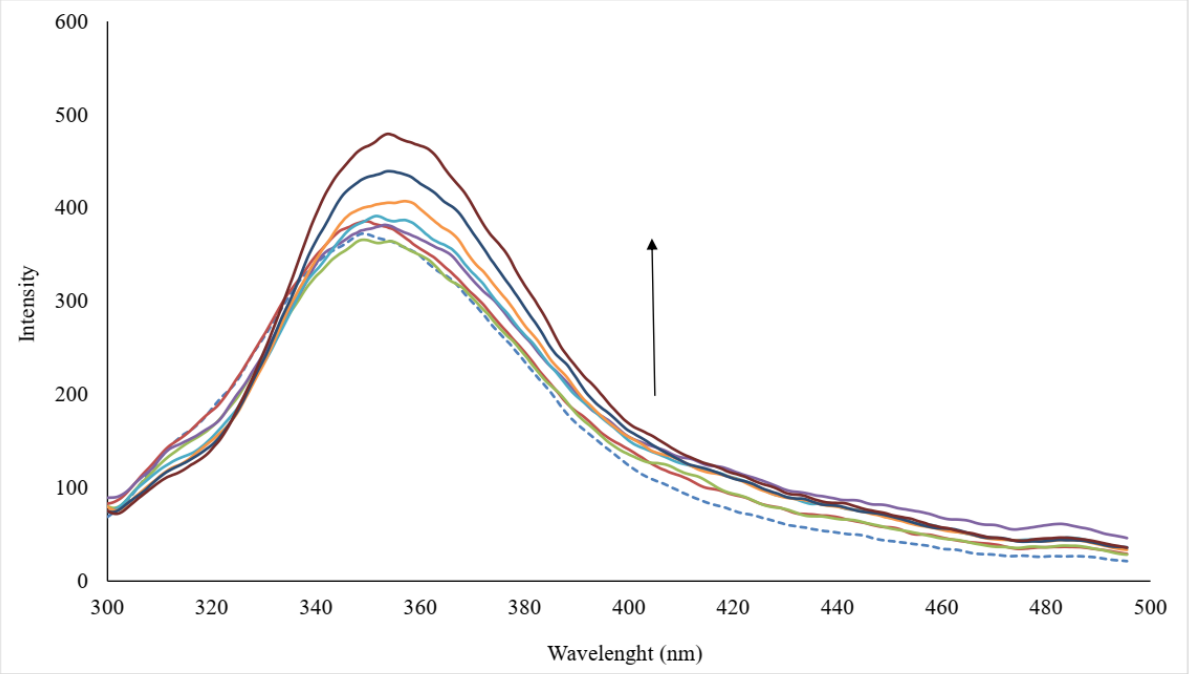

Figure S54: Fluorescence emission spectra of BSA in the absence(dashed line) and the presence of different concentrations of complex **4**.

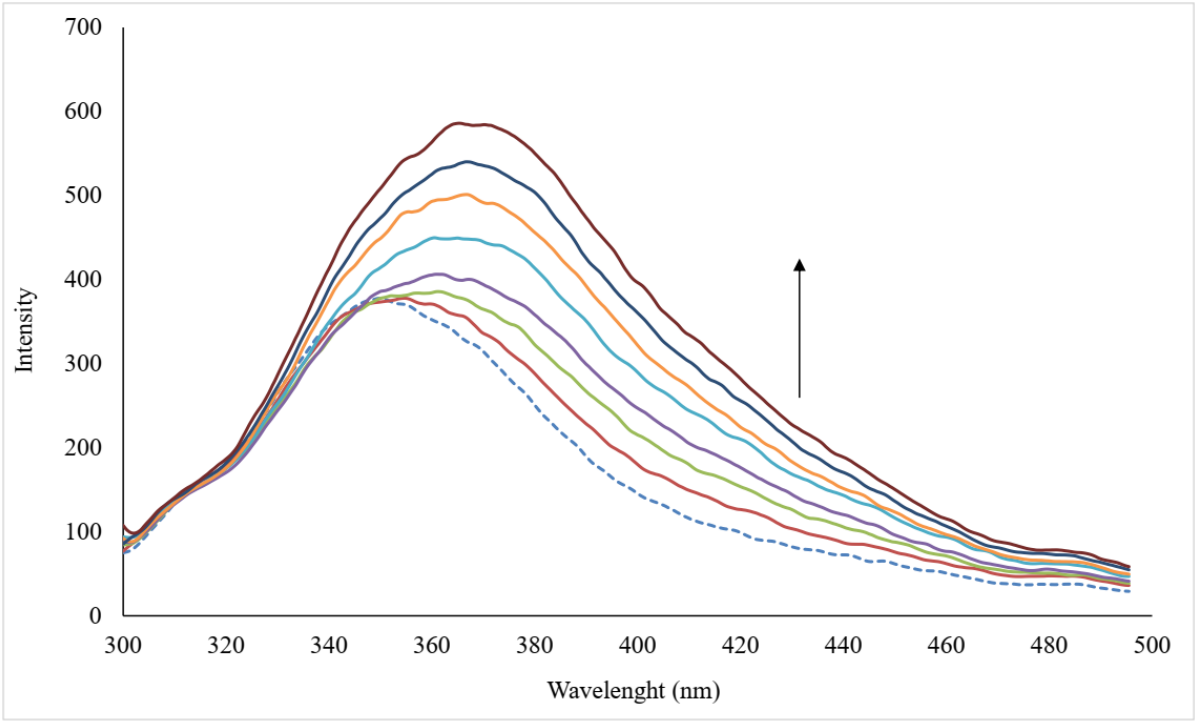

Figure S55: Fluorescence emission spectra of BSA in the absence(dashed line) and the presence of different concentration of complex **5**

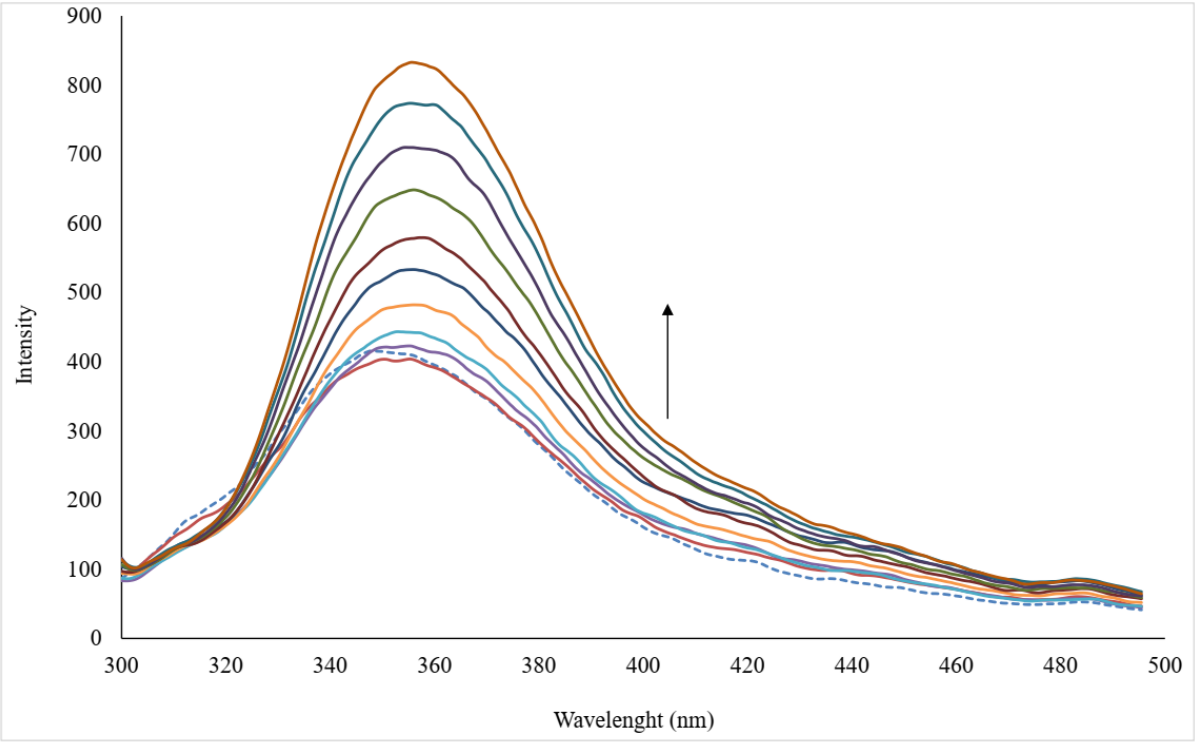

Figure S56: Fluorescence emission spectra of BSA in the absence(dashed line) and the presence of different concentrations of complex **8**.

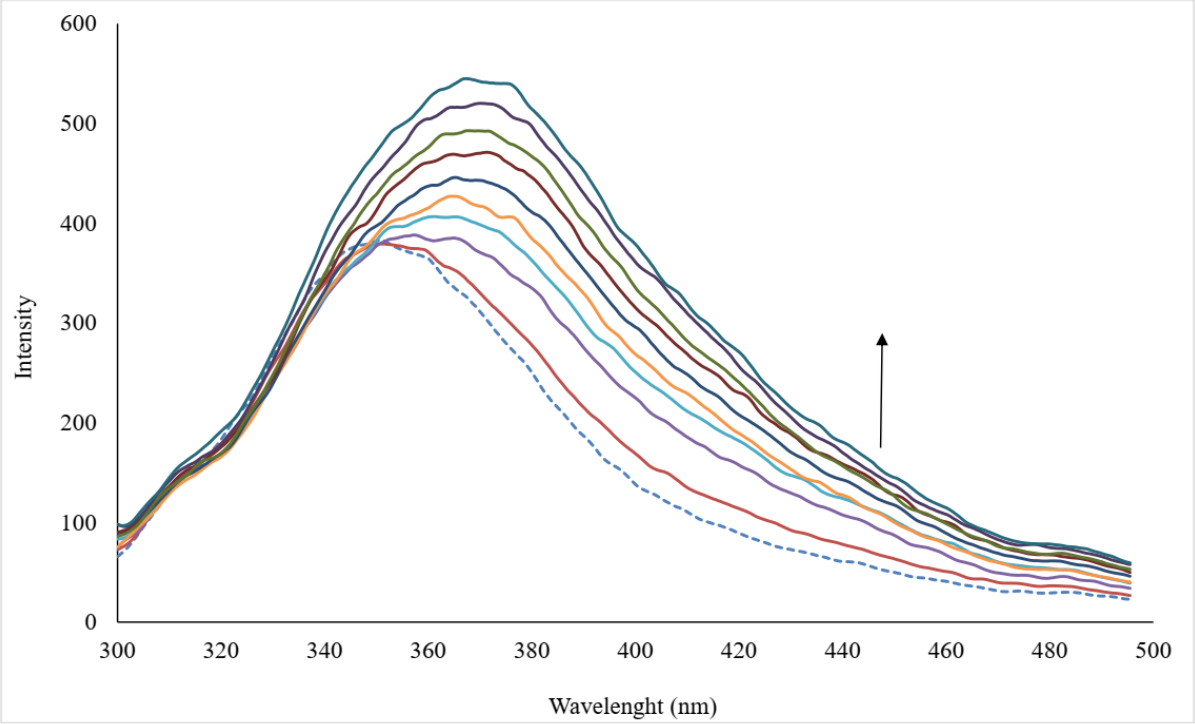

Figure S57: Fluorescence emission spectra of BSA in the absence(dashed line) and the presence of different concentrations of complex **9**. (inset) Stern-Volmer plot of complex **9** interaction with BSA

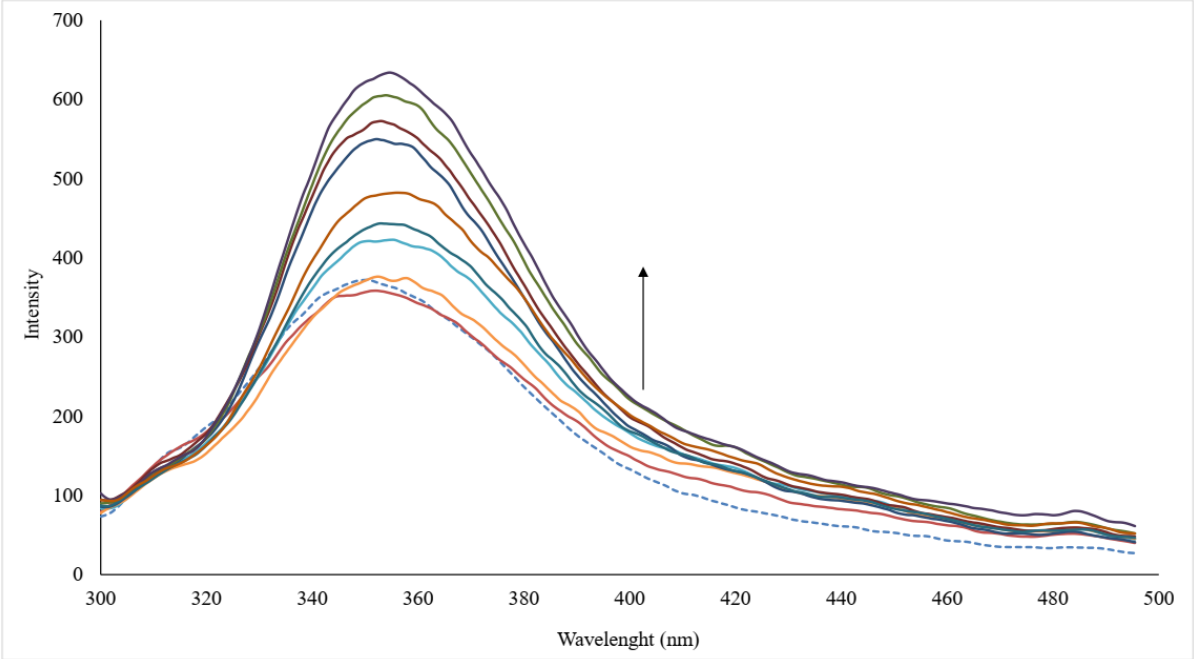

Figure S58: Fluorescence emission spectra of BSA in the absence(dashed line) and the presence of different concentrations of complex **12**. (inset) Stern-Volmer plot of complex **12** interaction with BSA

The double-logarithmic plot of BSA–Complexes interactions at room temperature.

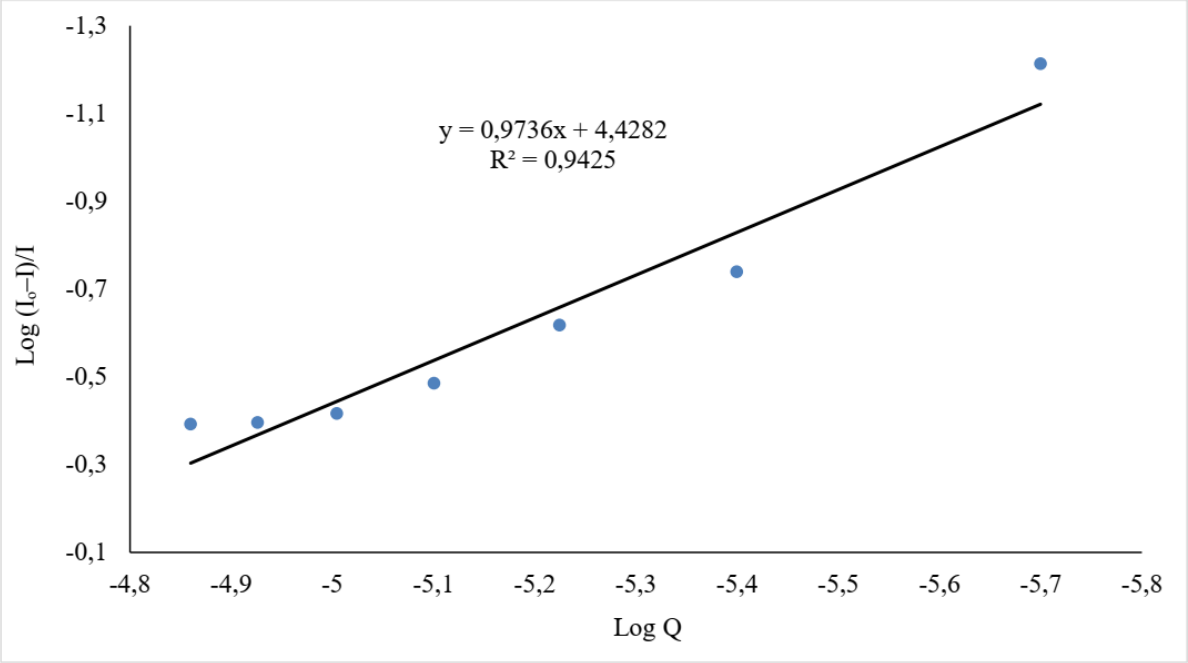

Figure S59: The double-logarithmic plot of BSA–Complex **2** interactions.

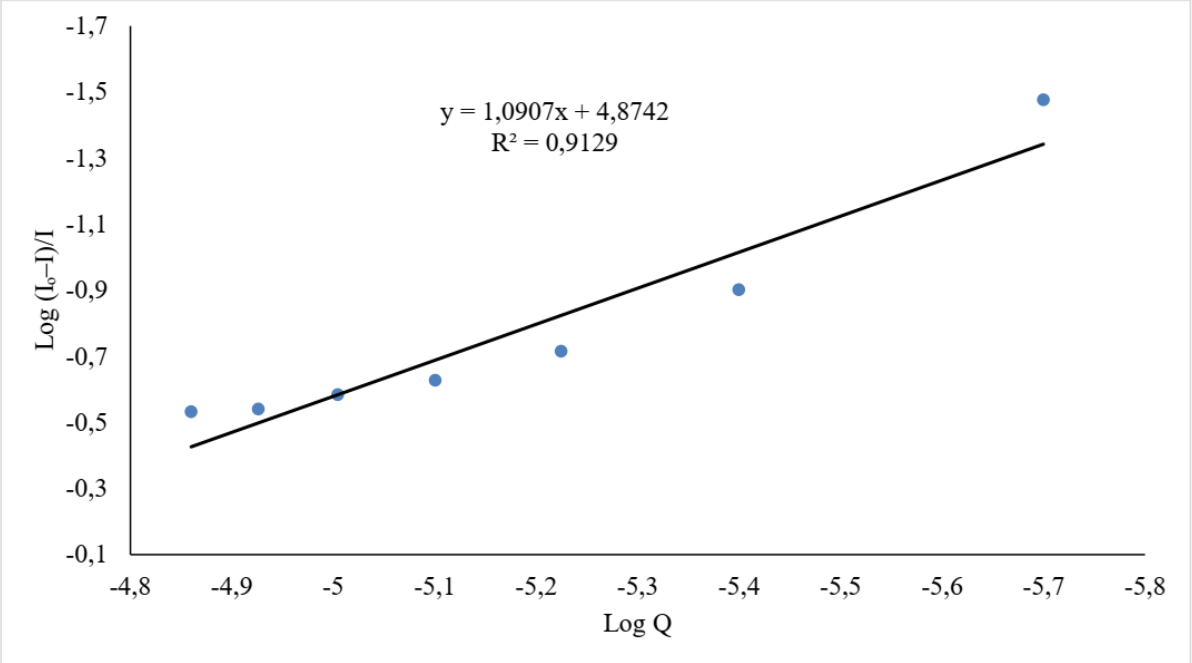

Figure S60: The double-logarithmic plot of BSA–Complex **3** interactions.

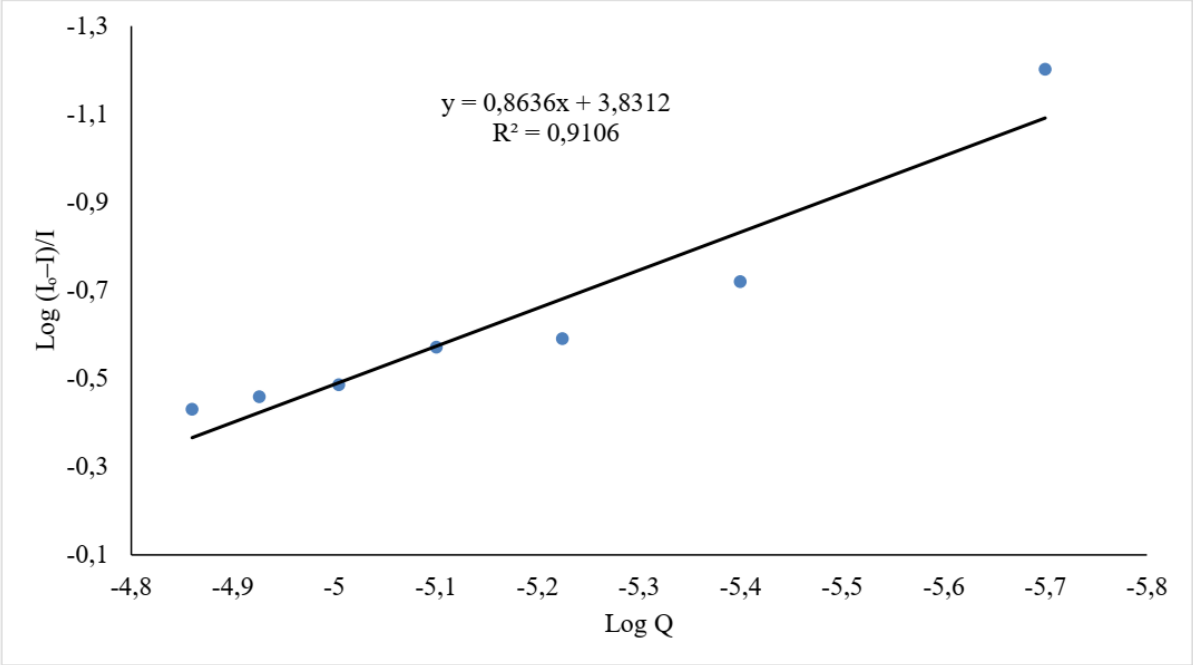

Figure S61: The double-logarithmic plot of BSA–Complex **6** interactions

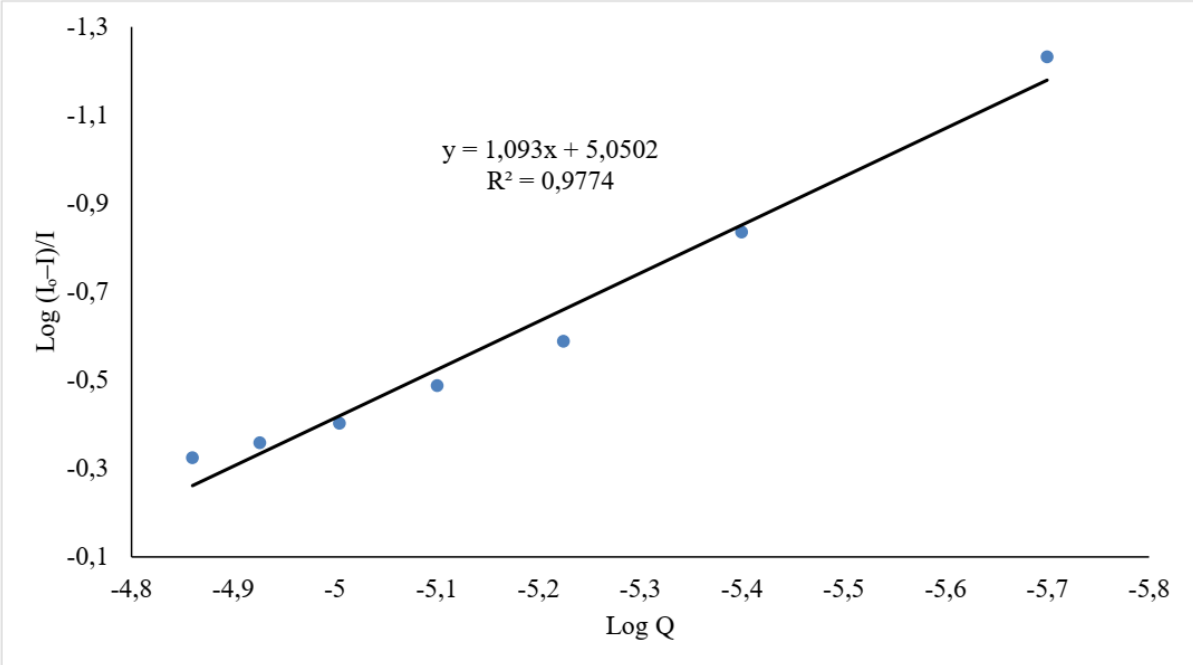

Figure S62: The double-logarithmic plot of BSA–Complex **7** interactions

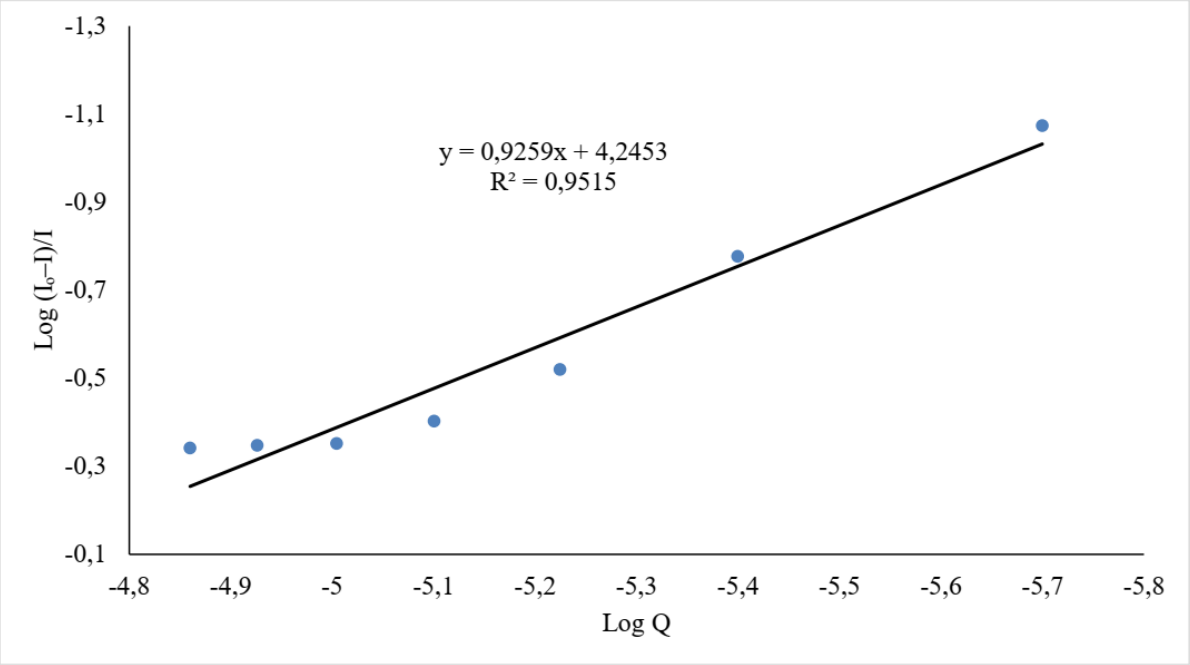

Figure S63: The double-logarithmic plot of BSA–Complex **11** interactions

^{1}H-NMR Spectra of Ligands E_{a-d}

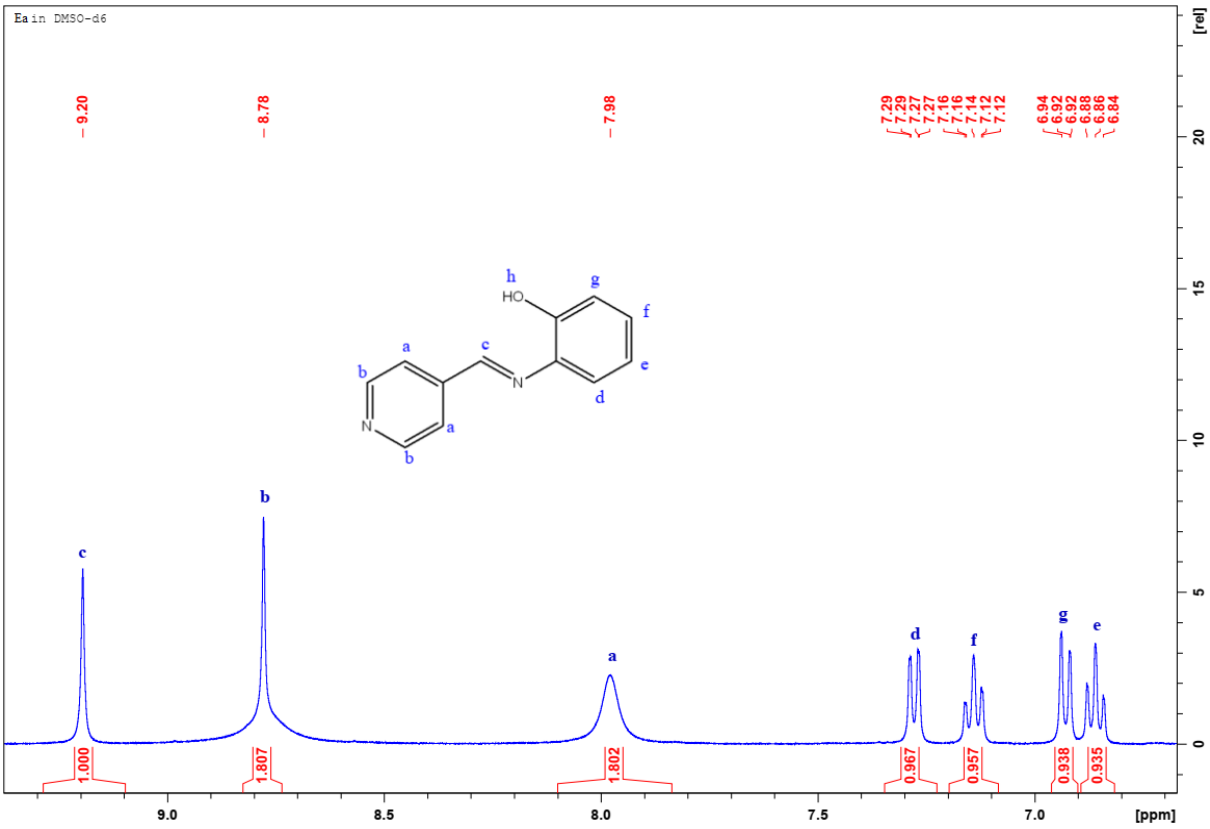

Figure S64: E)-2-((pyridin-4-ylmethylene)amino)phenol E_a

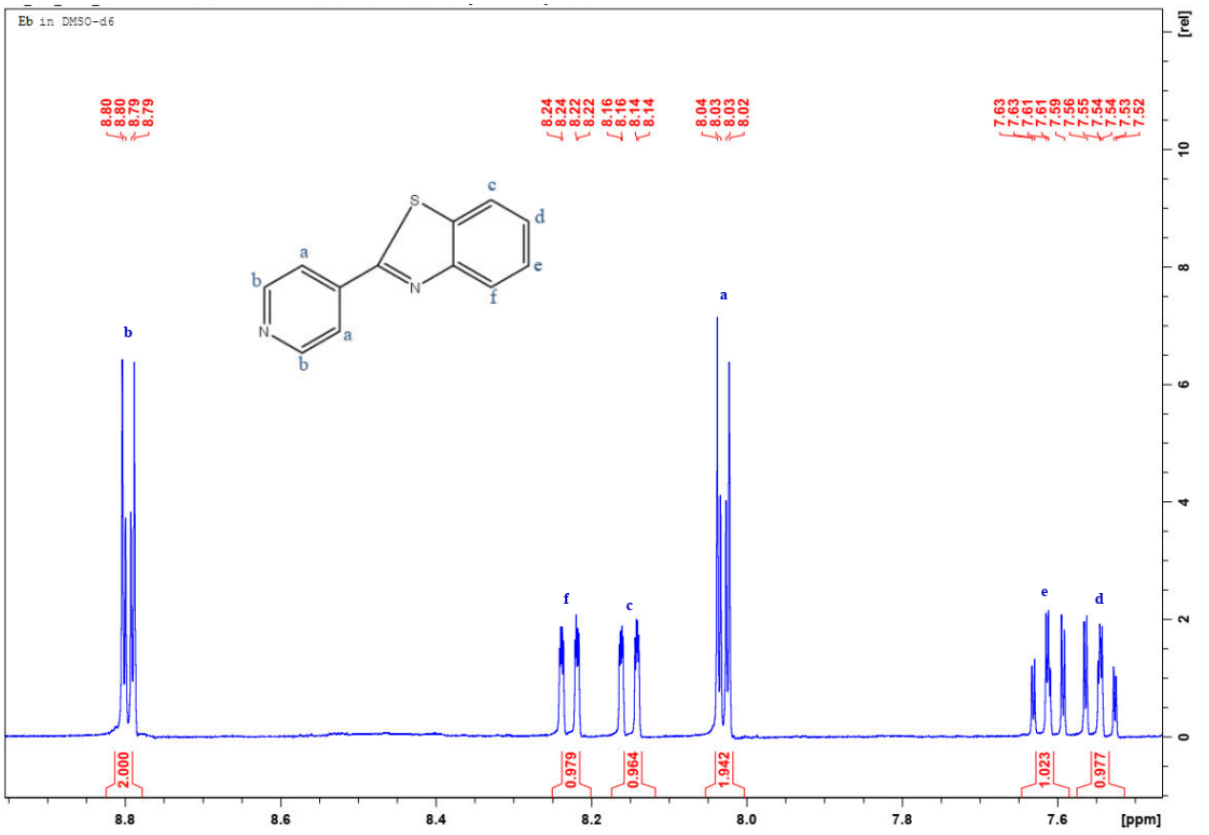

Figure S65: 2-(pyridin-4-yl)benzo[*d*]thiazole E_b

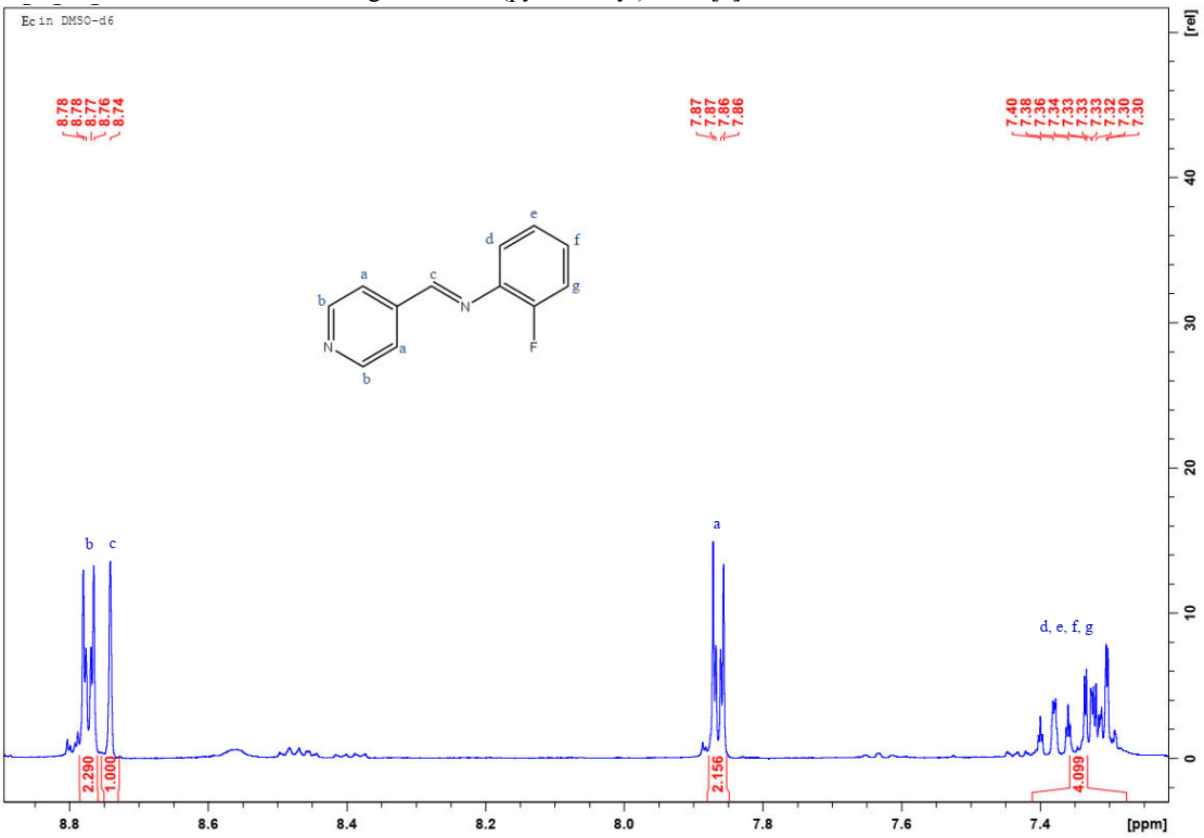

Figure S66: (E)-N-(2-fluorophenyl)-1-(pyridin-4-yl)methanimine E_c

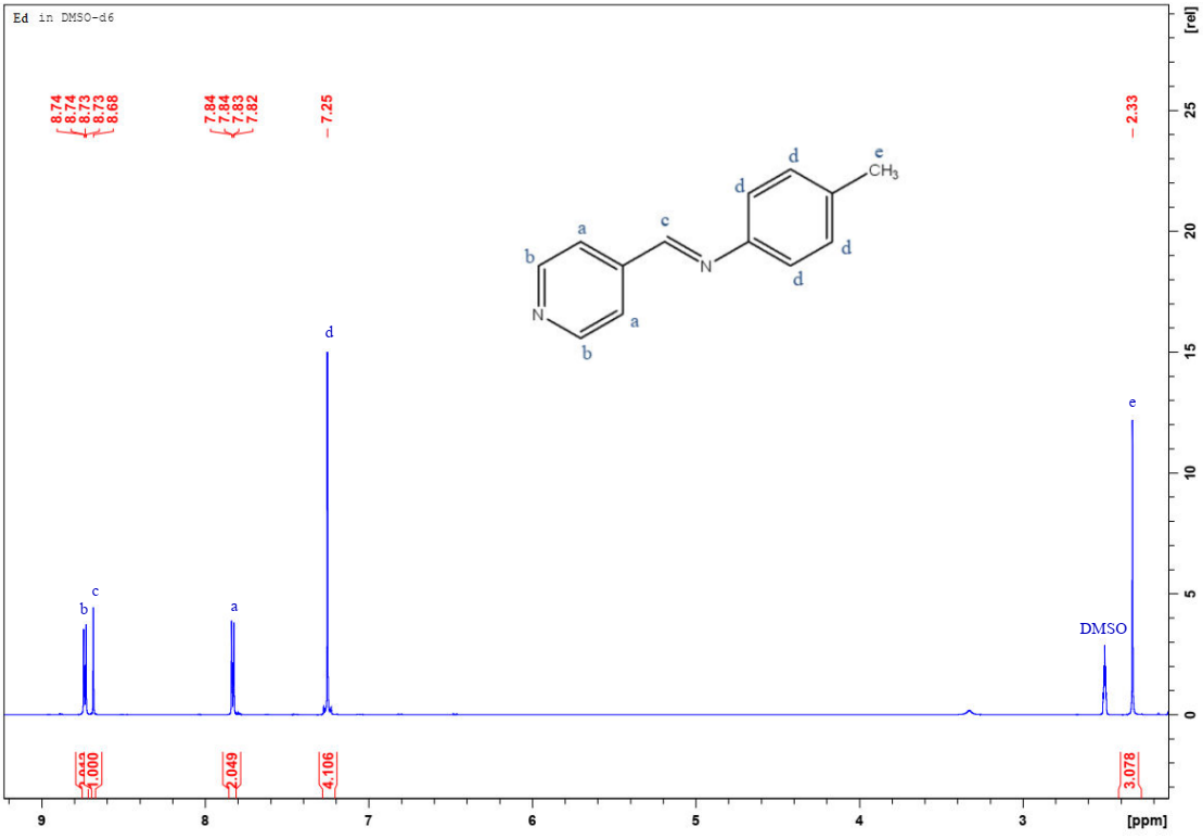

Figure S67: (E)-1-(pyridin-4-yl)-N-(p-tolyl)methanimine E_d

^{1}H-NMR SPECTRA OF COMPLEXES 1-12

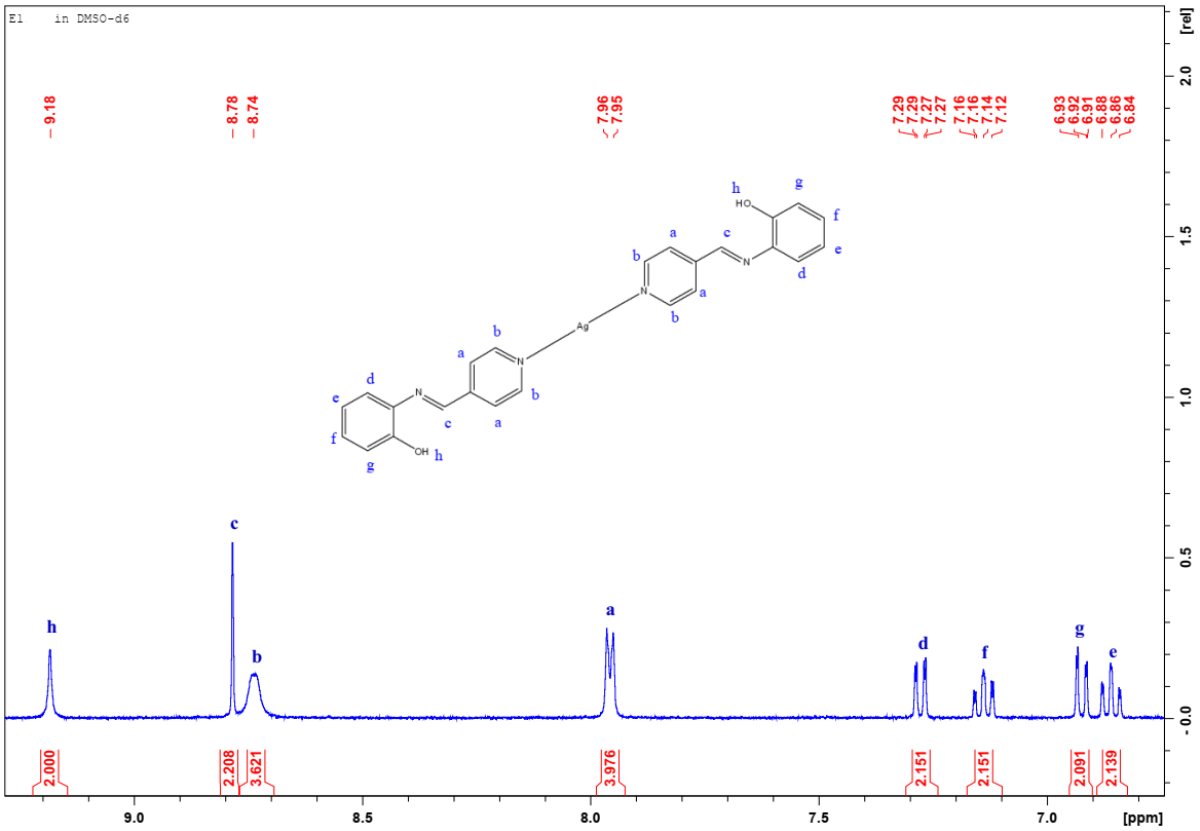

Figure S68: $[Ag(E_a)_2]NO_3$ 1

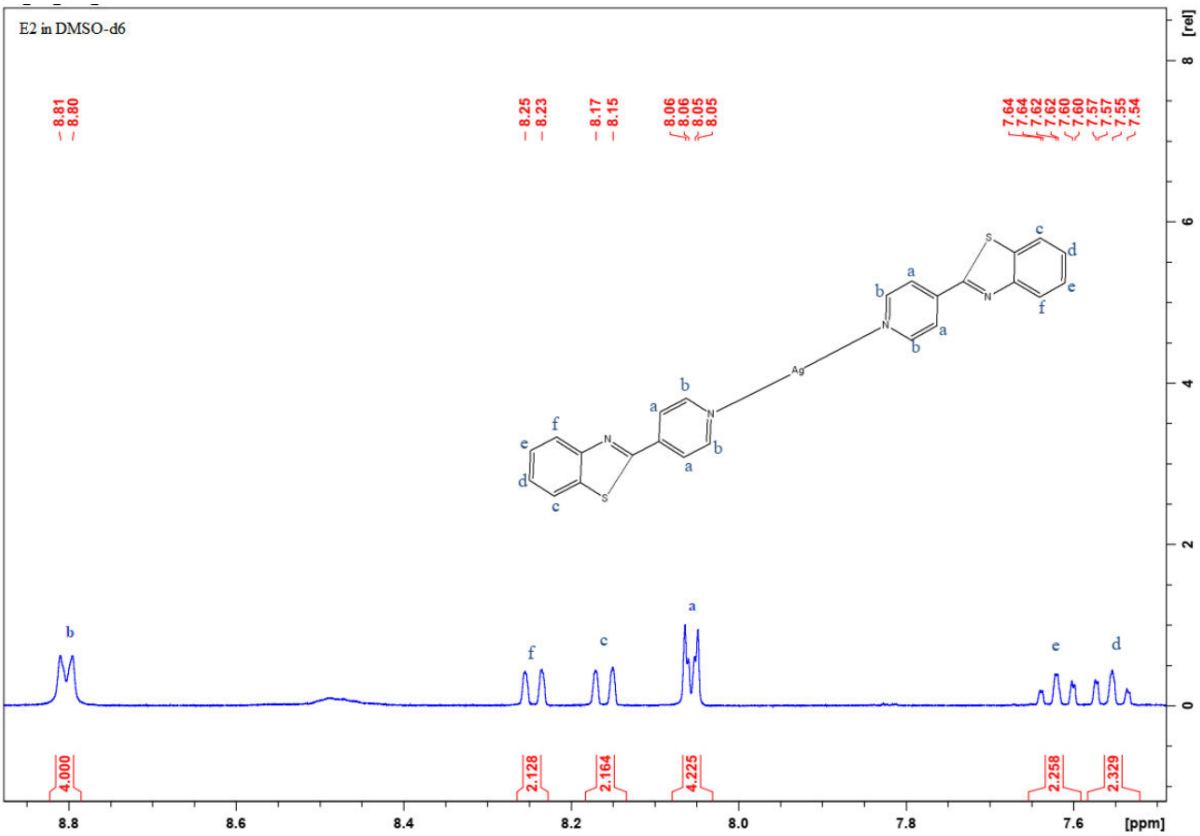

Figure S69: $[Ag(E_b)_2]NO_3$ 2

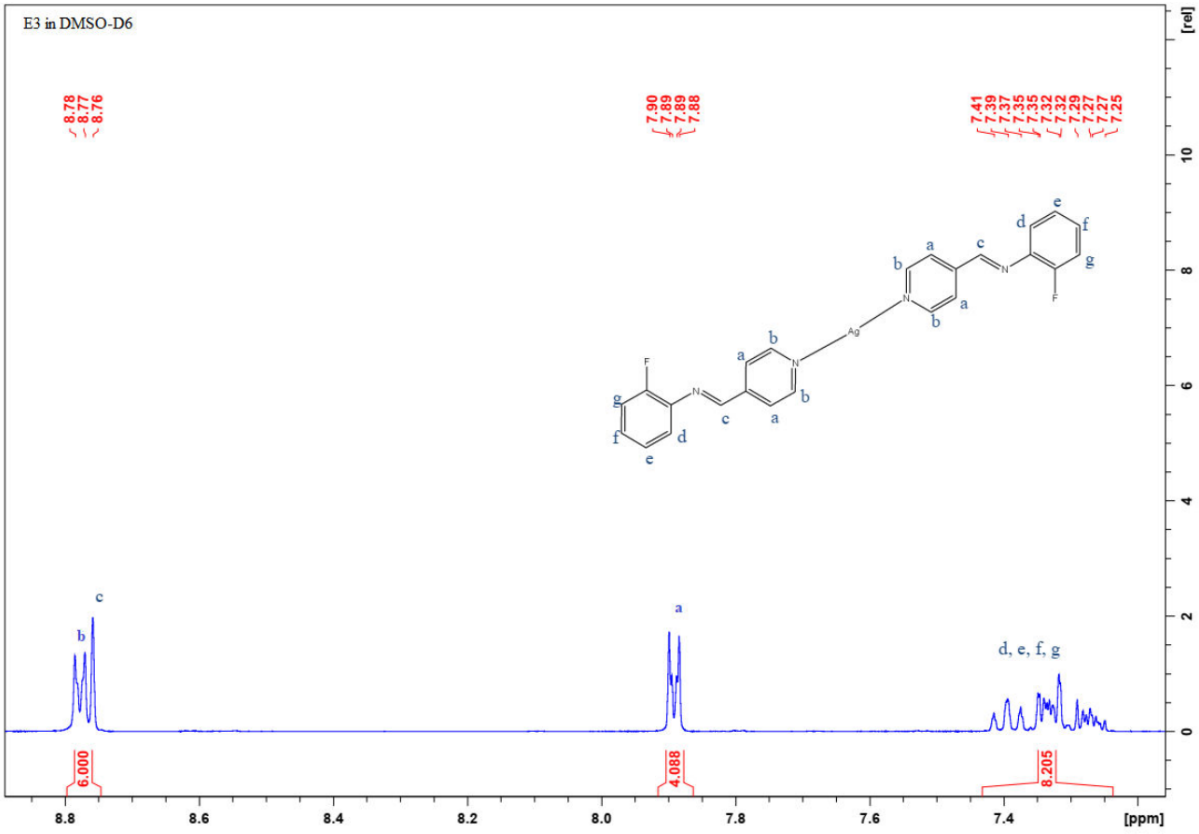

Figure S70: $[Ag(E_c)_2]NO_3$ 3

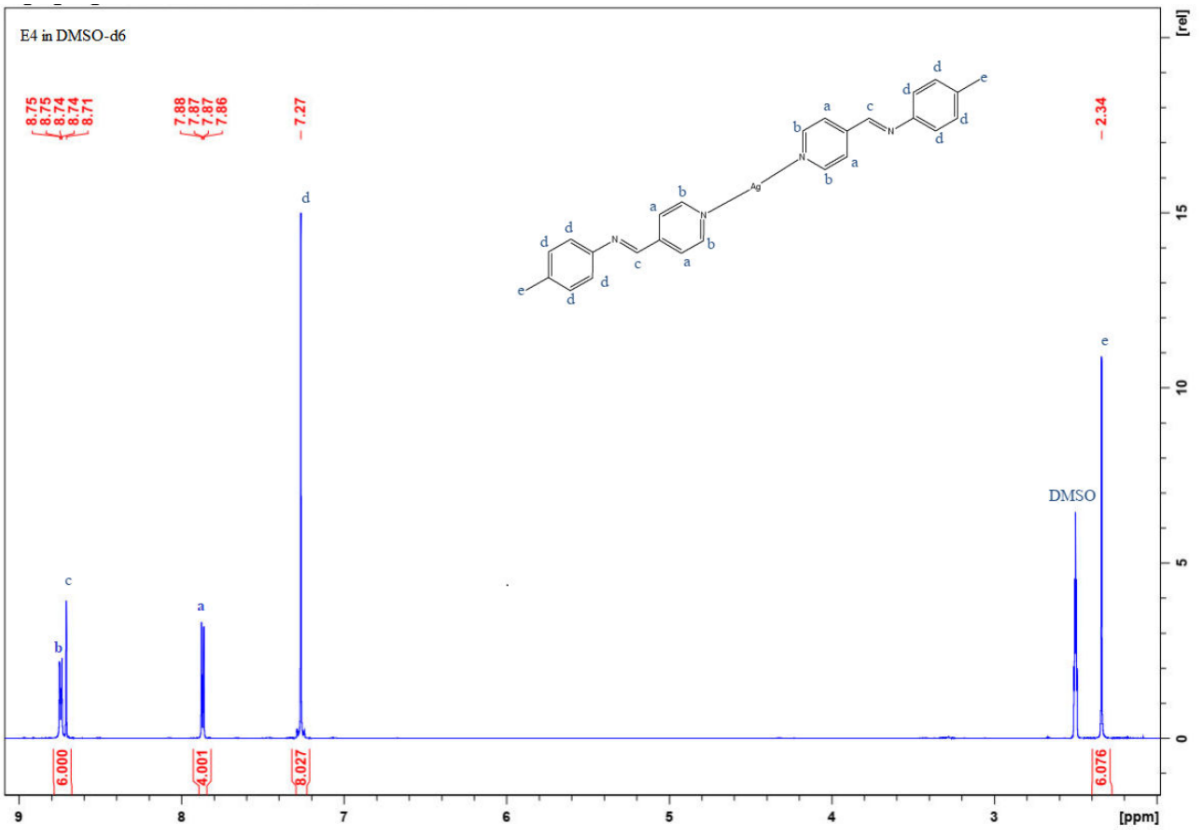

Figure S71: $[Ag(E_d)_2]NO_3$ 4

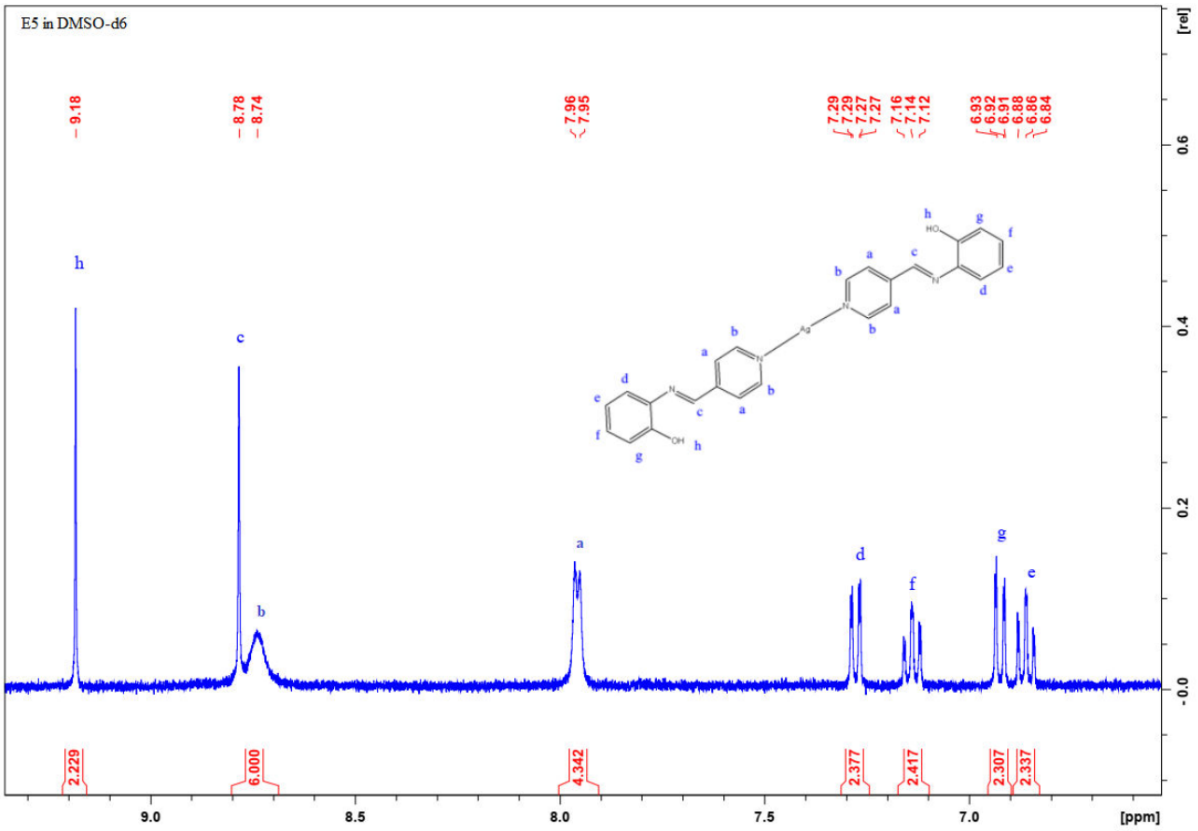

Figure S72: $[Ag(E_a)_2]ClO_4$ 5

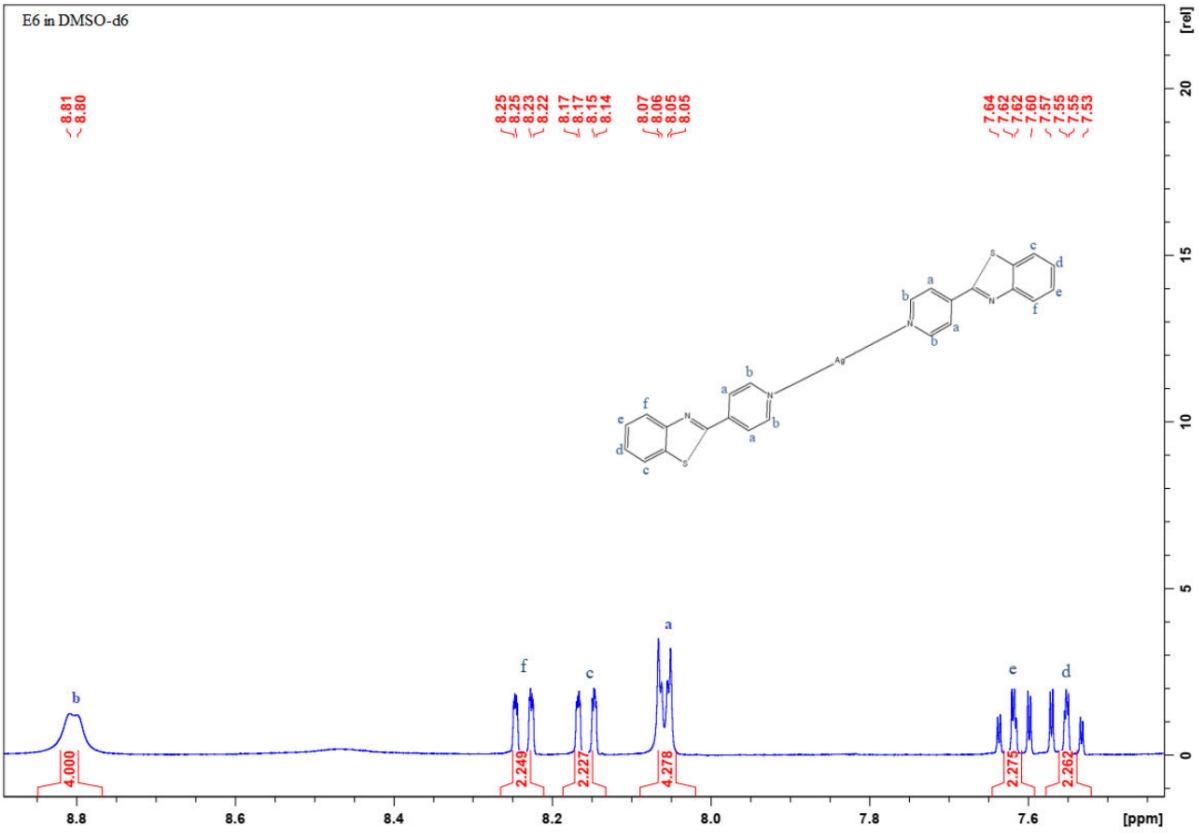

Figure S73: $[Ag(E_b)_2]ClO_4$ 6

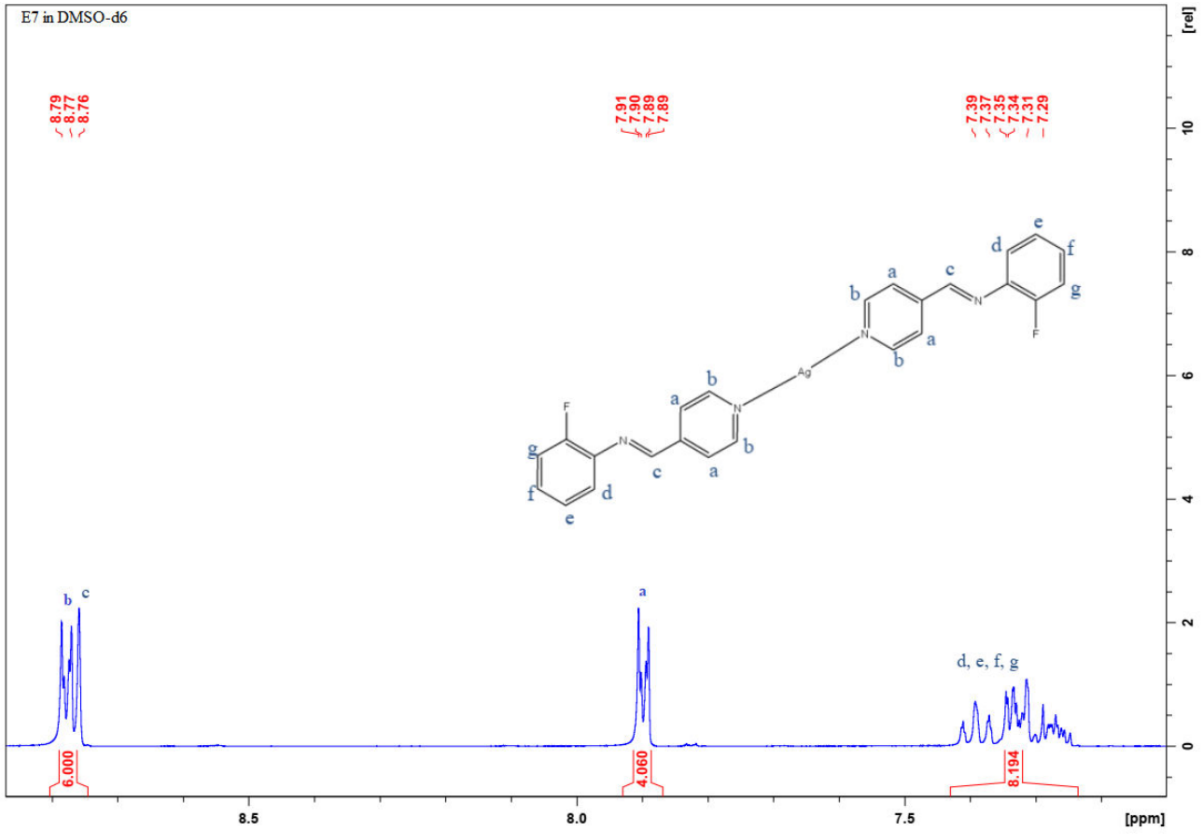

Figure S74: $[Ag(E_c)_2]ClO_4$ 7

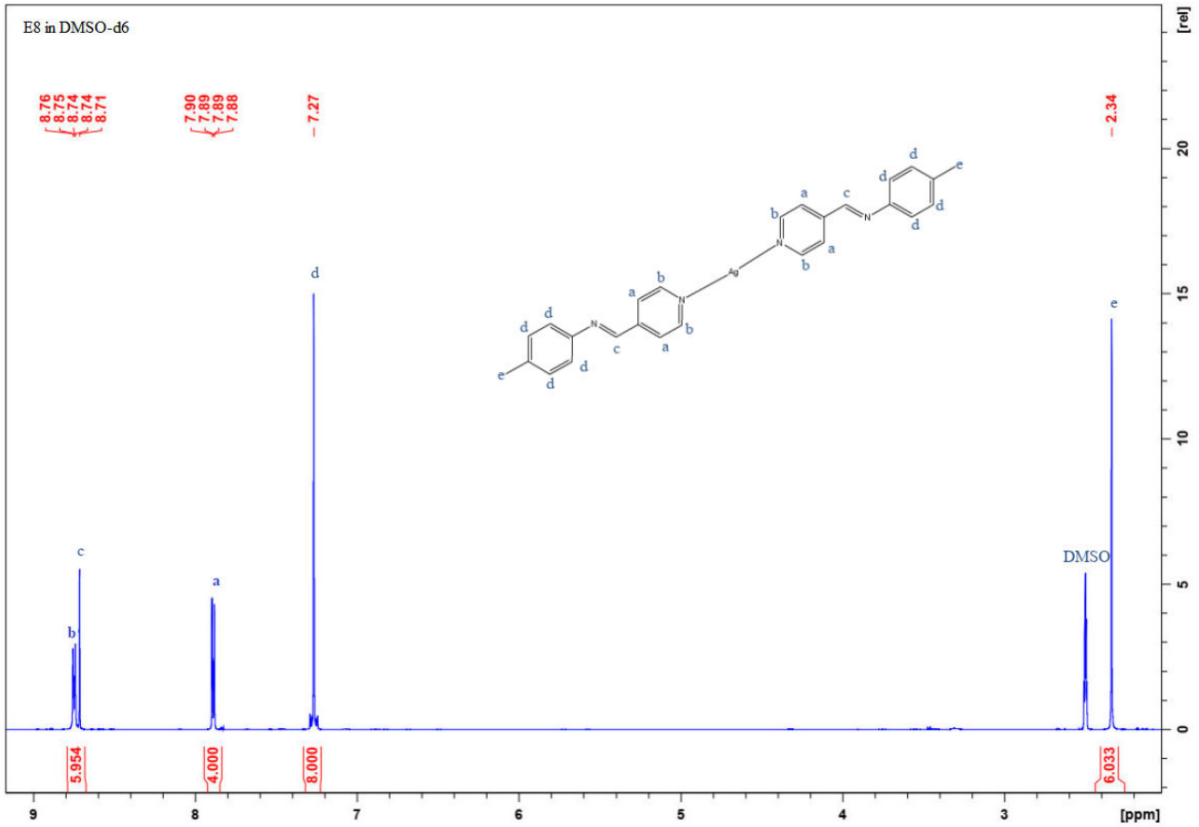

Figure S75: $[Ag(E_d)_2]ClO_4$ 8

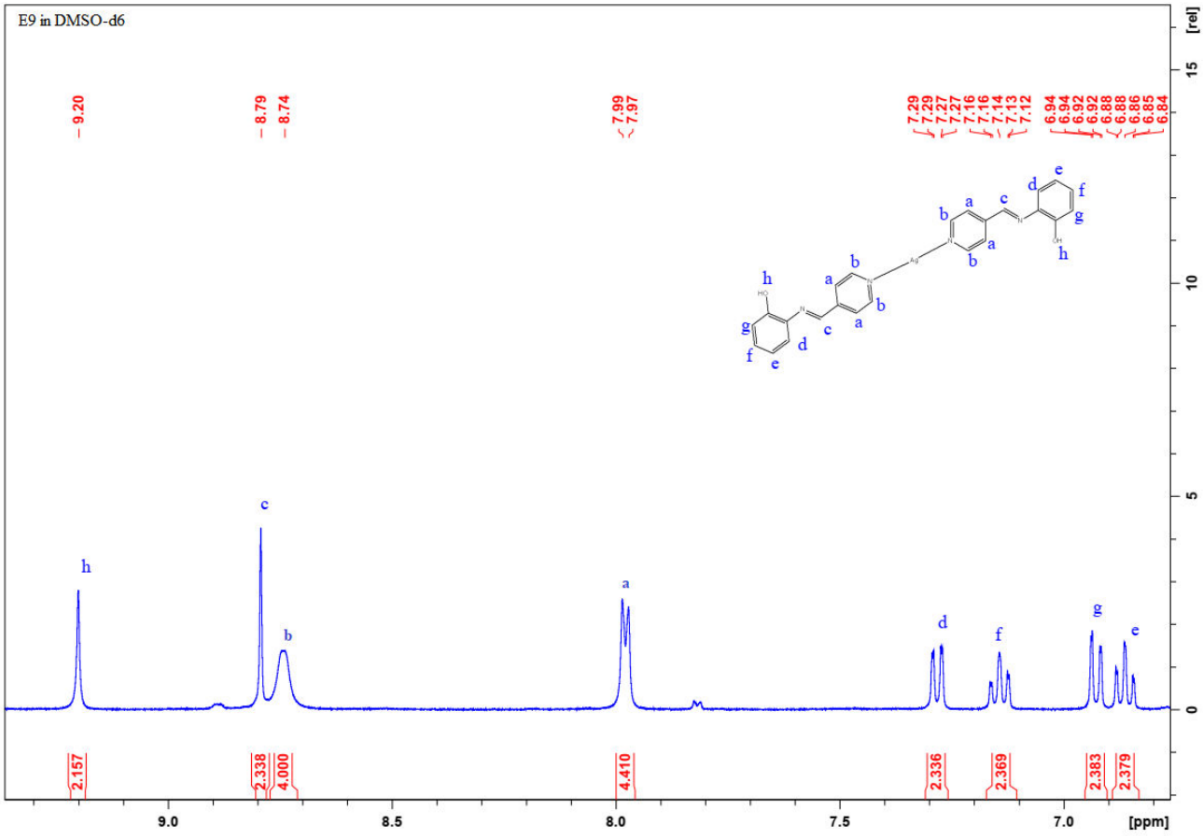

Figure S76: $[Ag(E_a)_2]CF_3SO_3$ 9

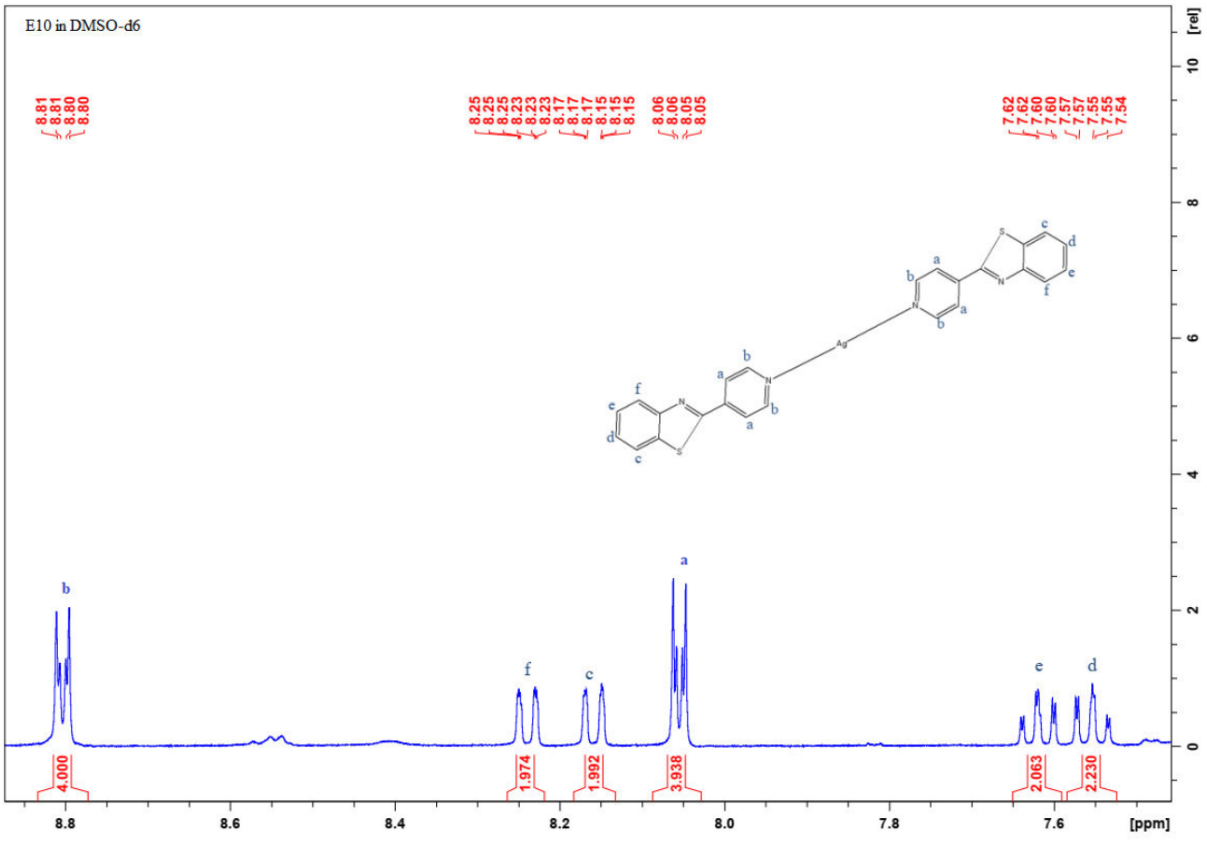

Figure S77: $[Ag(E_b)_2]CF_3SO_3$ 10

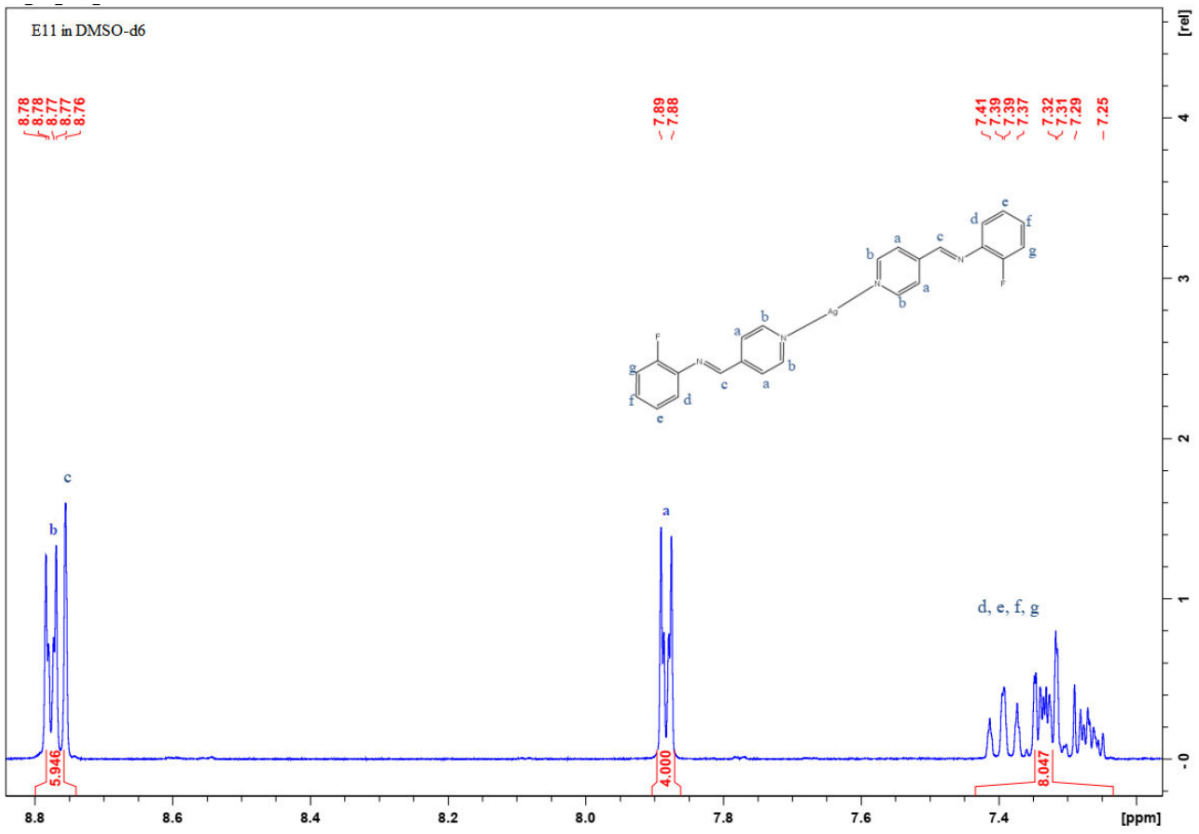

Figure S78: $[Ag(E_c)_2]CF_3SO_3$ 11

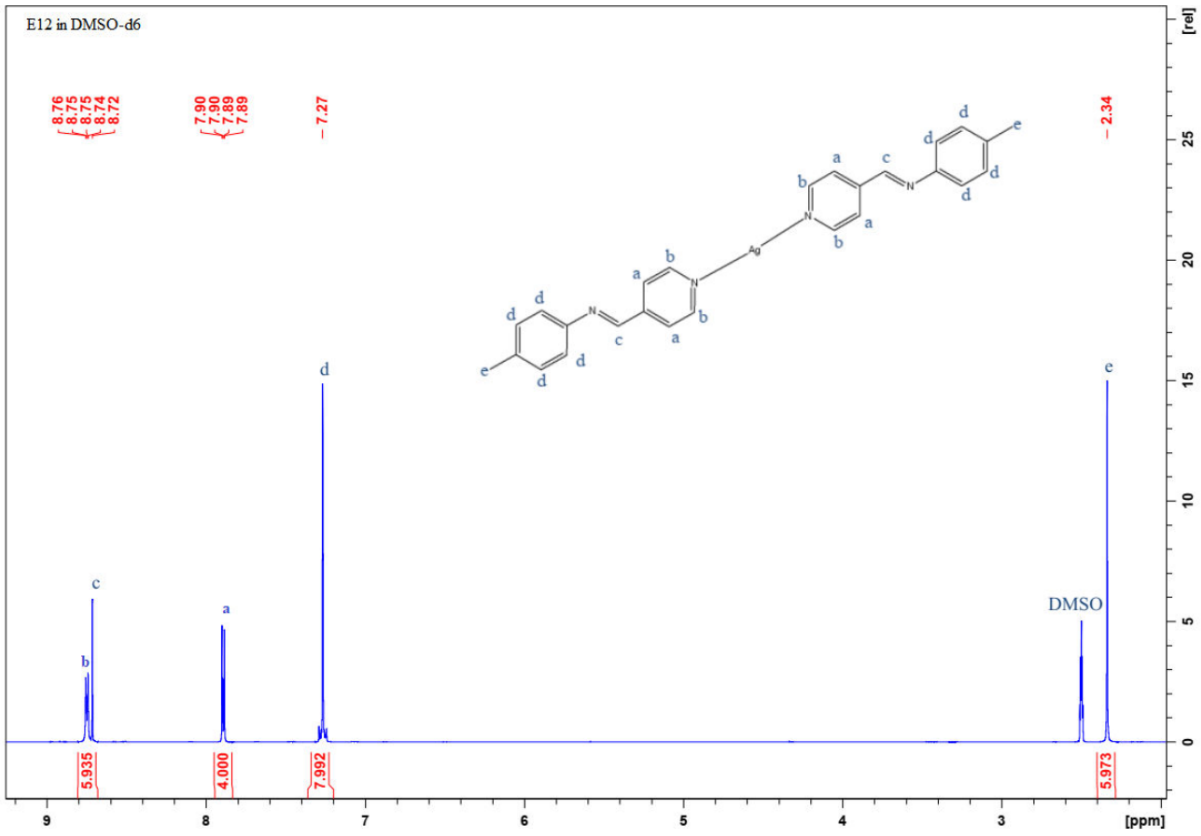

Figure S79: $[Ag(E_d)_2]CF_3SO_3$ 12

^{1}H NMR spectra of the complexes **1**, **6**, **7** and **12** between 0-48 h

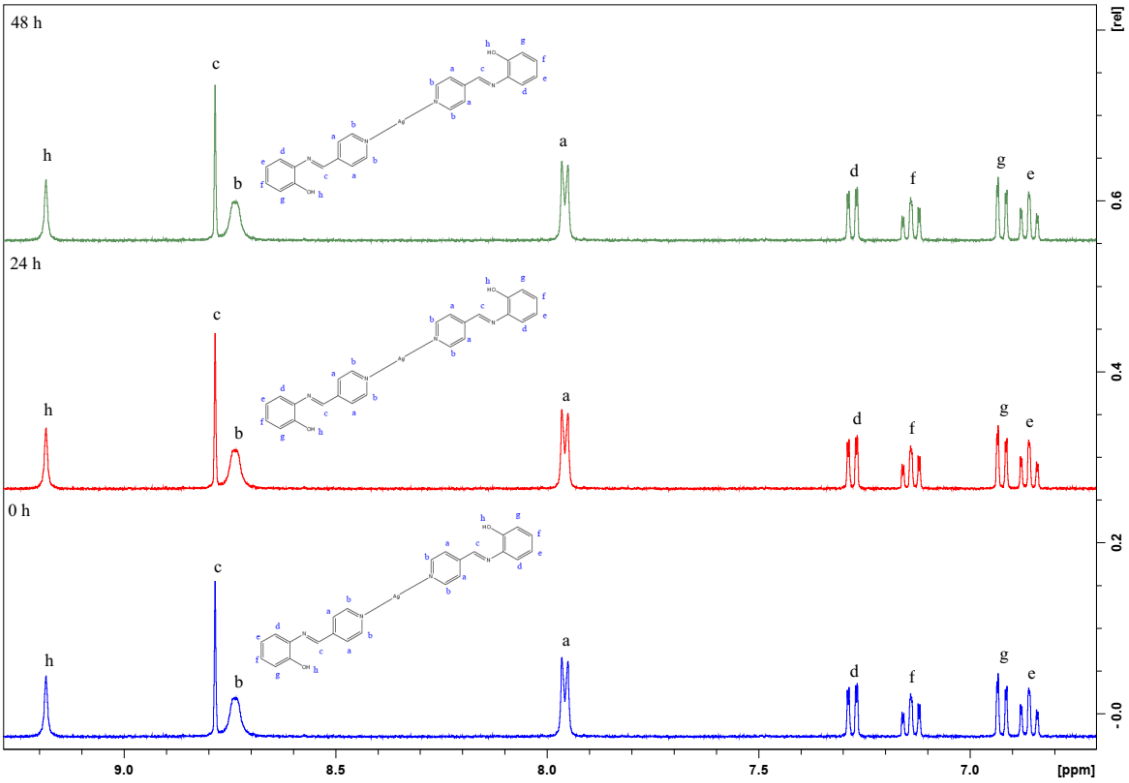

Figure S80: Time dependent ^{1}H NMR spectra of $[Ag(E_a)_2]NO_3$ 1

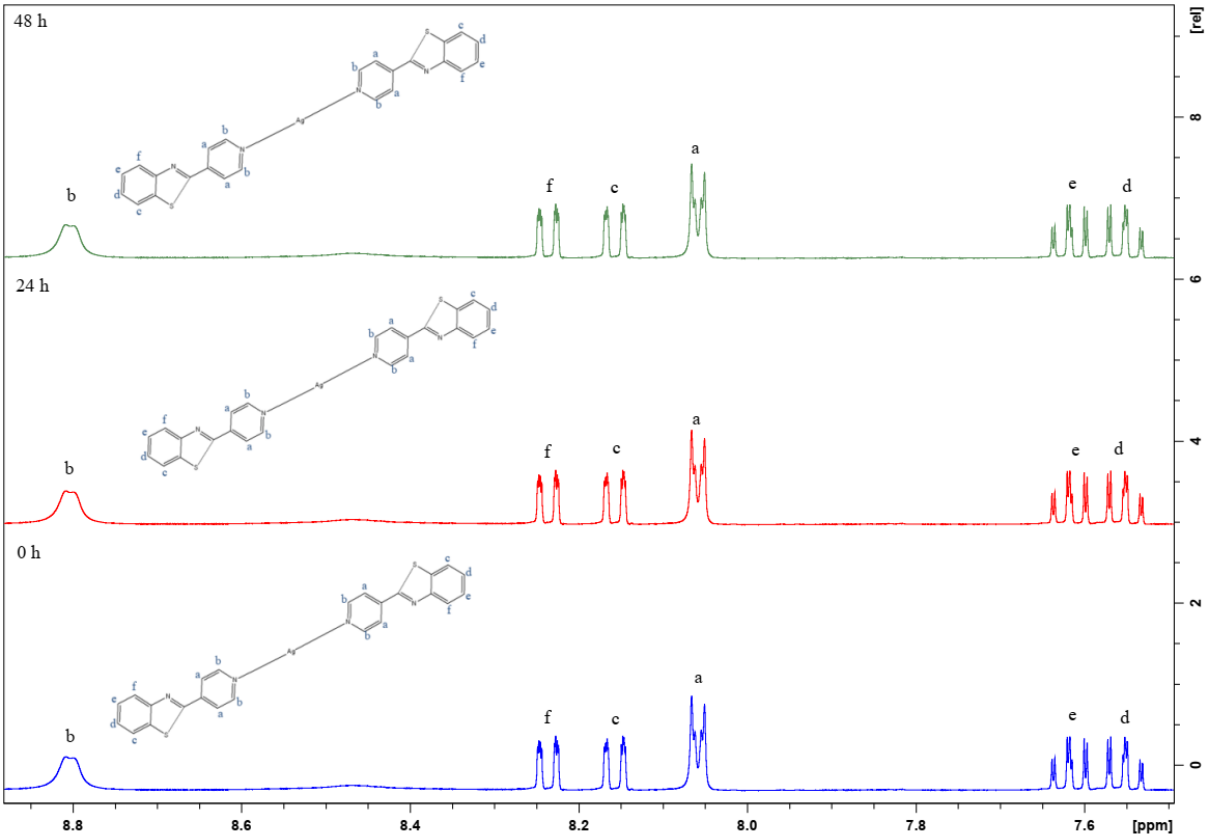

Figure S81: **Time dependent ^{1}H NMR spectra of *$[Ag(E_b)_2]ClO_4$* 6**

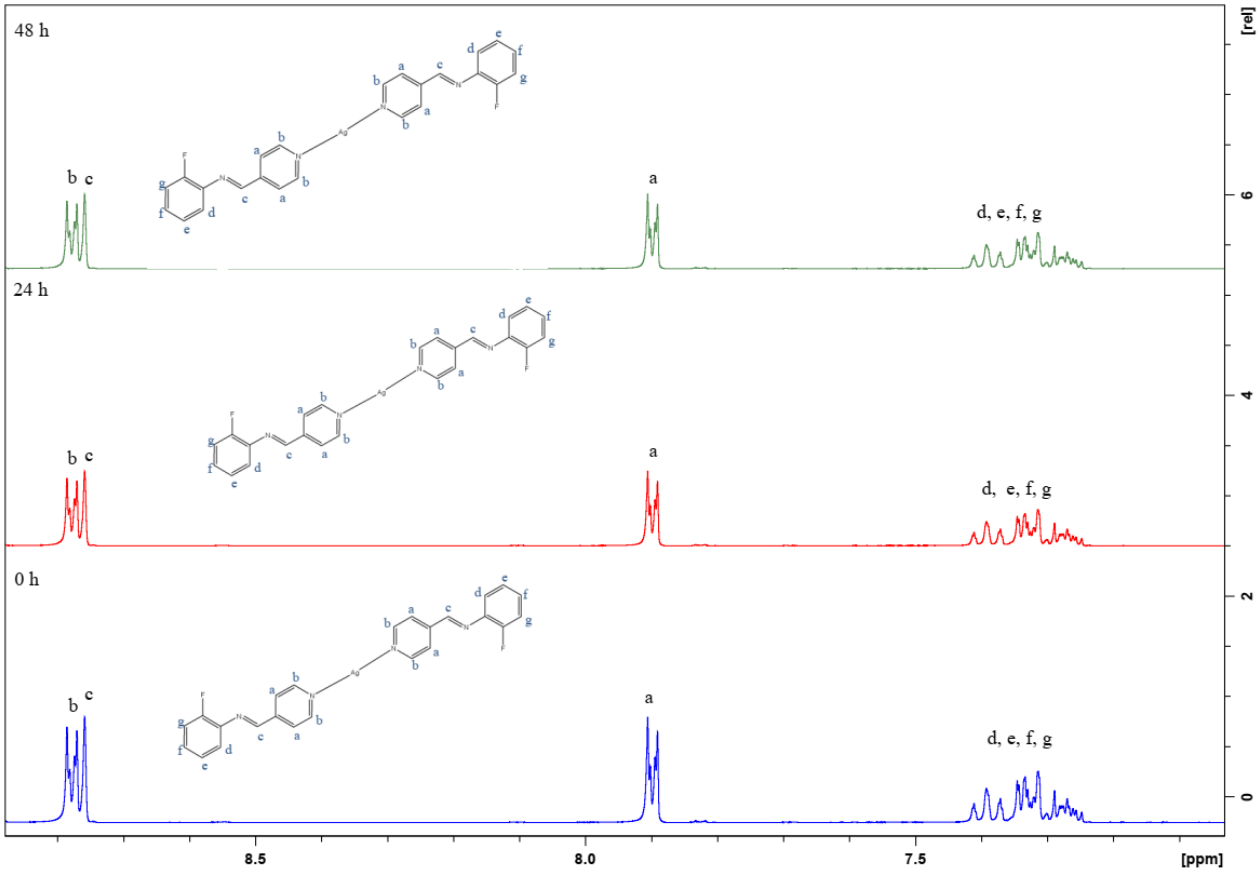

Figure S82: **Time dependent ^{1}H NMR spectra of $[Ag(E_c)_2]ClO_4$ 7**

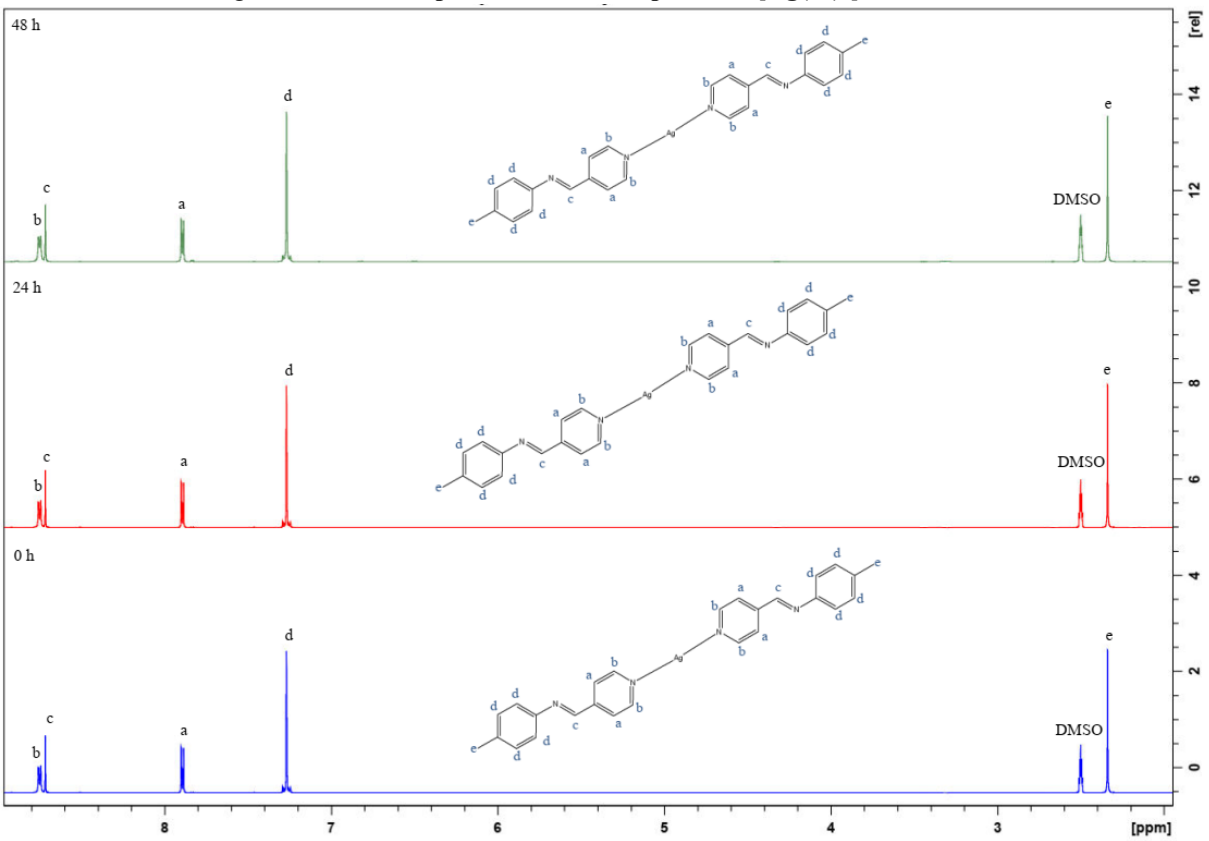

Figure S83: Time dependent ^{1}H NMR spectra of $[Ag(E_d)_2]CF_3SO_3$ 12

^{15}N-NMR SPECTRA OF E_{a-d}

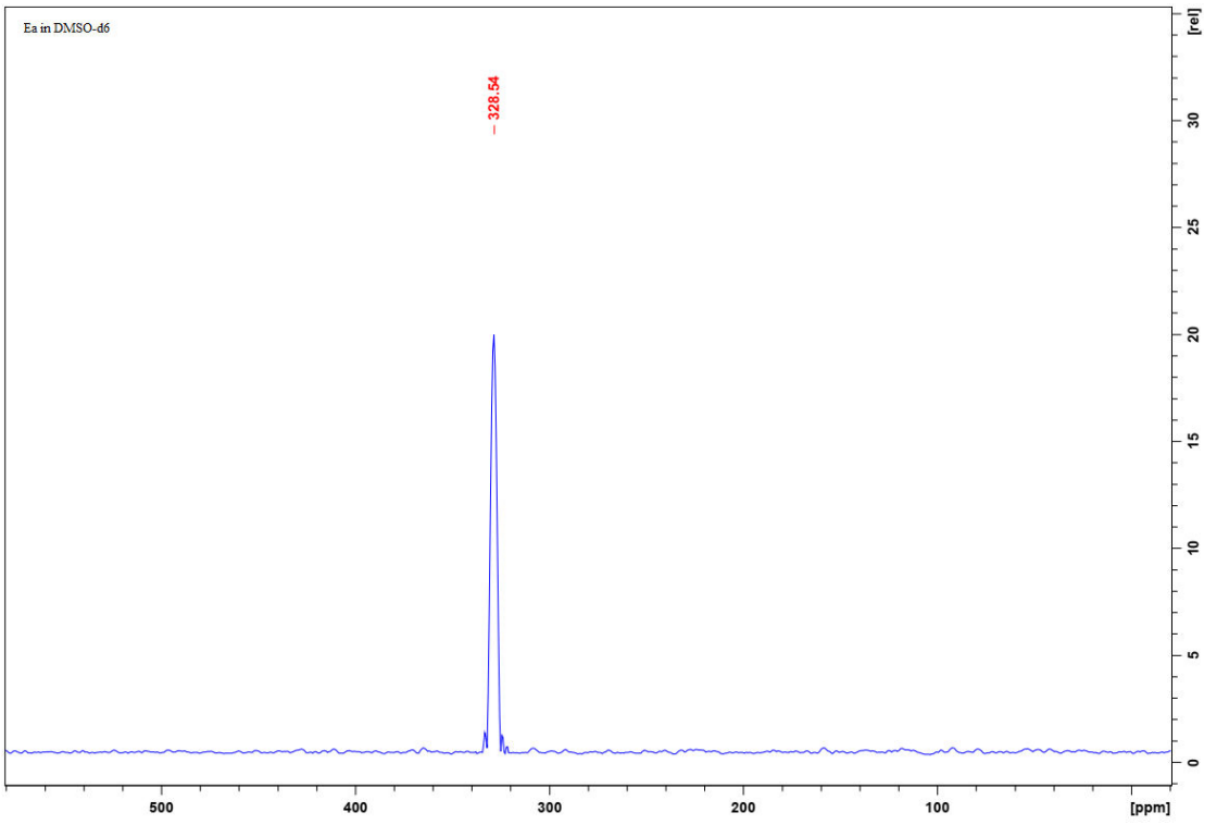

Figure S84: ^{15}N NMR spectrum of E)-2-((pyridin-4-ylmethylene)amino)phenol E_a

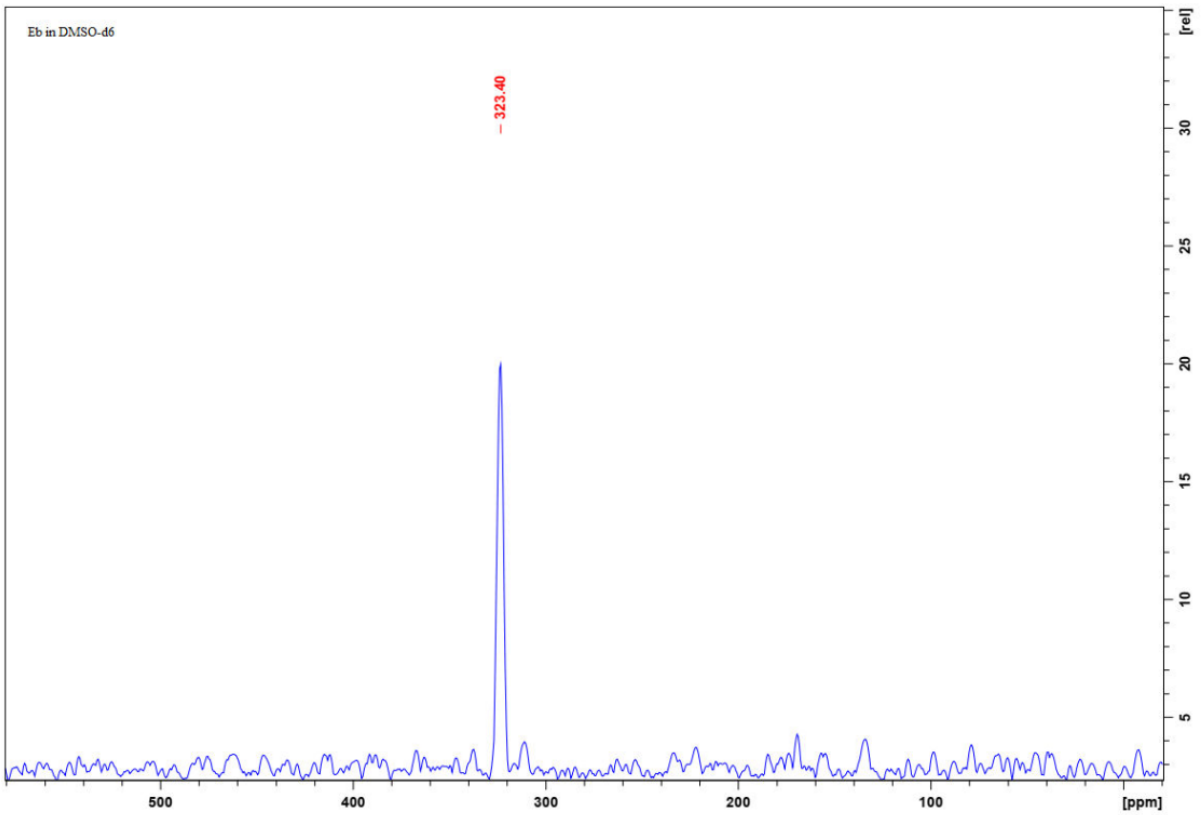

Figure S85: ^{15}N NMR spectrum of 2-(pyridin-4-yl)benzo[*d*]thiazole E_b

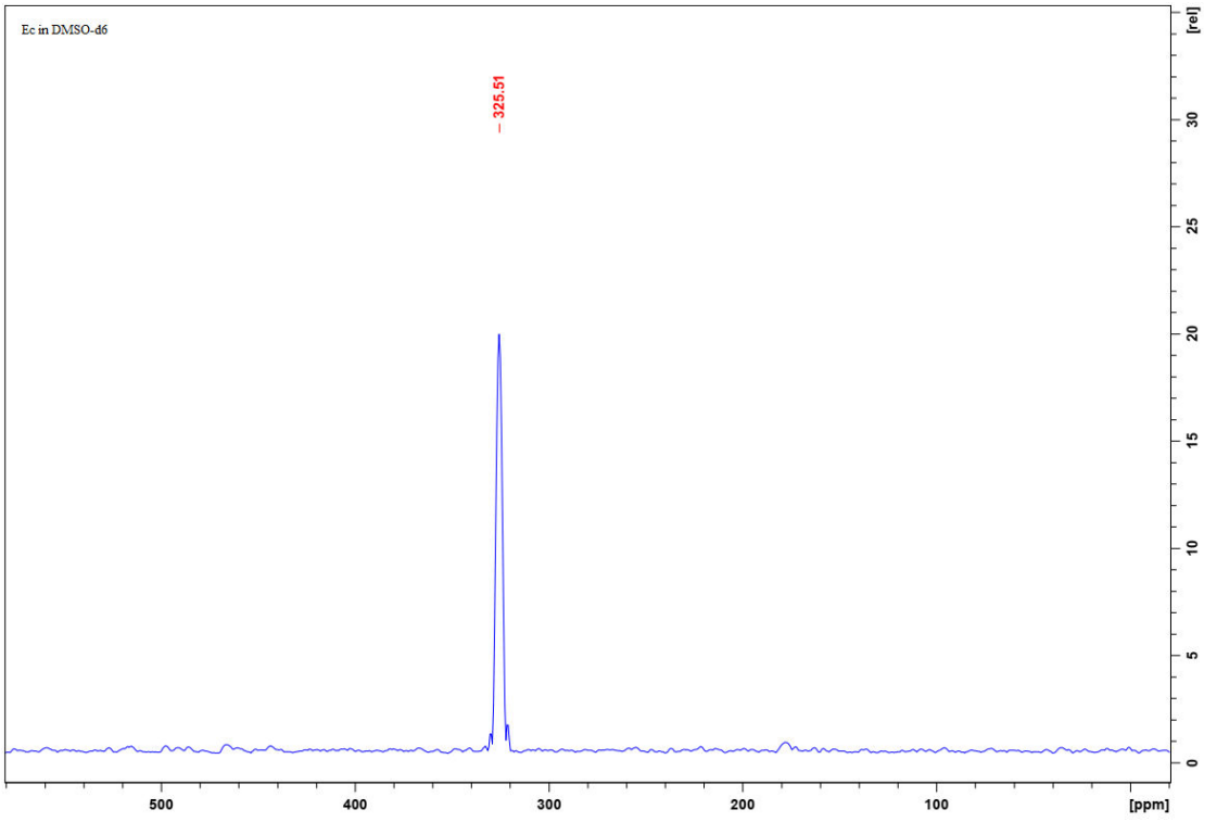

Figure S86: ^{15}N NMR spectrum of (E)-N-(2-fluorophenyl)-1-(pyridin-4-yl)methanimine E_c

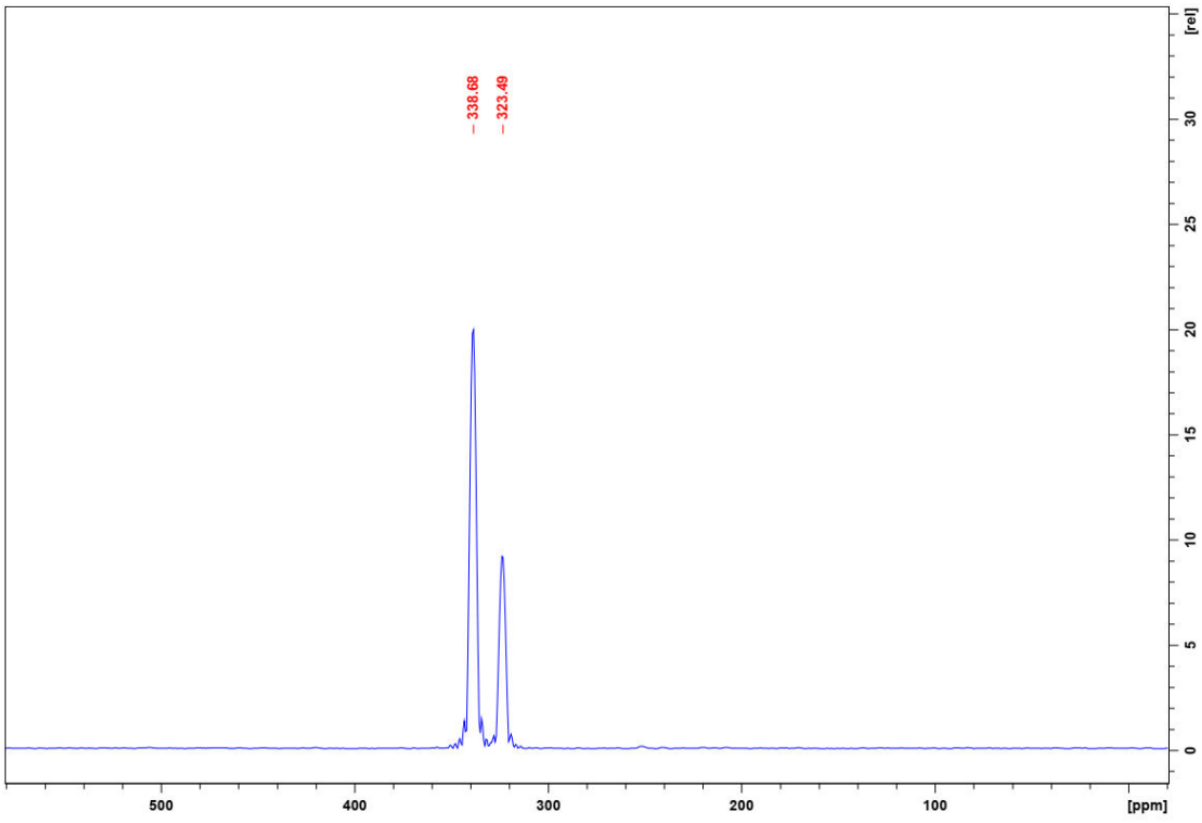

Figure S87: ^{15}N NMR spectrum of (E)-1-(pyridin-4-yl)-N-(p-tolyl)methanimine E_d

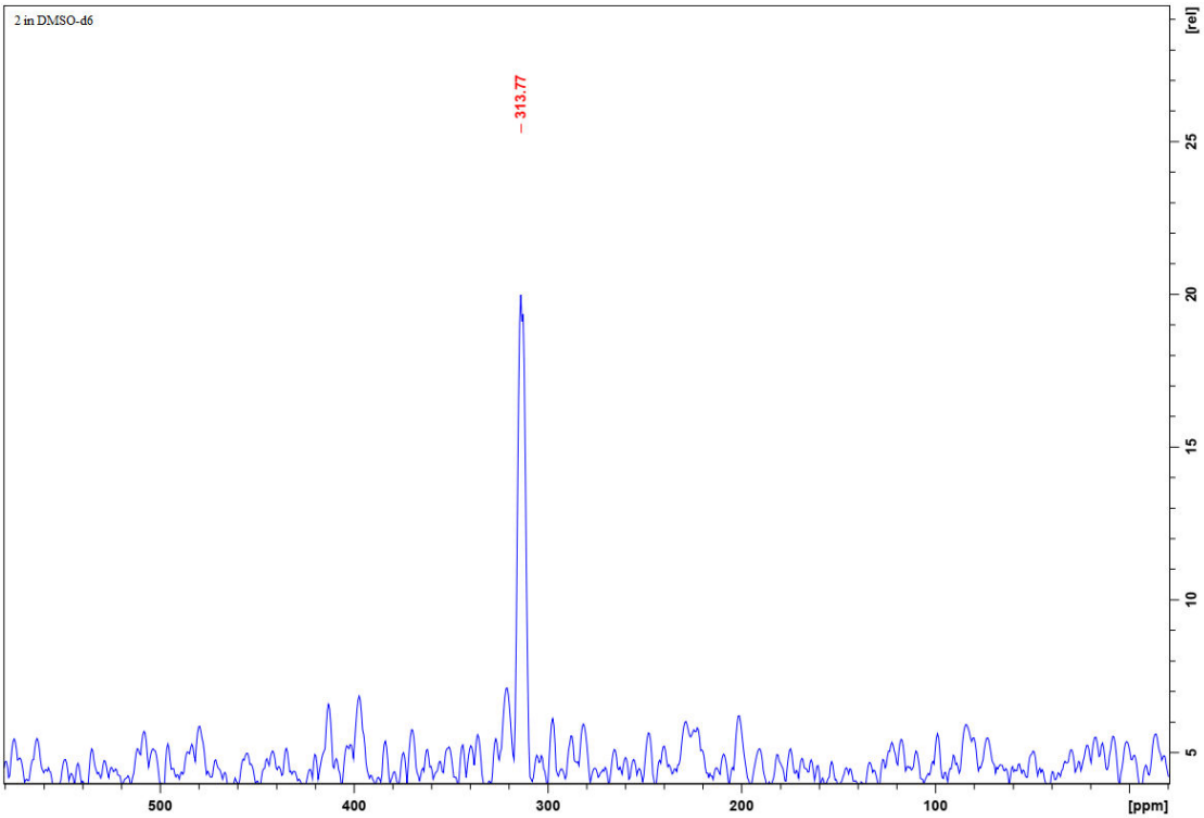

Figure S88: ^{15}N NMR spectrum of $[Ag(E_b)_2]NO_3$ 2

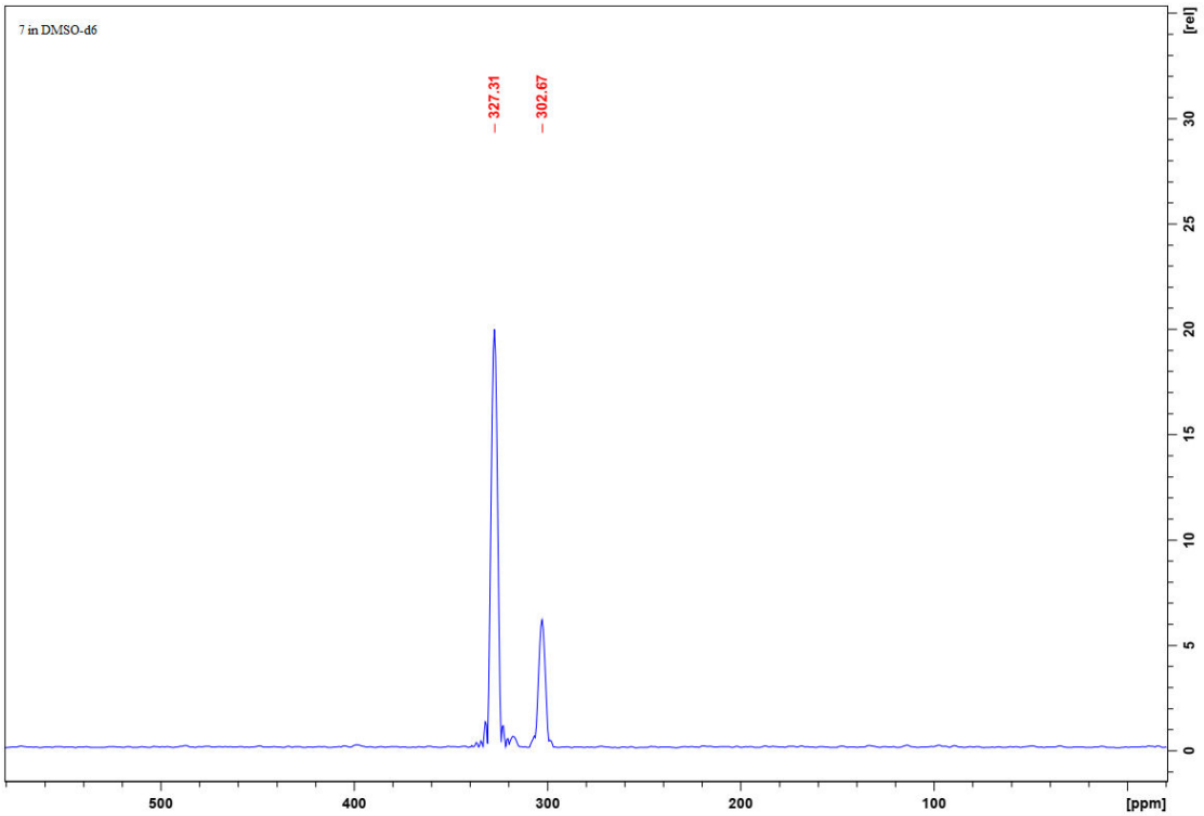

Figure S89: ^{15}N NMR spectrum of $[Ag(E_c)_2]ClO_4$ 7

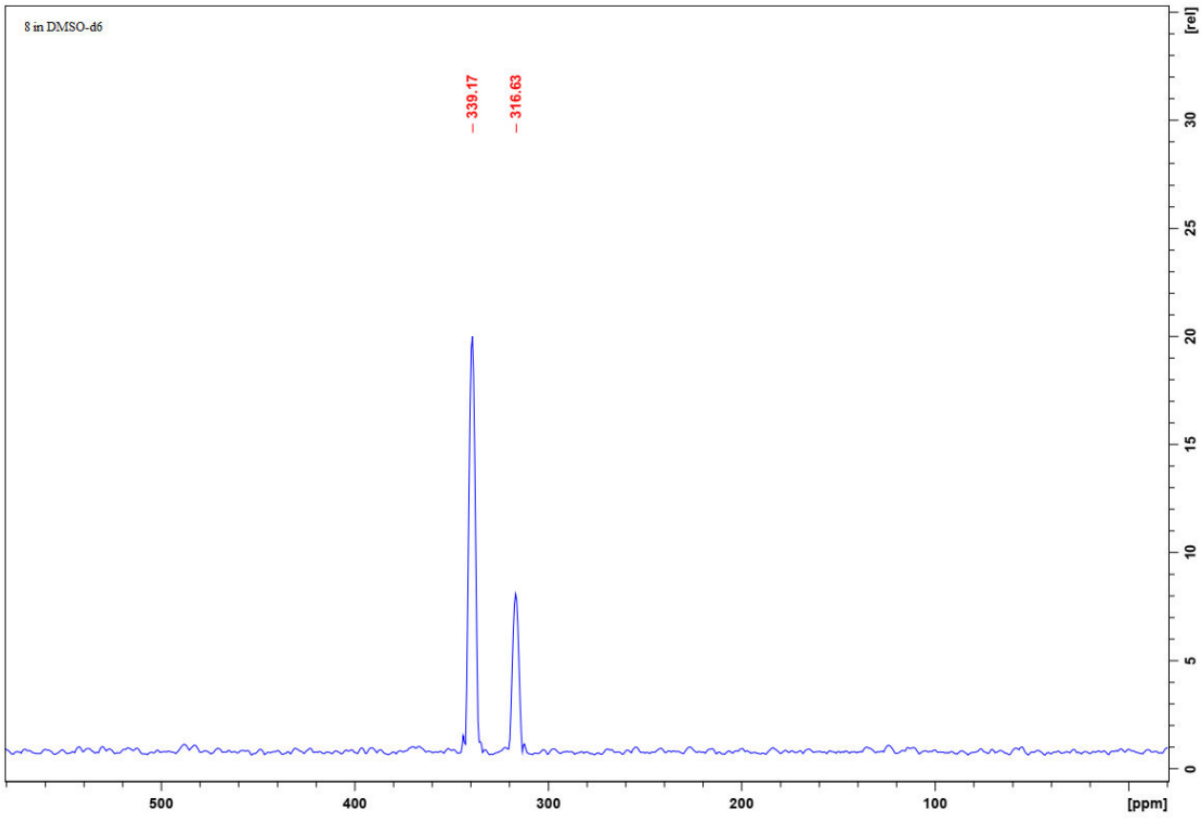

Figure S90: ^{15}N NMR spectrum of $[Ag(E_d)_2]ClO_4$ 8

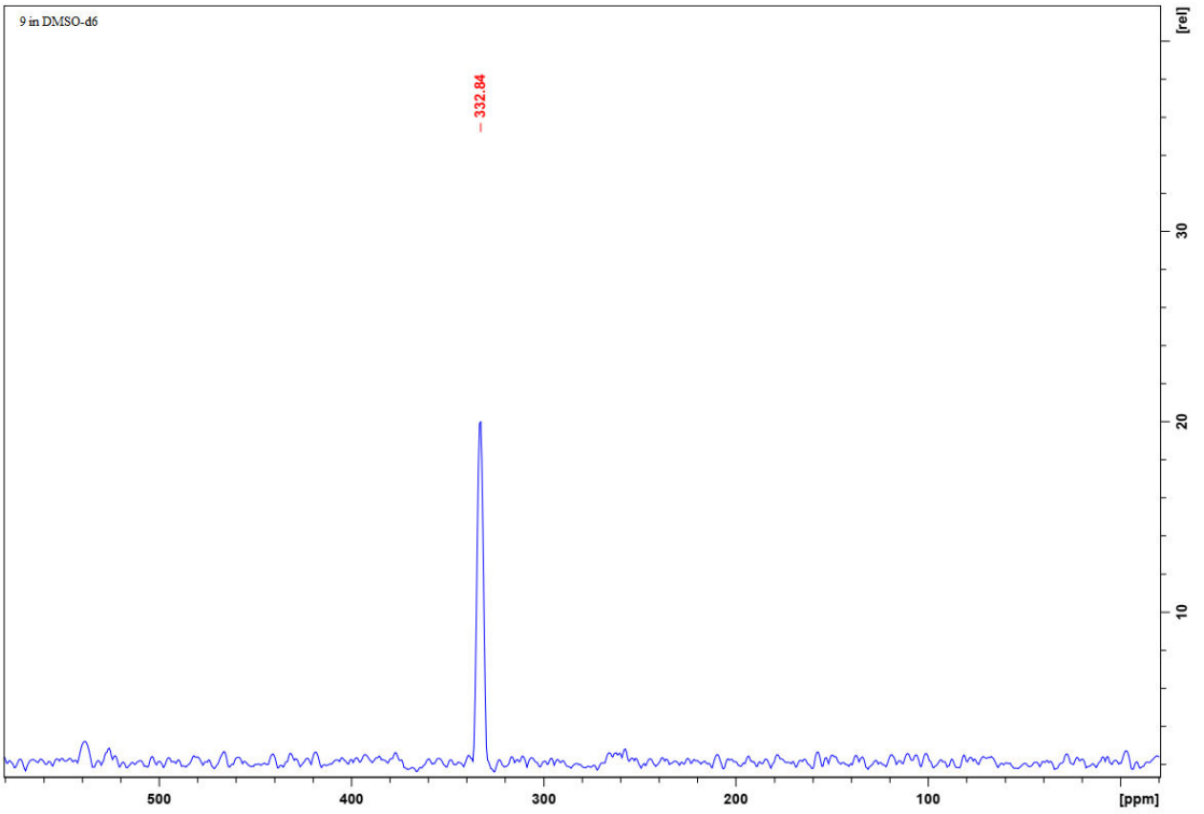

Figure S91: ^{15}N NMR spectrum of $[Ag(E_a)_2]CF_3SO_3$ 9

^{13}C-NMR SPECTRA OF E_{a-d}

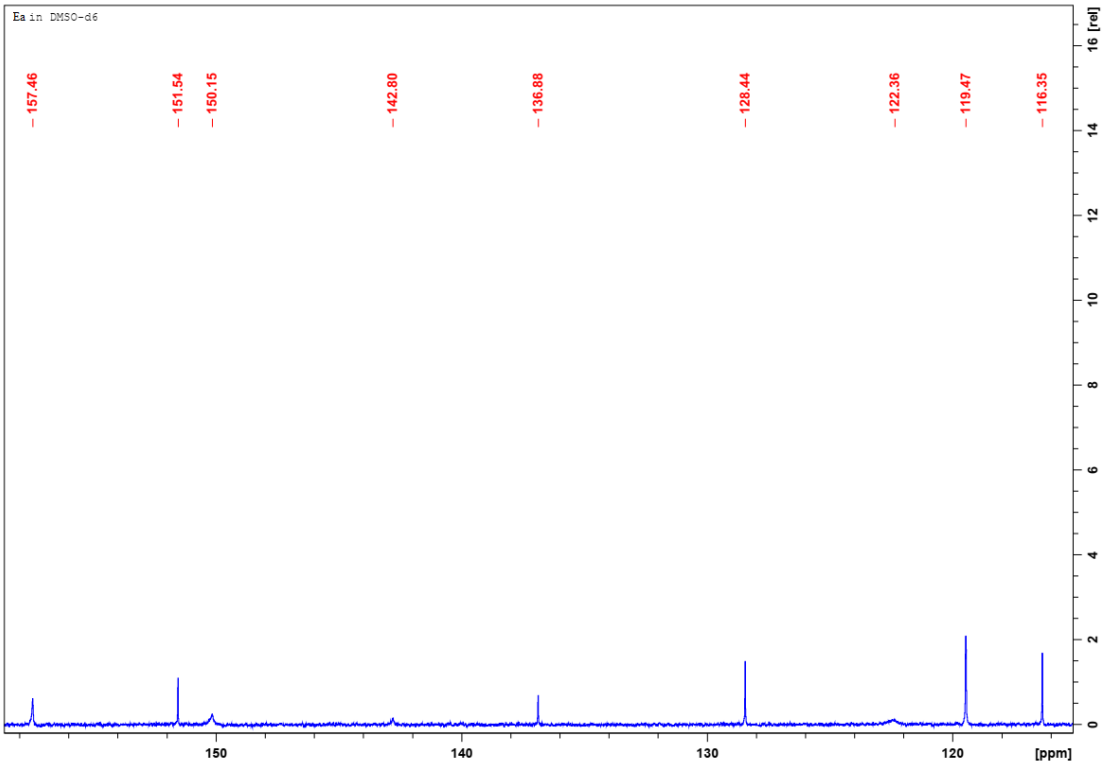

Figure S92: E)-2-((pyridin-4-ylmethylene)amino)phenol E_a

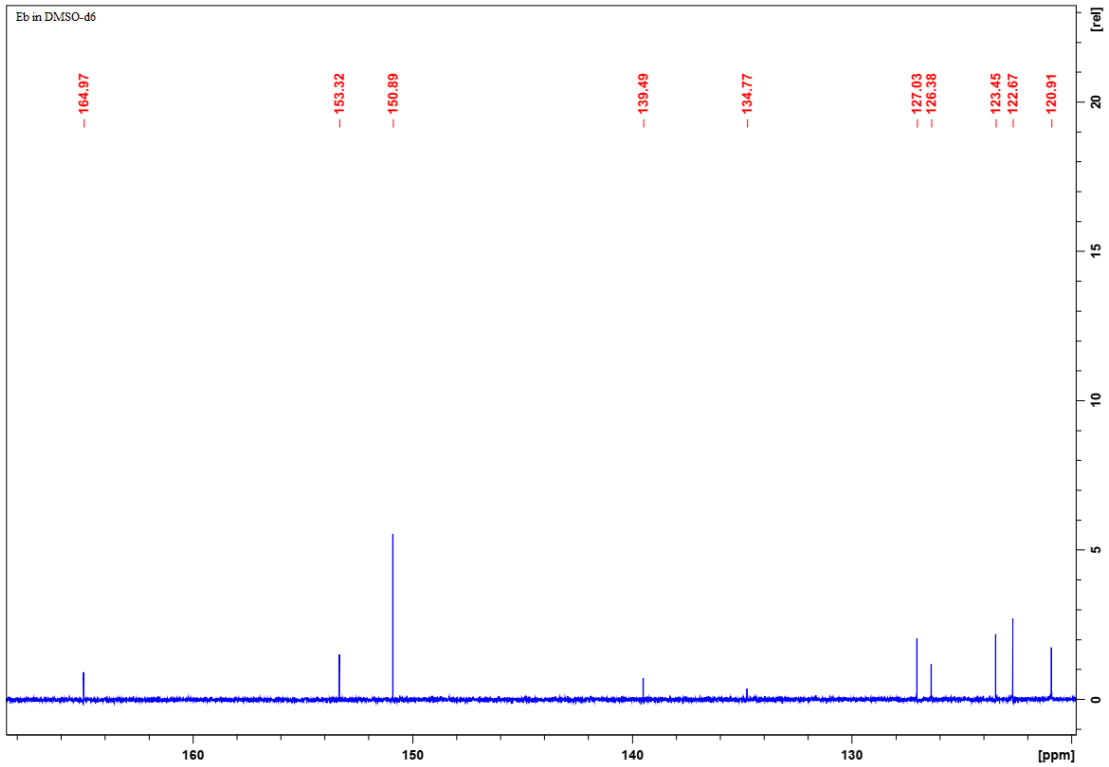

Figure S93: 2-(pyridin-4-yl)benzo[*d*]thiazole E_b

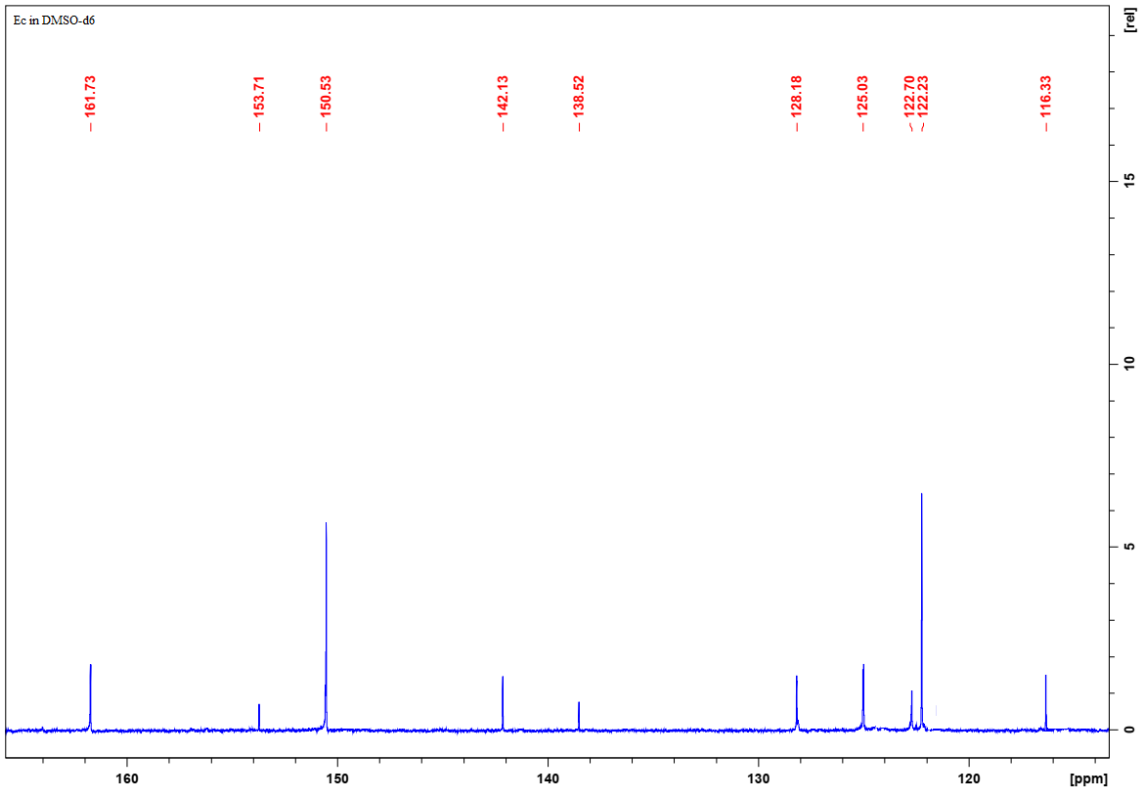

Figure S94: (E)-N-(2-fluorophenyl)-1-(pyridin-4-yl)methanimine E_c

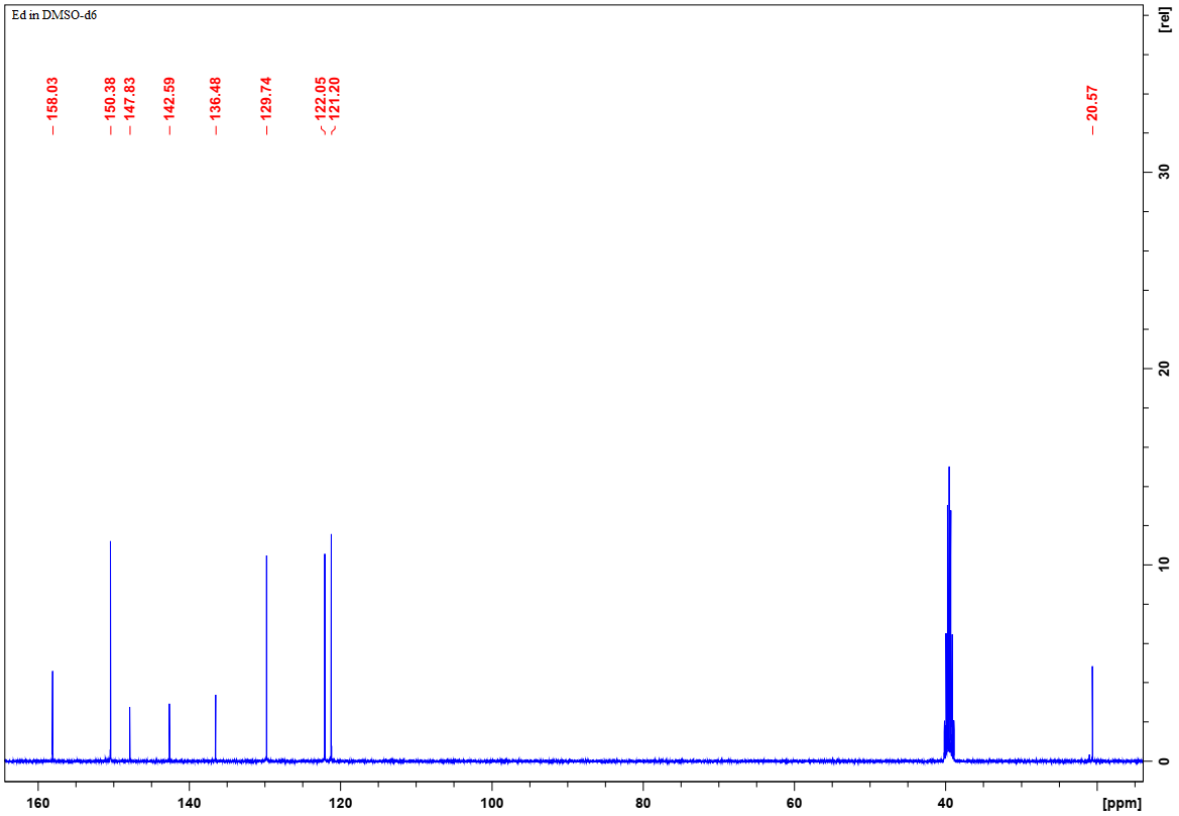

Figure S95: (E)-1-(pyridin-4-yl)-N-(p-tolyl)methanimine E_d

^{13}C-NMR SPECTRA OF COMPLEXES 1-12

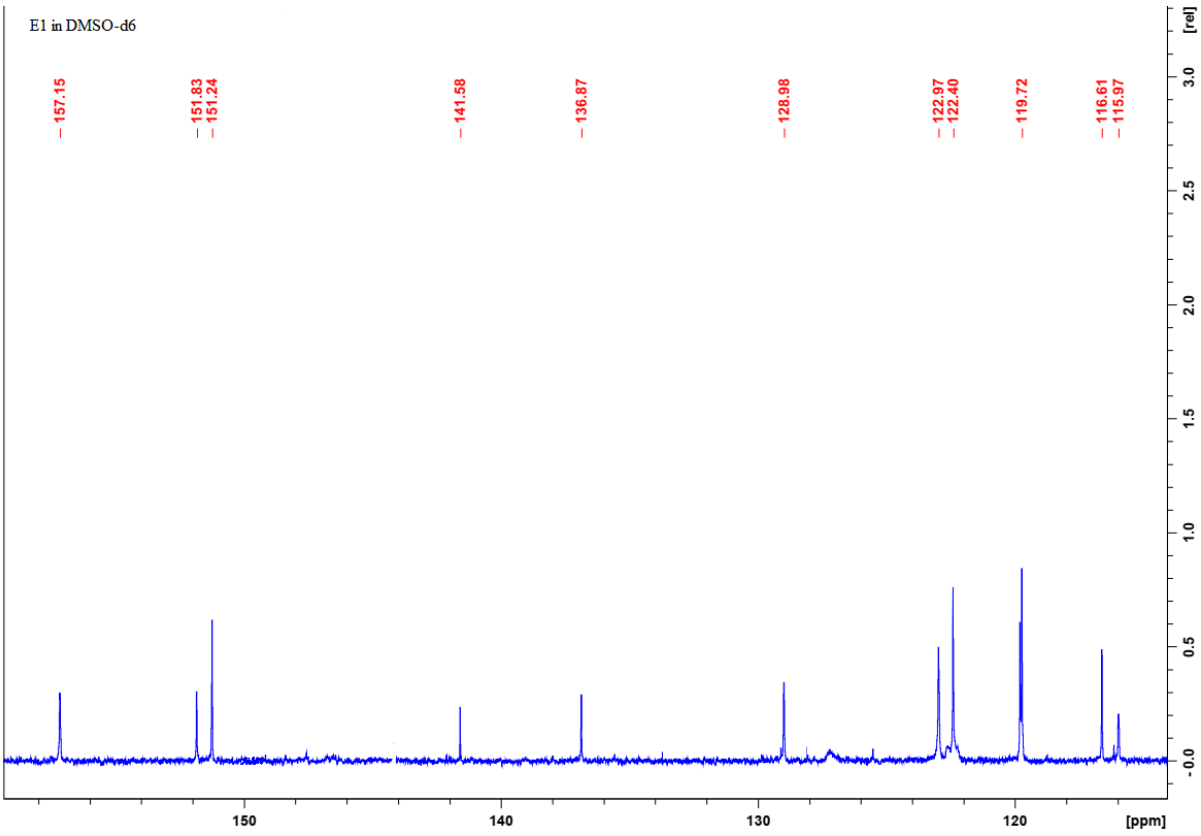

Figure S96: $[Ag(E_a)_2]NO_3$ 1

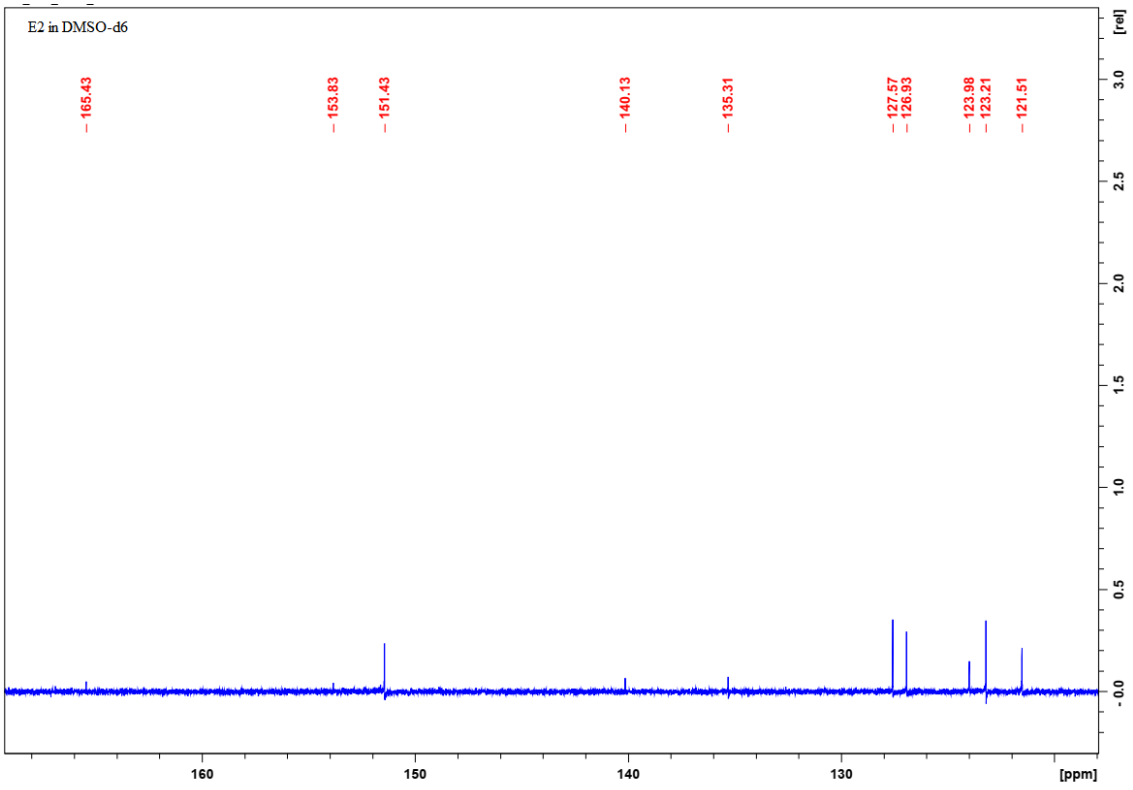

Figure S97: $[Ag(E_b)_2]NO_3$ 2

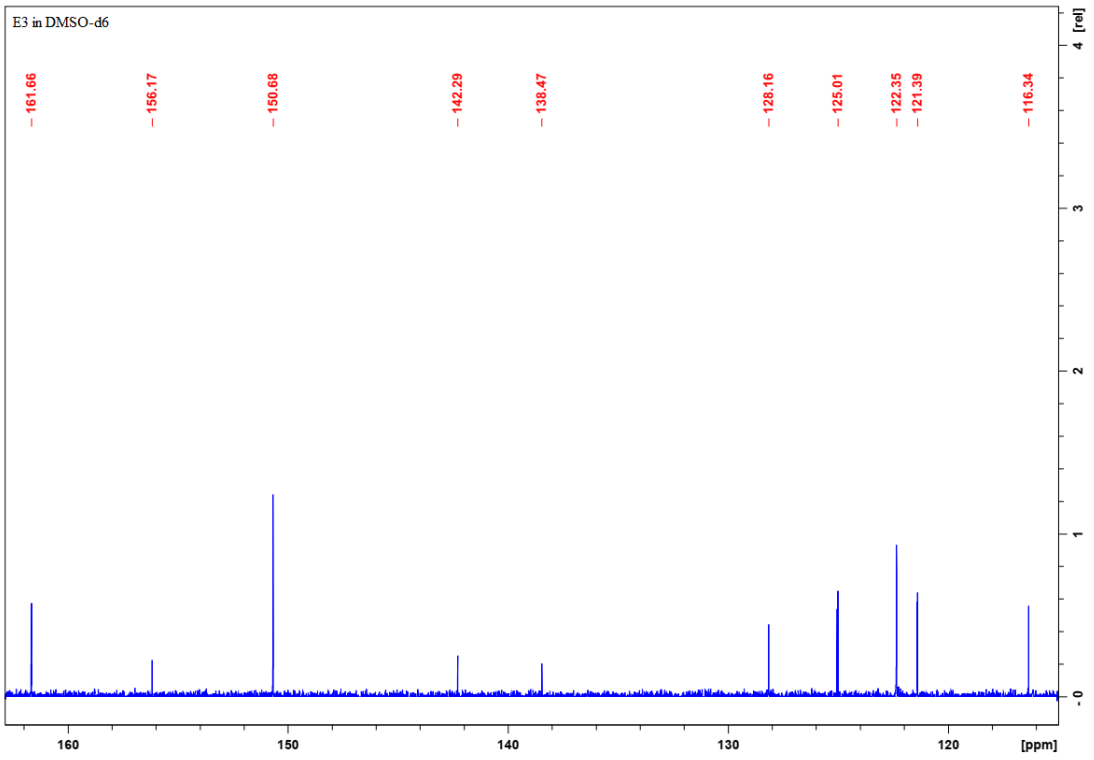

Figure S98: $[Ag(E_c)_2]NO_3$ 3

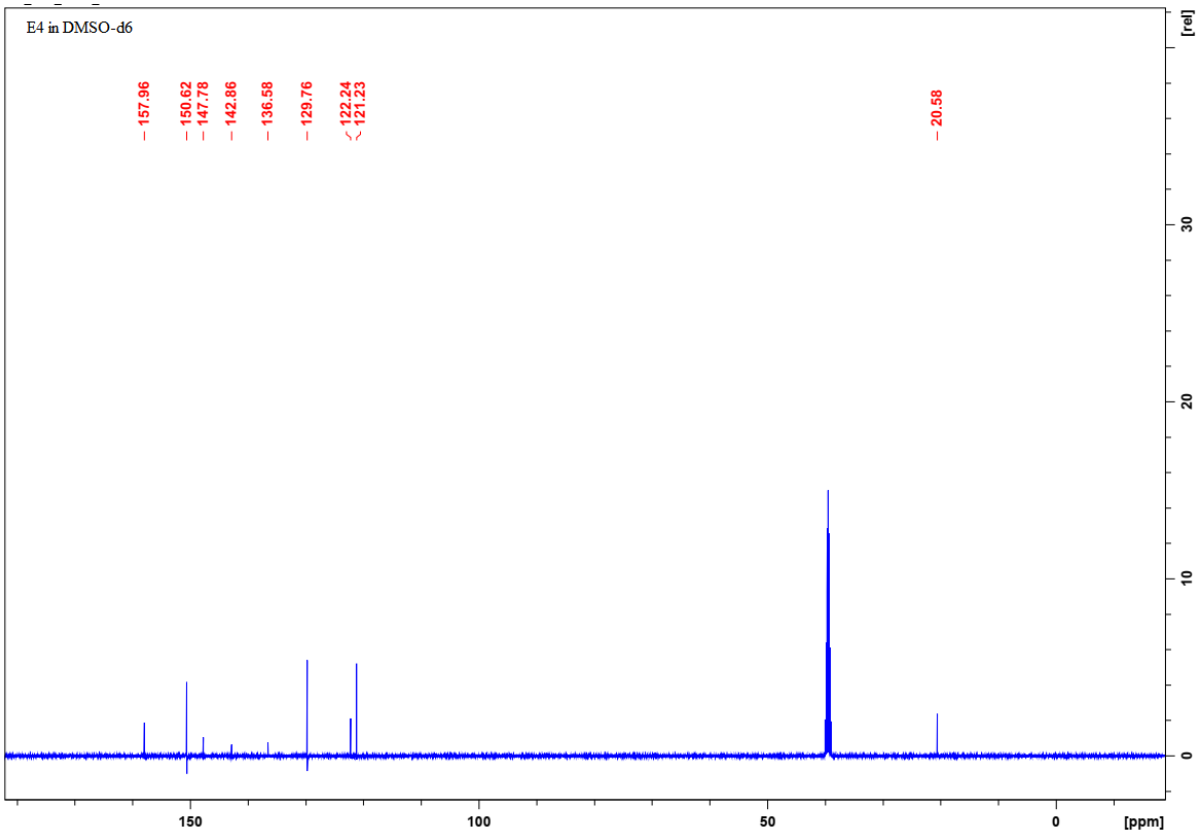

Figure S99: $[Ag(E_d)_2]NO_3$ 4

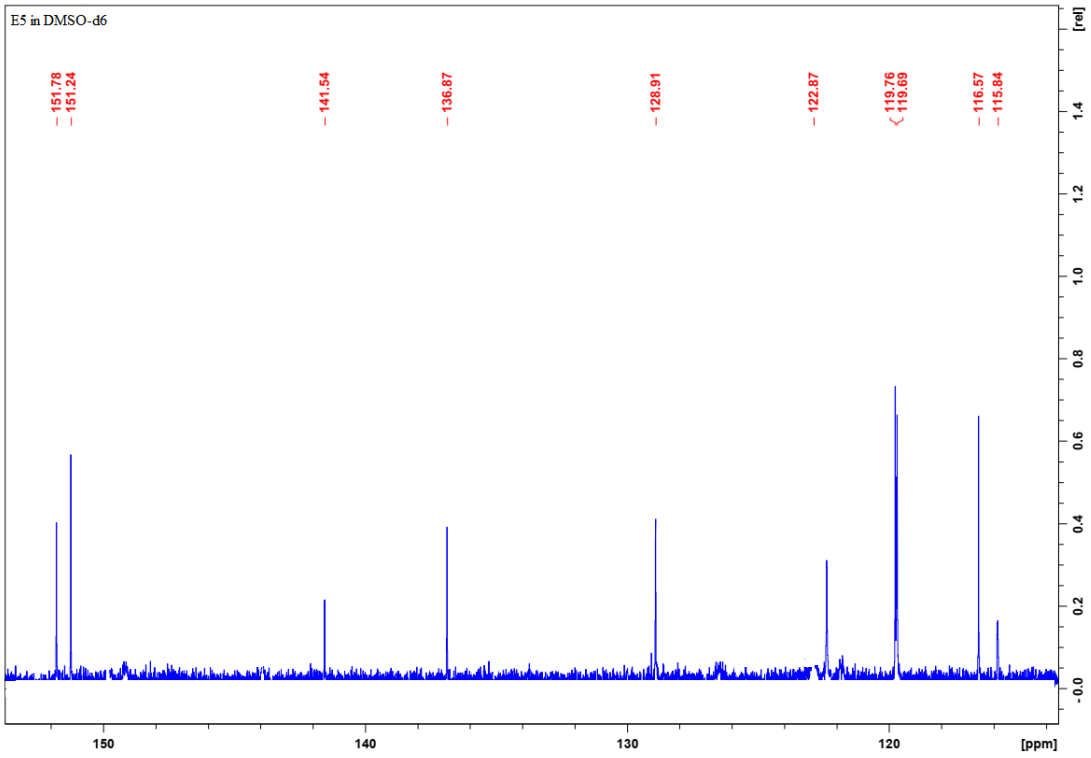

Figure S100: $[Ag(E_a)_2]ClO_4$ 5

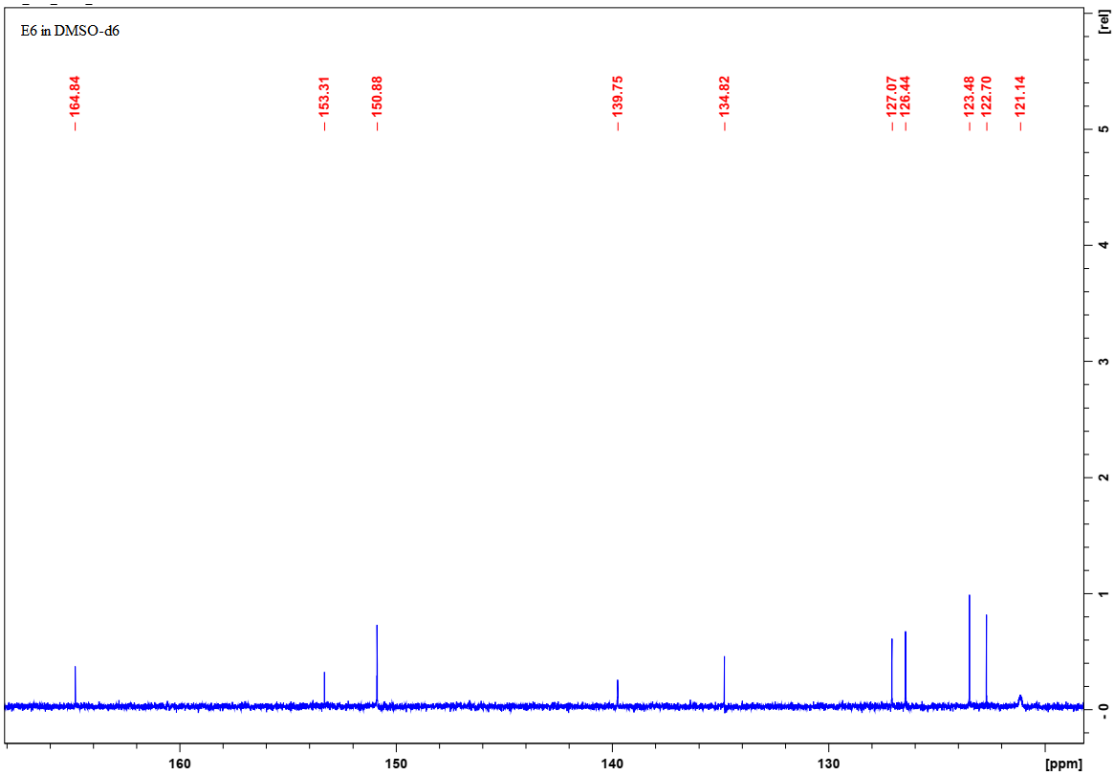

Figure S101: $[Ag(E_b)_2]ClO_4$ 6

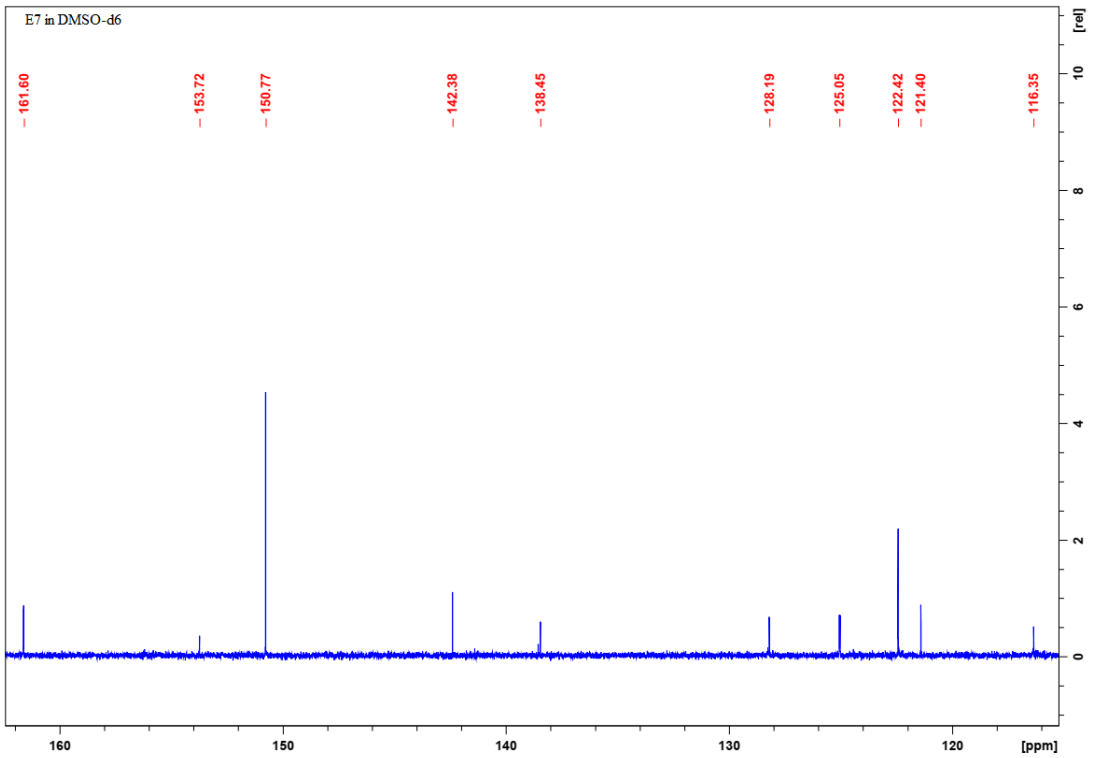

Figure S102: $[Ag(E_c)_2]ClO_4$ 7

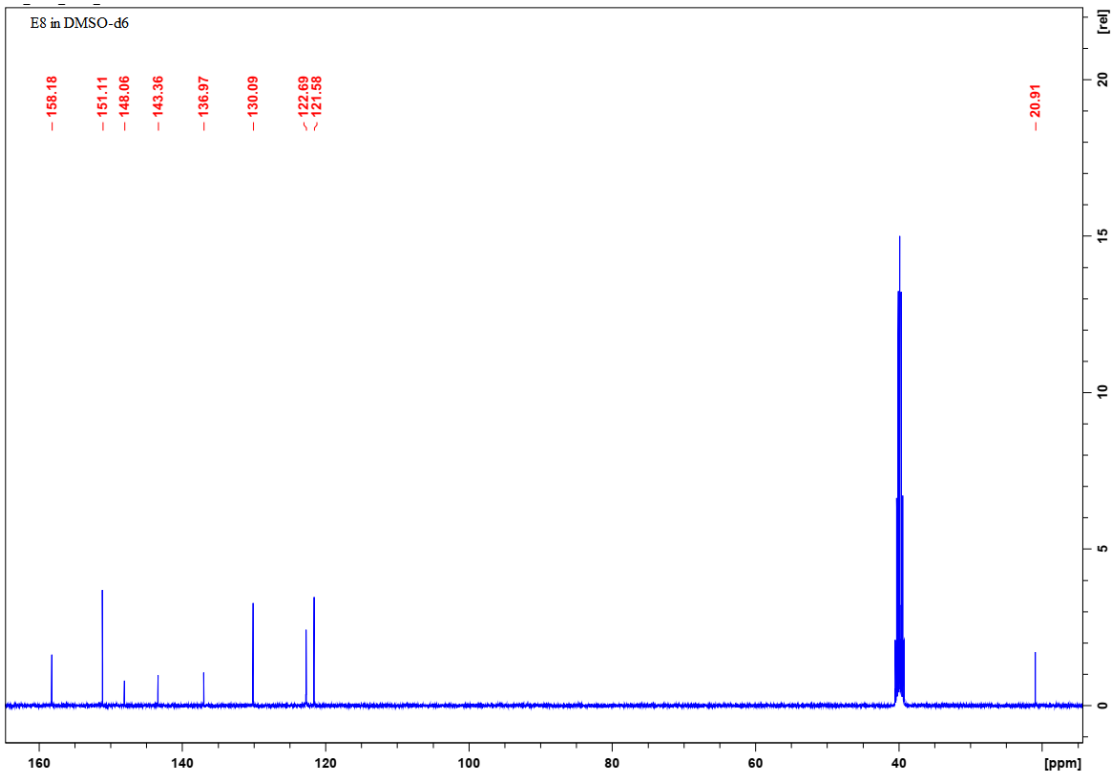

Figure S103: $[Ag(E_d)_2]ClO_4$ 8

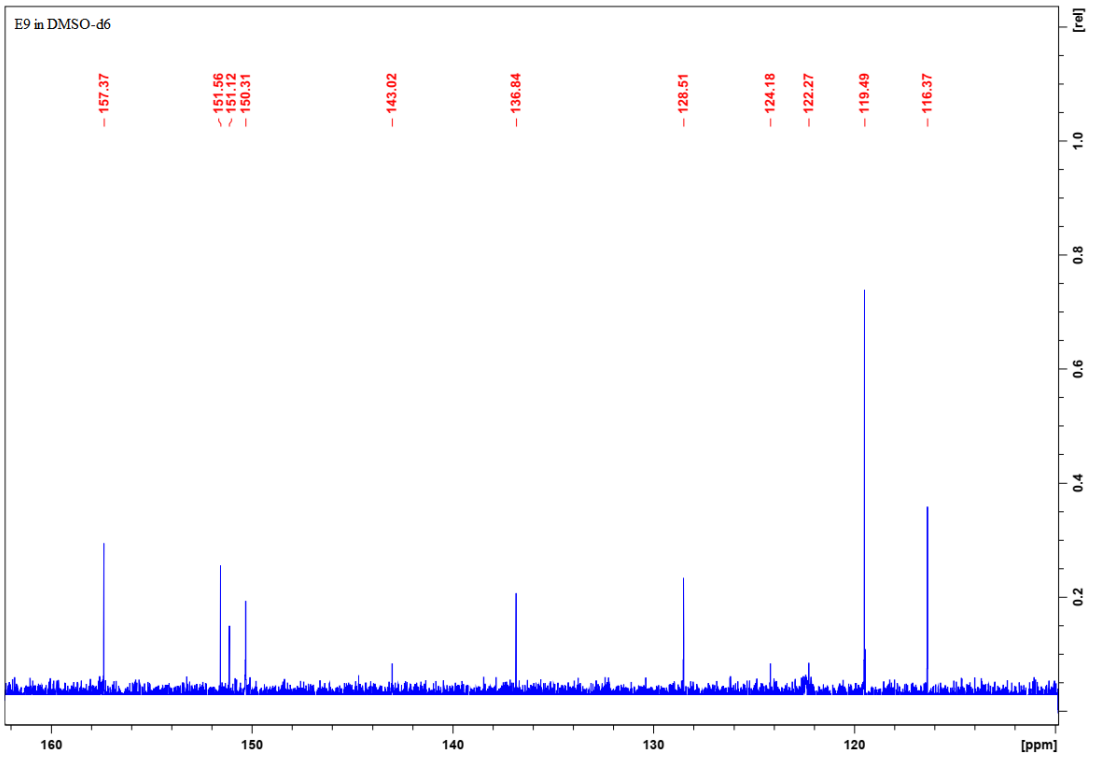

Figure S104: $[Ag(E_a)_2]CF_3SO_3$ 9

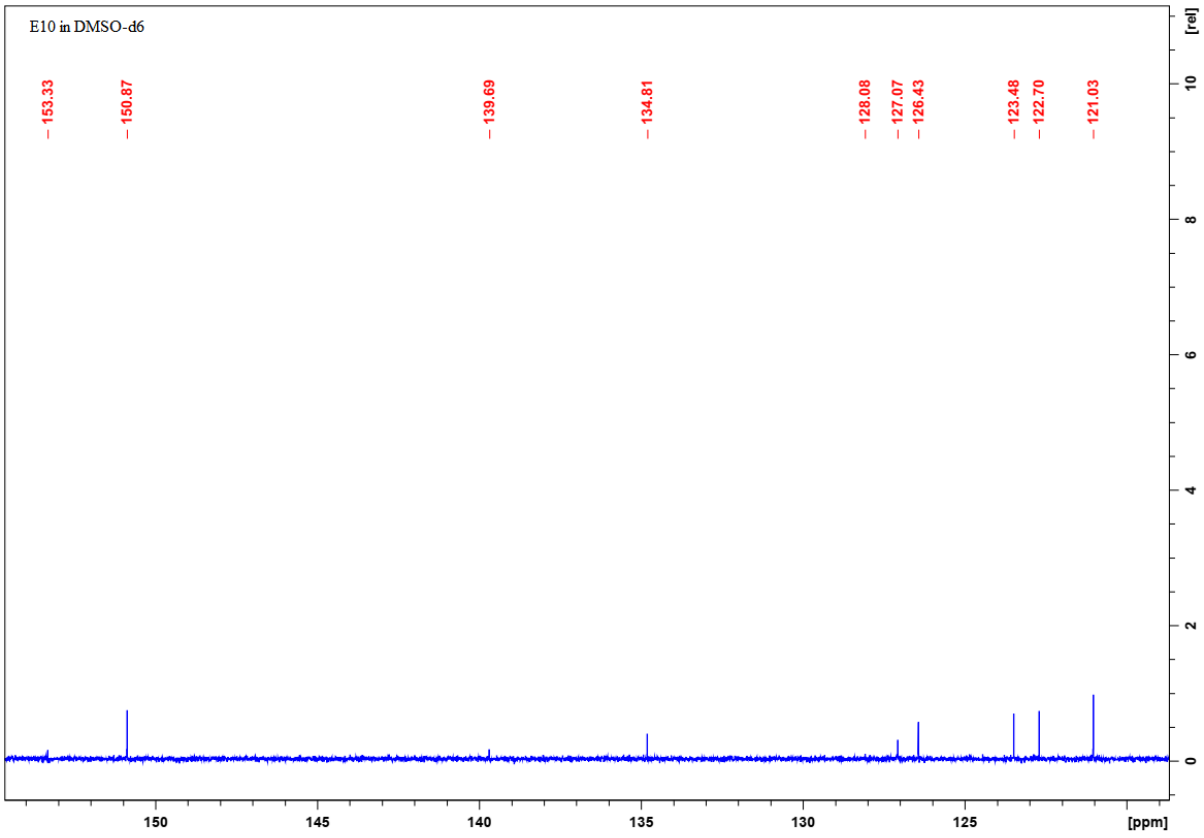

Figure S105: $[Ag(E_b)_2]CF_3SO_3$ 10

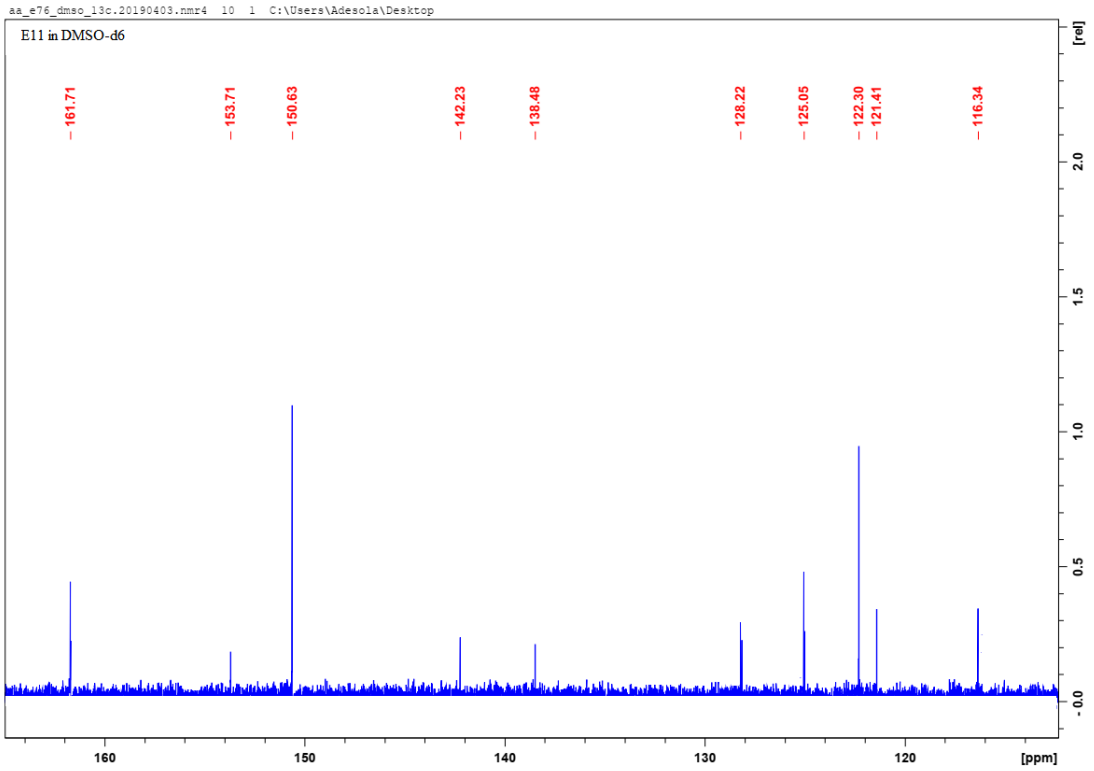

Figure S106: $[Ag(E_c)_2]CF_3SO_3$ 11

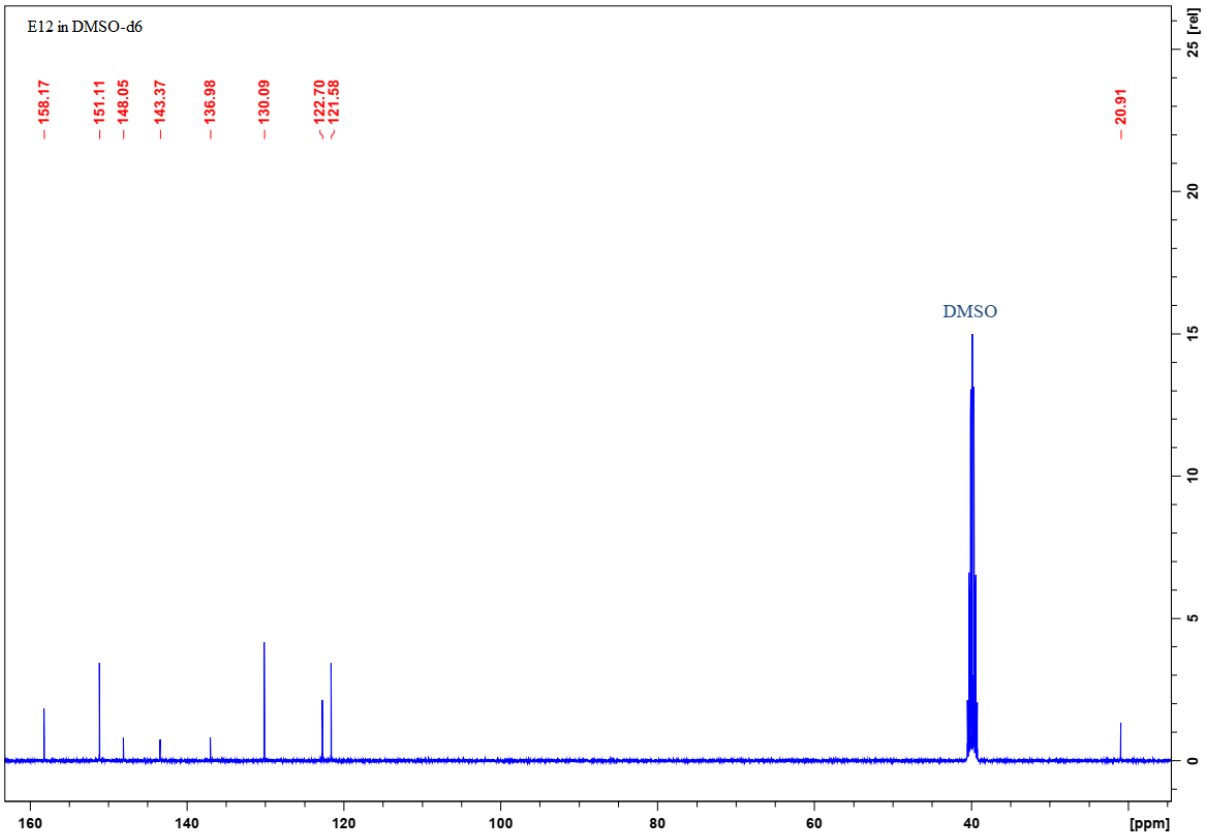

Figure S107: $[Ag(E_d)_2]CF_3SO_3$ 12

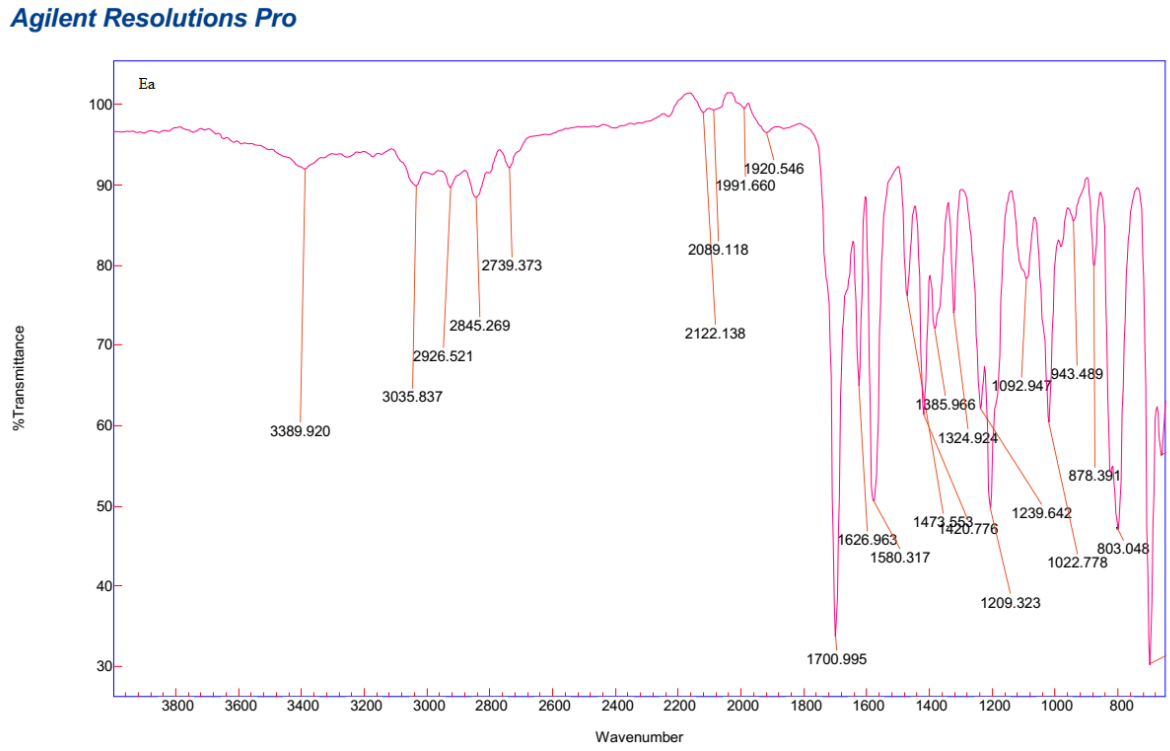

Figure S108: (E)-2-((pyridin-4-ylmethylene)amino)phenol E_a

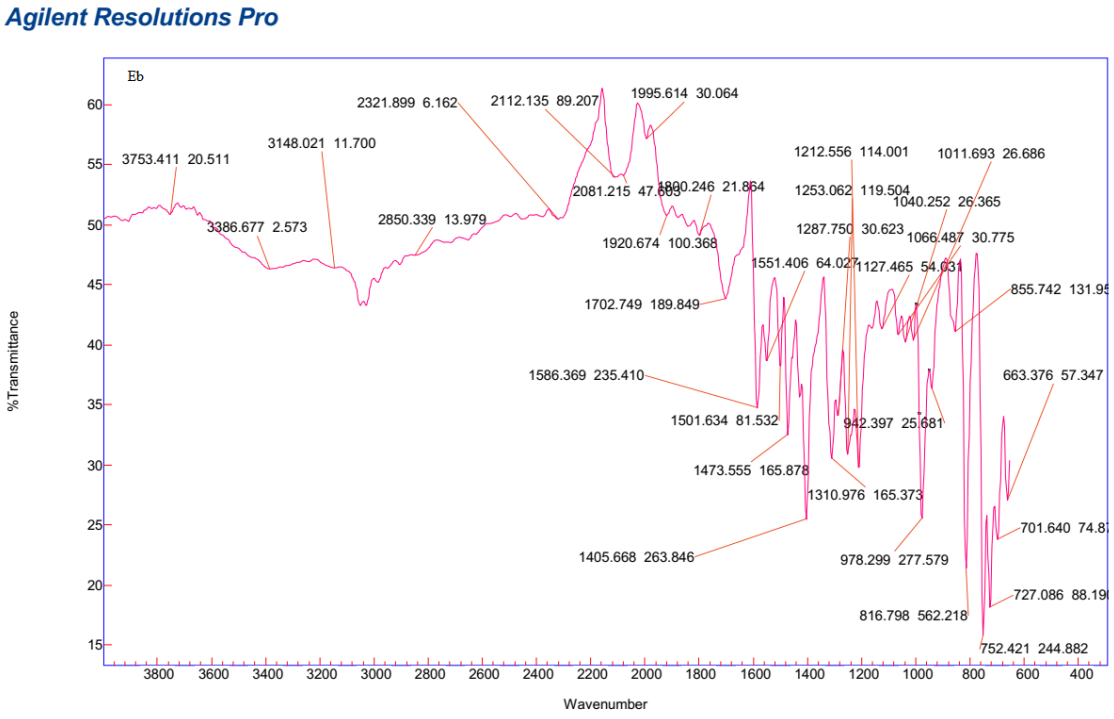

Figure S109: 2-(pyridin-4-yl)benzo[*d*]thiazole E_b

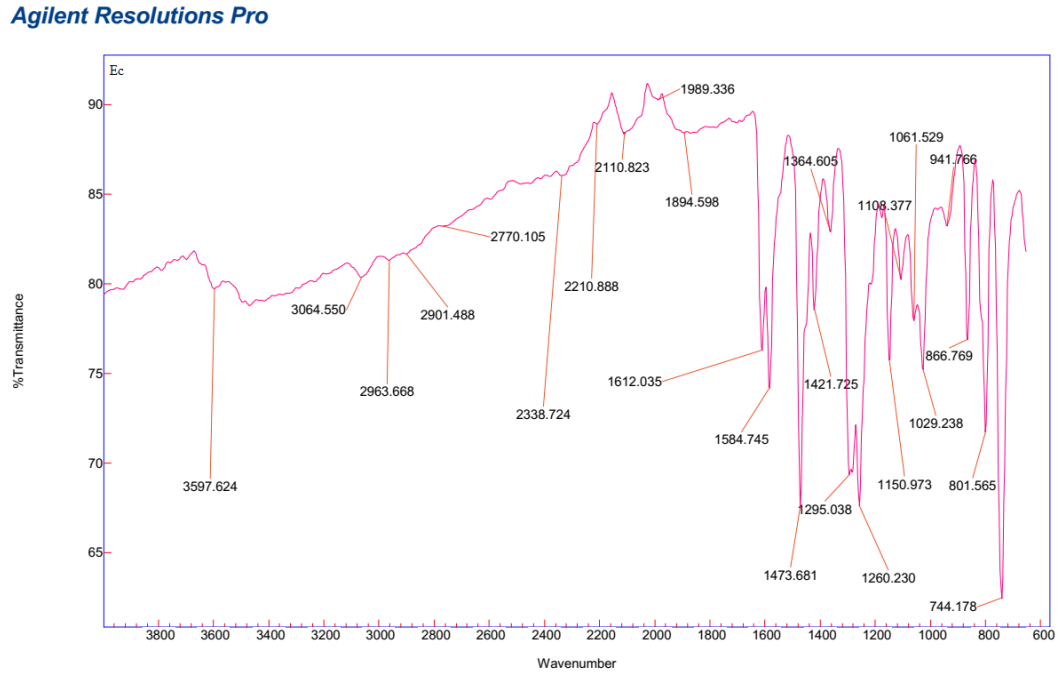

Figure S110: (E)-N-(2-fluorophenyl)-1-(pyridin-4-yl)methanimine E_c

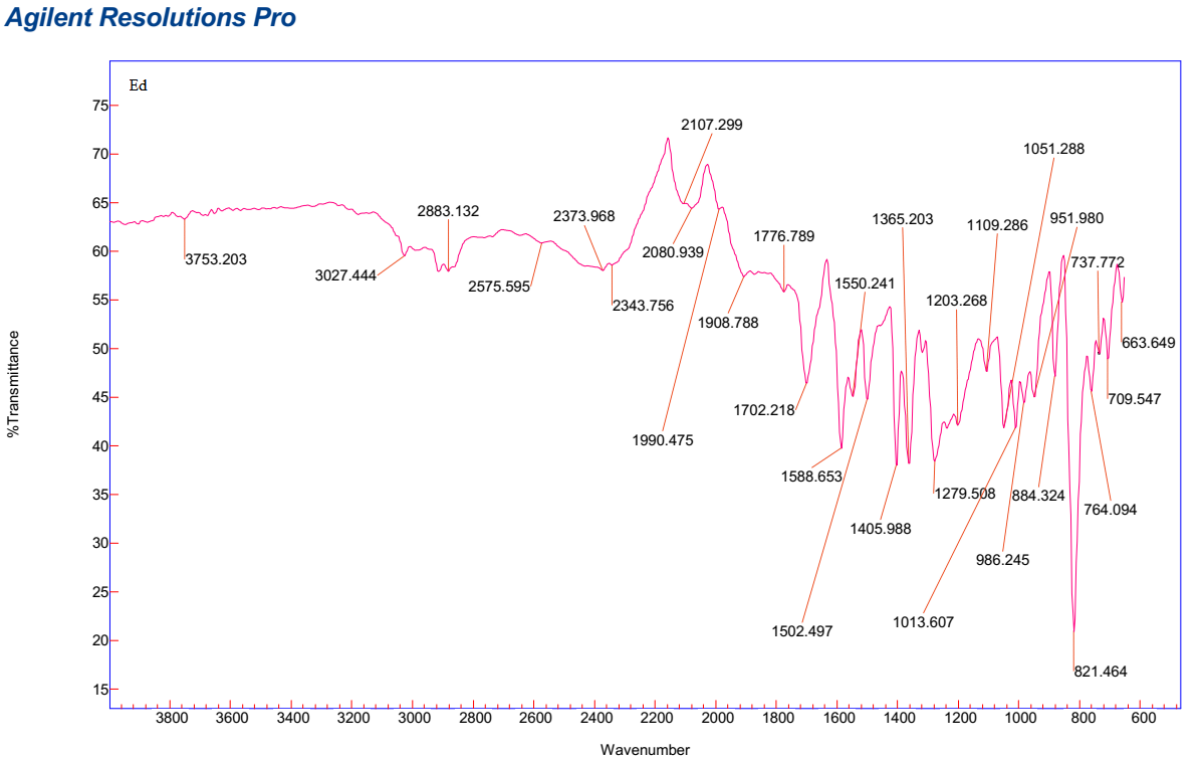

Figure S111: (E)-1-(pyridin-4-yl)-N-(p-tolyl)methanimine E_d

IR SPECTRA OF COMPLEXES 1-12

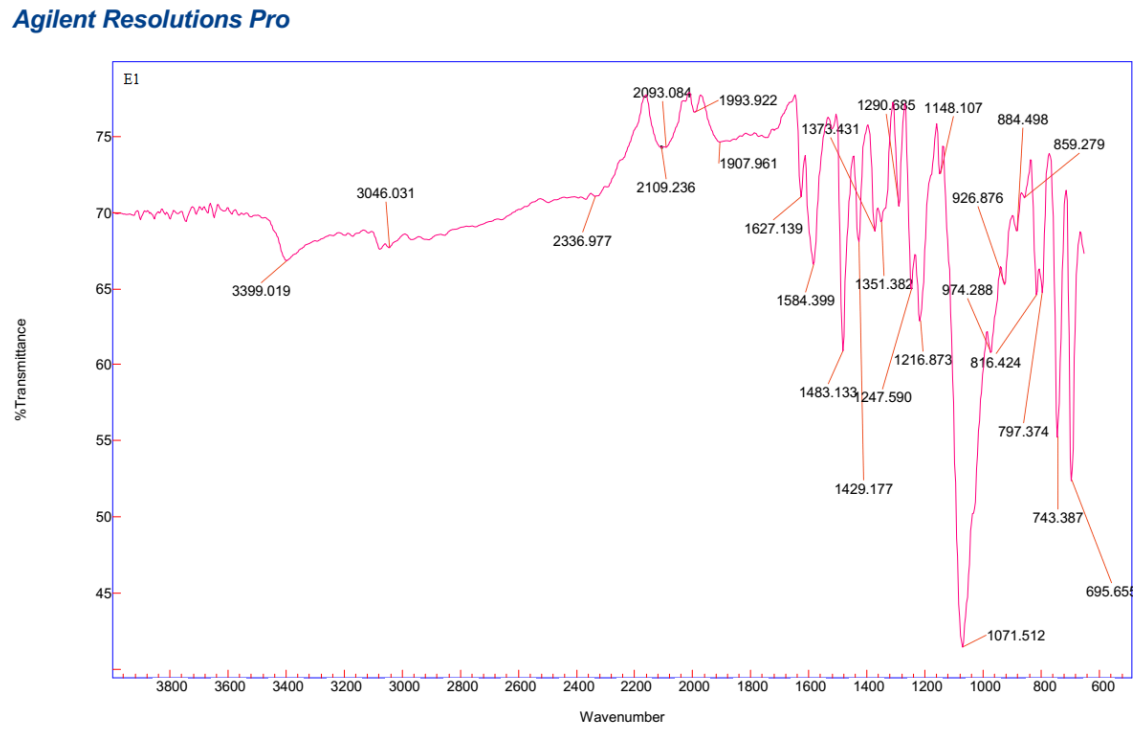

Figure S112: $[Ag(E_a)_2]NO_3$ 1

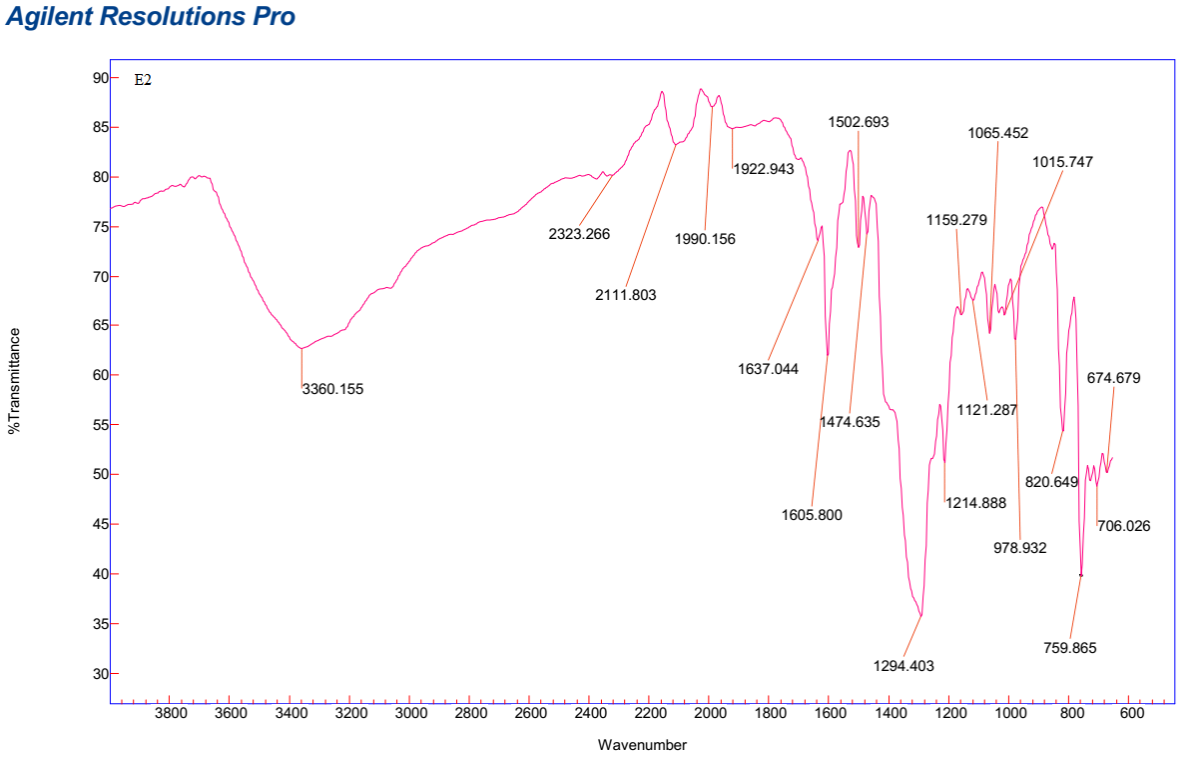

Figure S113: $[Ag(E_b)_2]NO_3$ 2

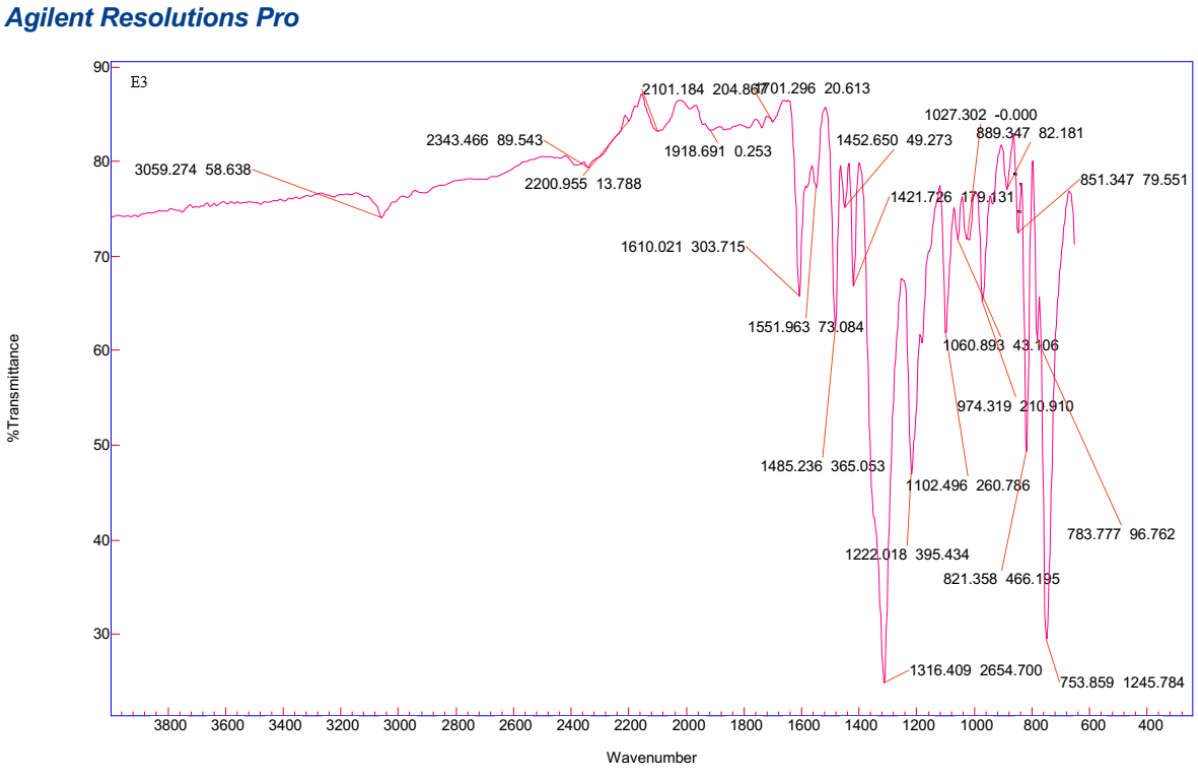

Figure S114: $[Ag(E_c)_2]NO_3$ 3

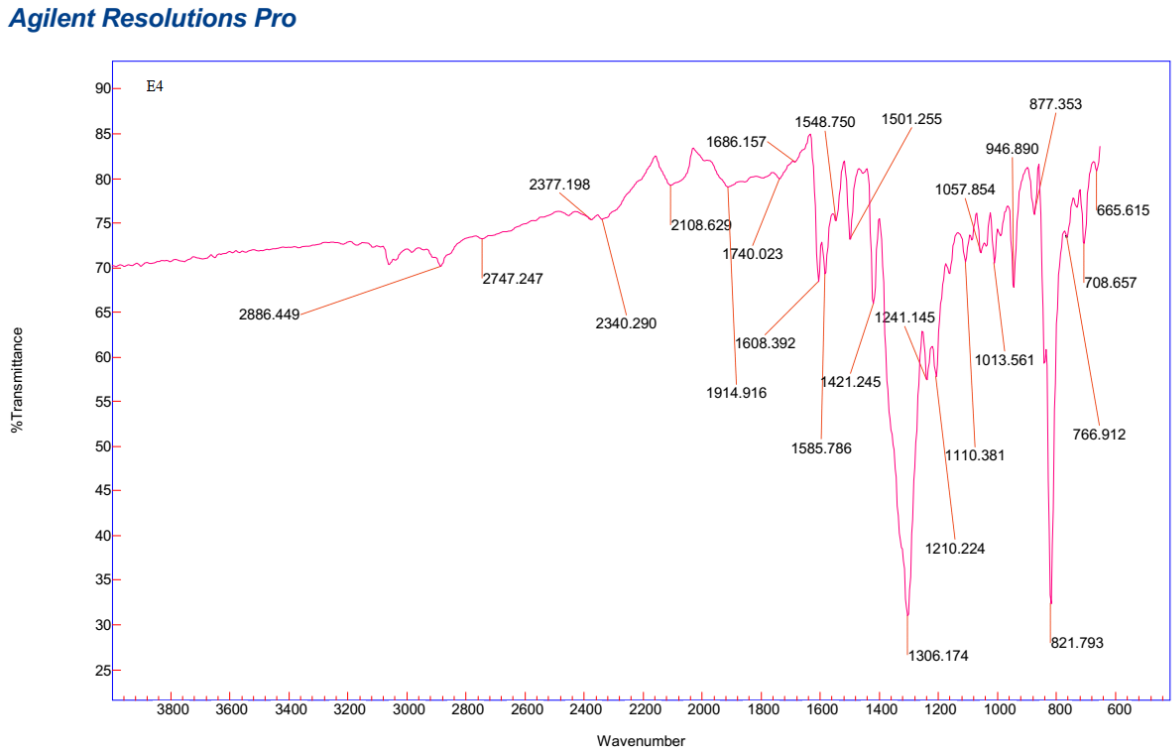

Figure S115: $[Ag(E_d)_2]NO_3$ 4

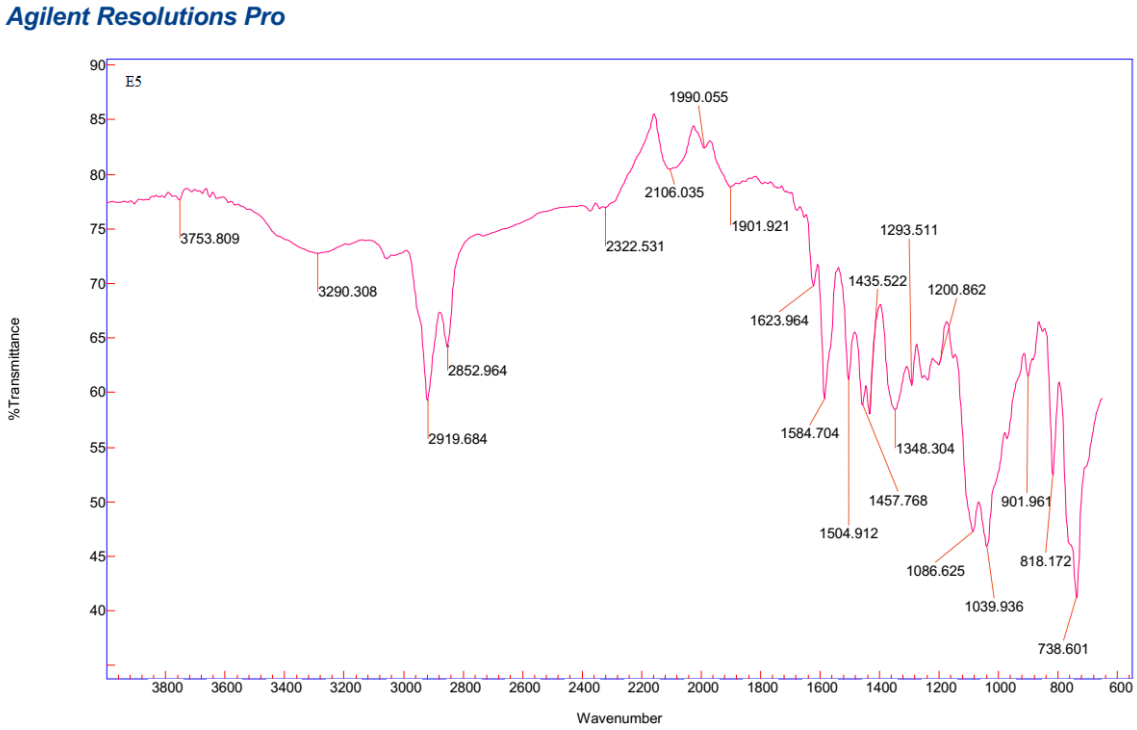

Figure S116: $[Ag(E_a)_2]ClO_4$ 5

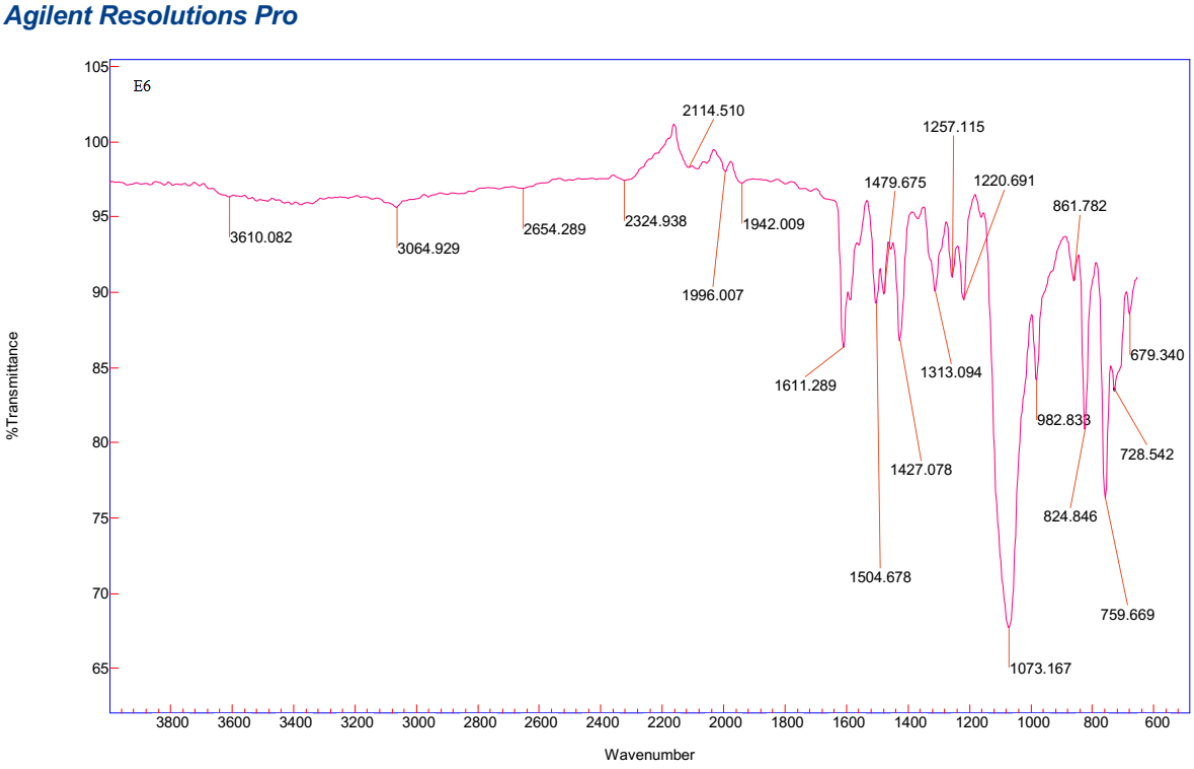

Figure S117: $[Ag(E_b)_2]ClO_4$ 6

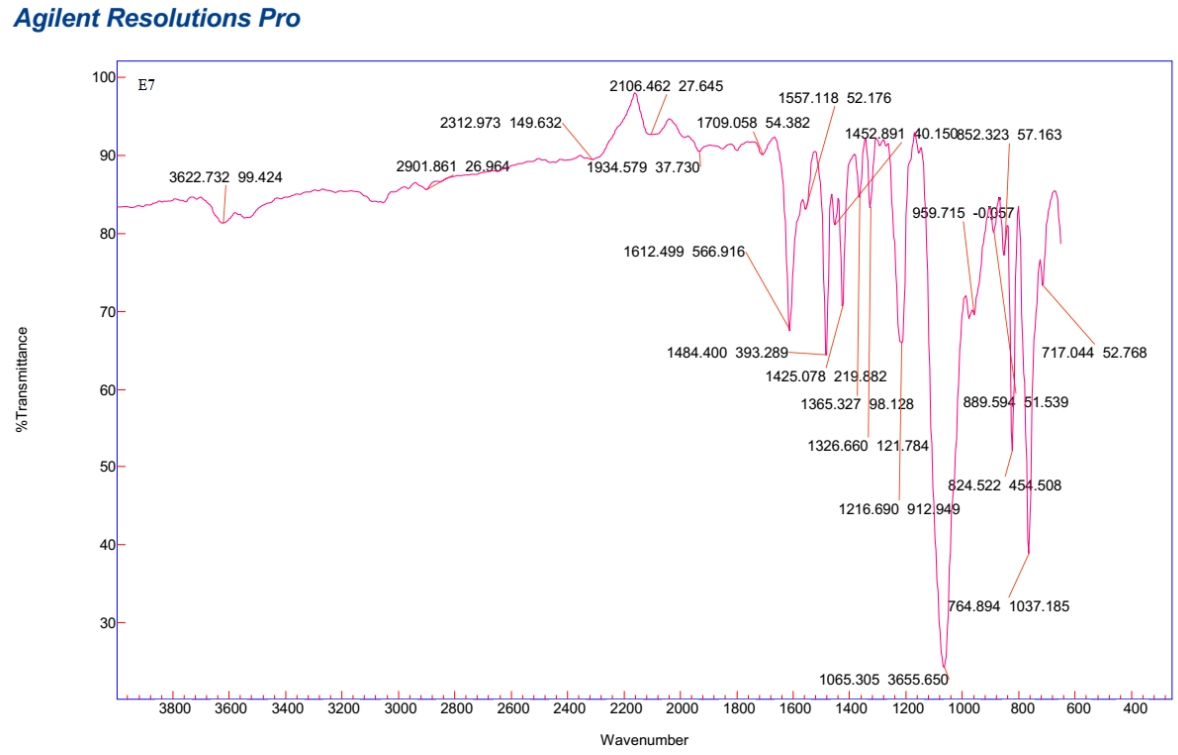

Figure S118: $[Ag(E_c)_2]ClO_4$ 7

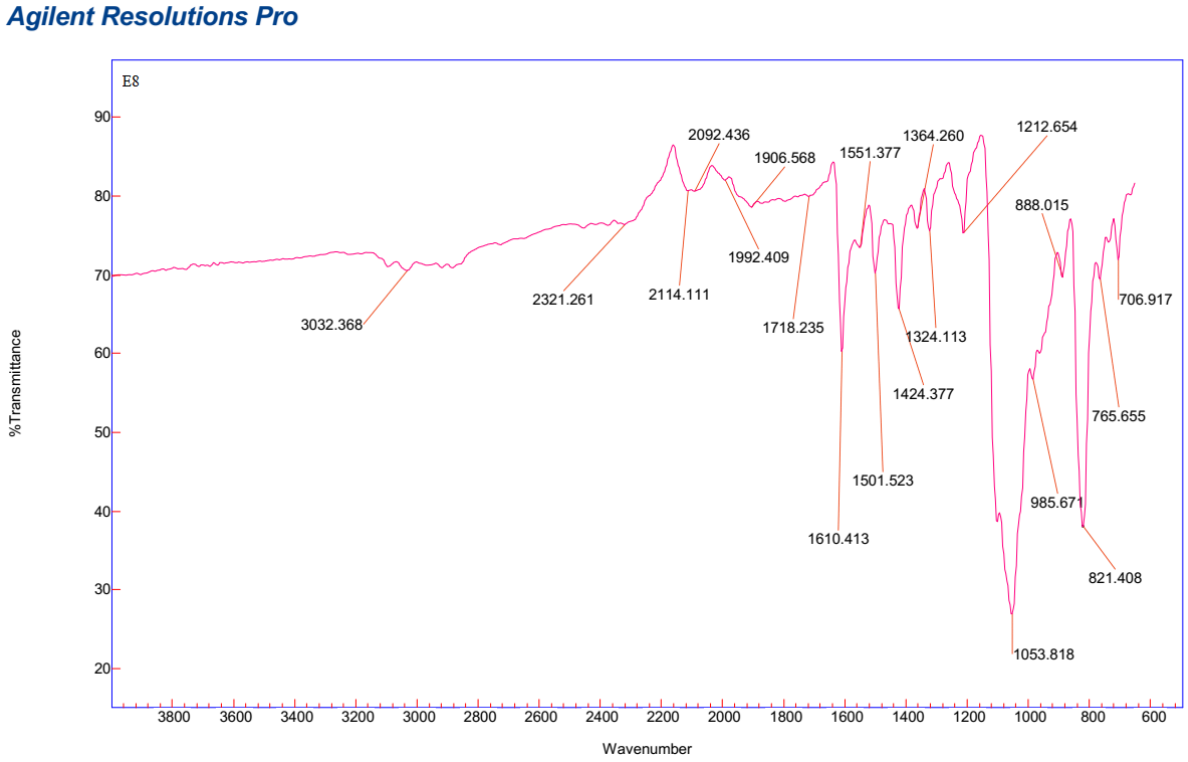

Figure S119: $[Ag(E_d)_2]ClO_4$ 8

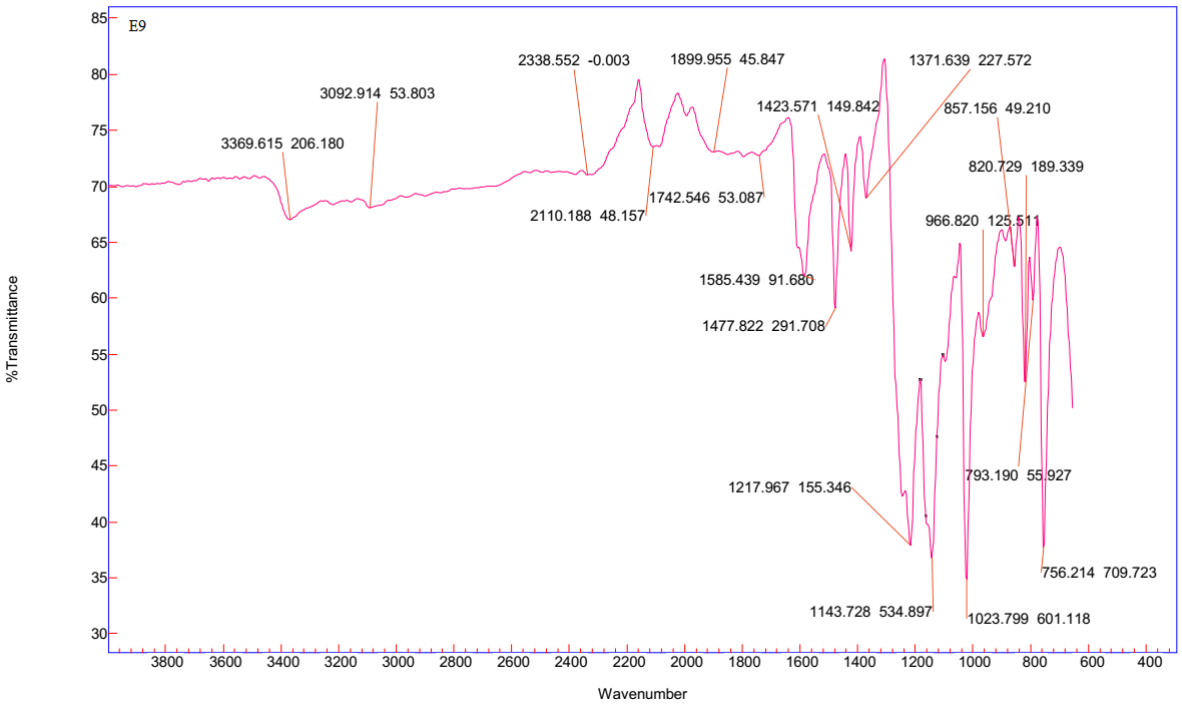

Figure S120: $[Ag(E_a)_2]CF_3SO_3$ 9

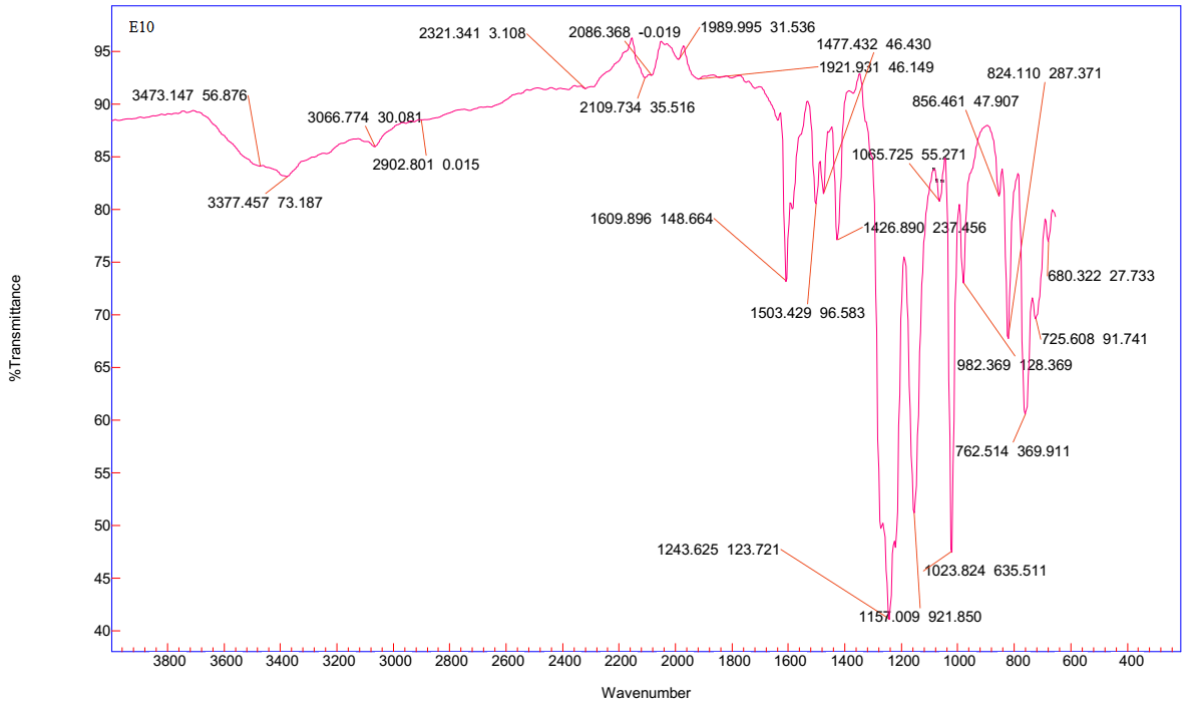

Figure S121: $[Ag(E_b)_2]CF_3SO_3$ 10

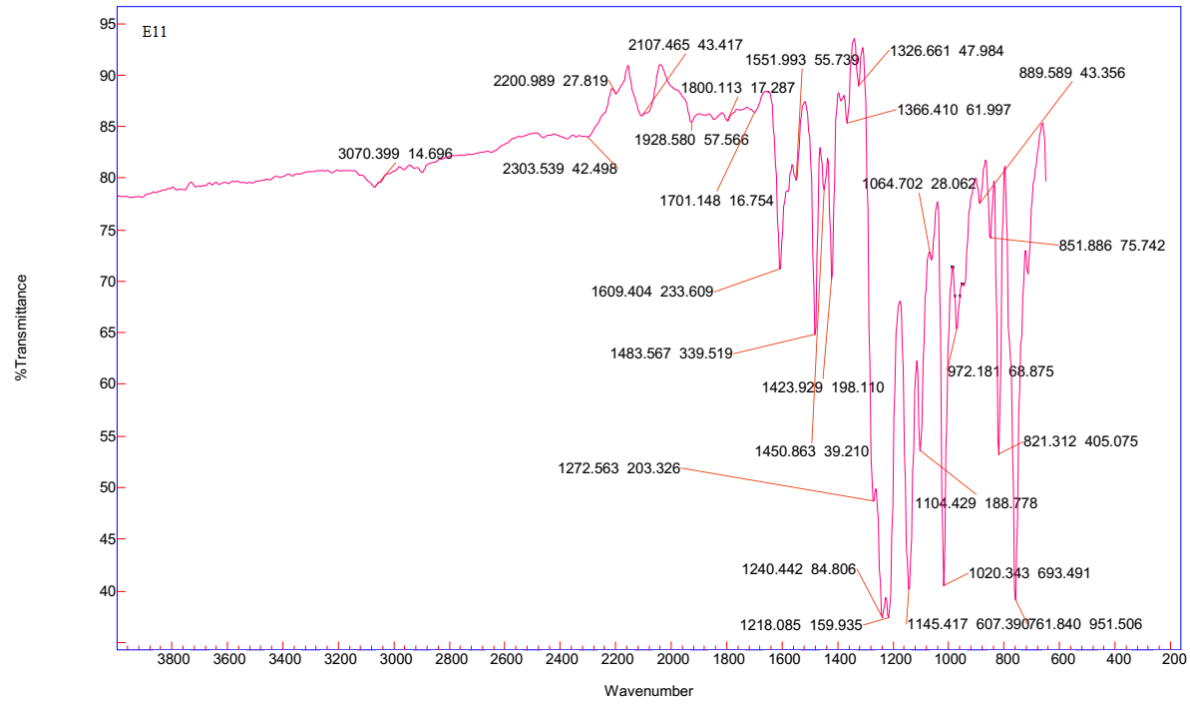

Figure S122: $[Ag(E_c)_2]CF_3SO_3$ 11

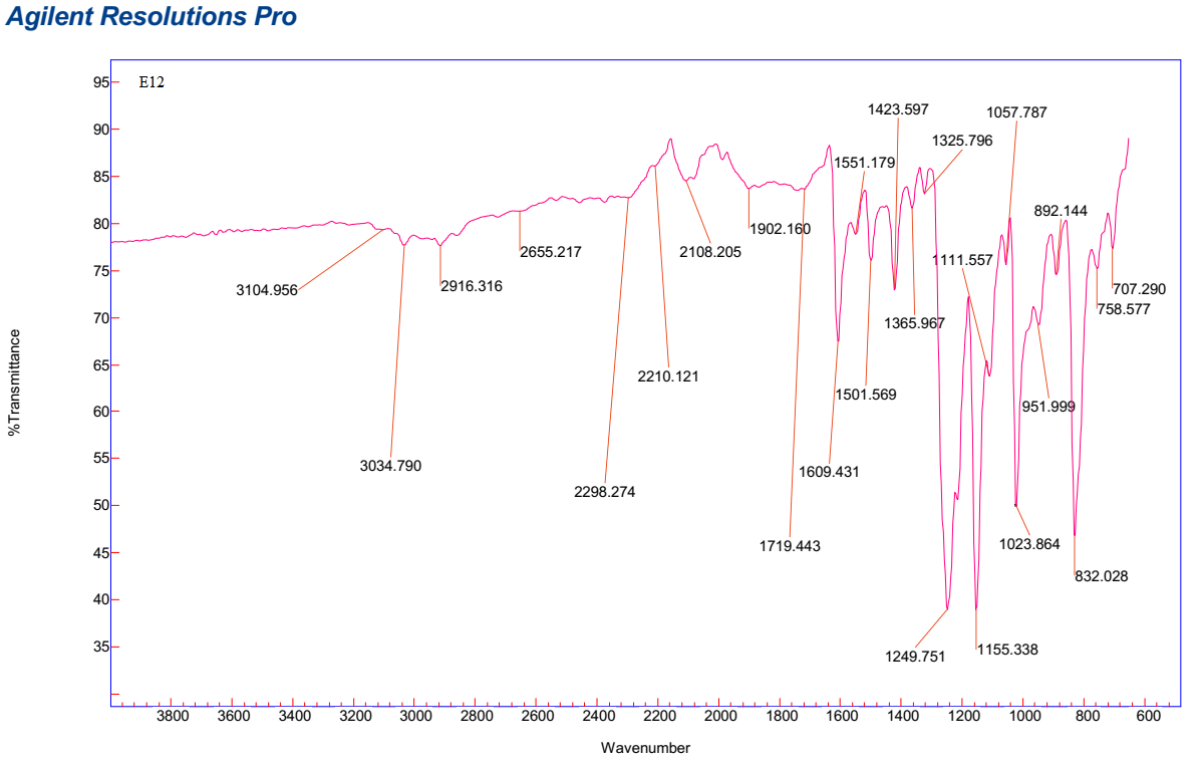

Figure S123: $[Ag(E_d)_2]CF_3SO_3$ 12

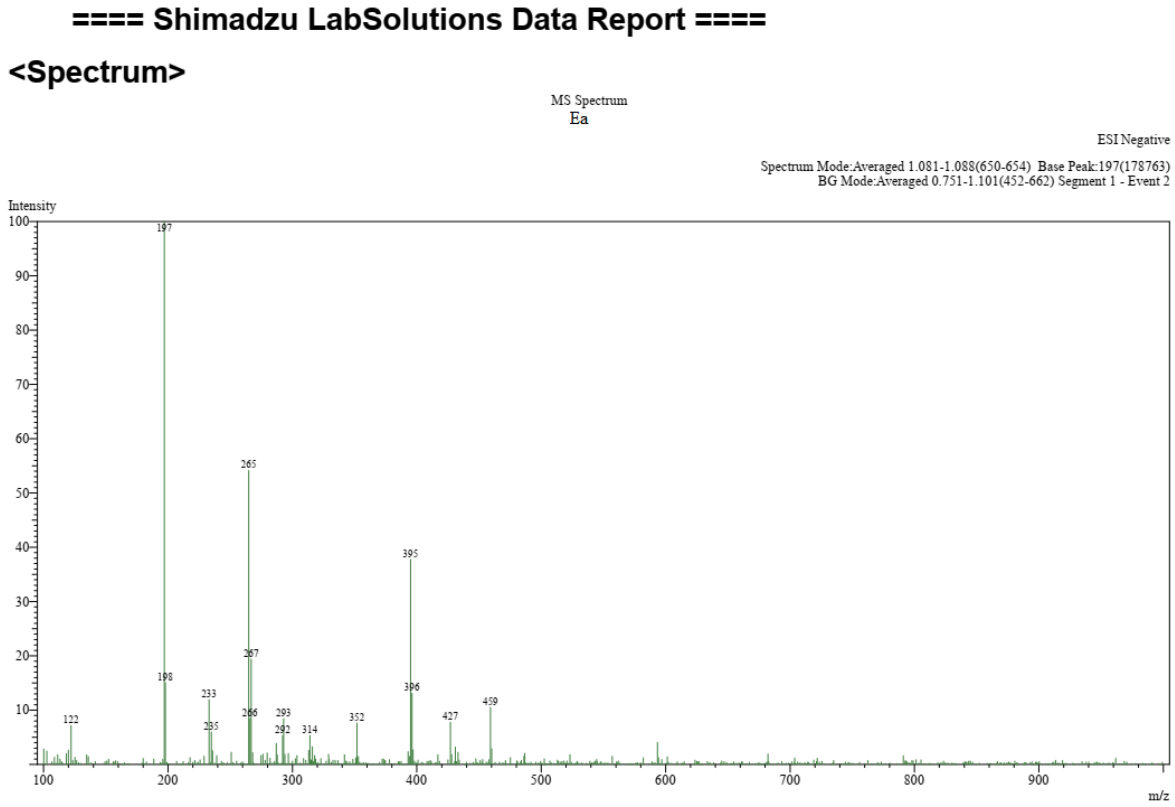

Figure S124: (E)-2-((pyridin-4-ylmethylene)amino)phenol E_a

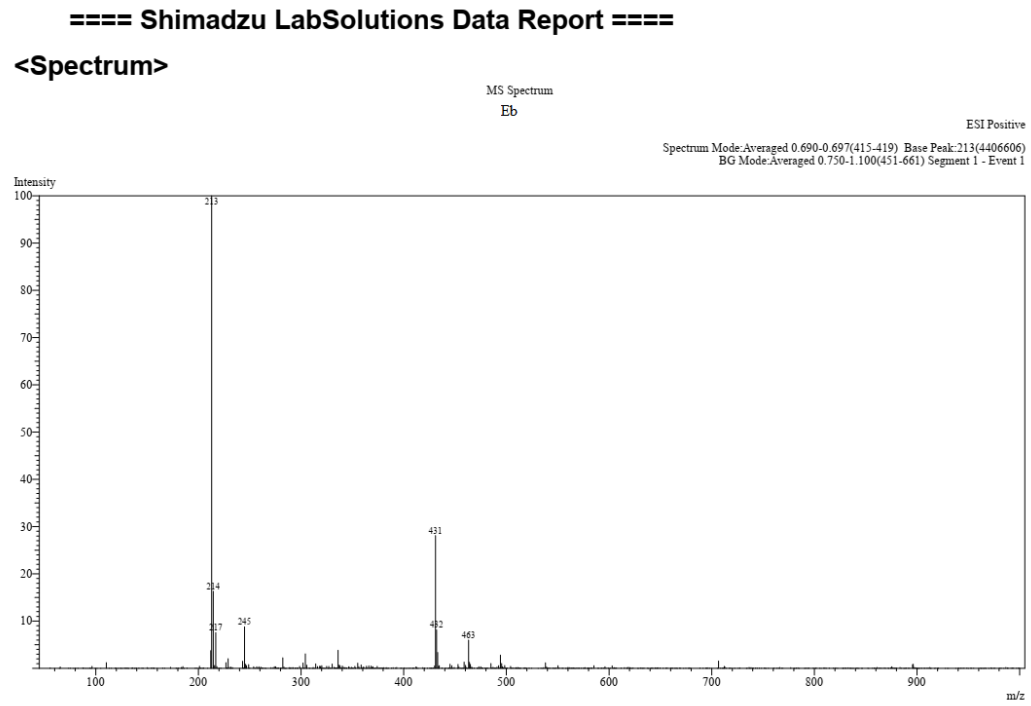

Figure S125: 2-(pyridin-4-yl)benzo[*d*]thiazole E_b

==== Shimadzu LabSolutions Data Report ====

<Spectrum>

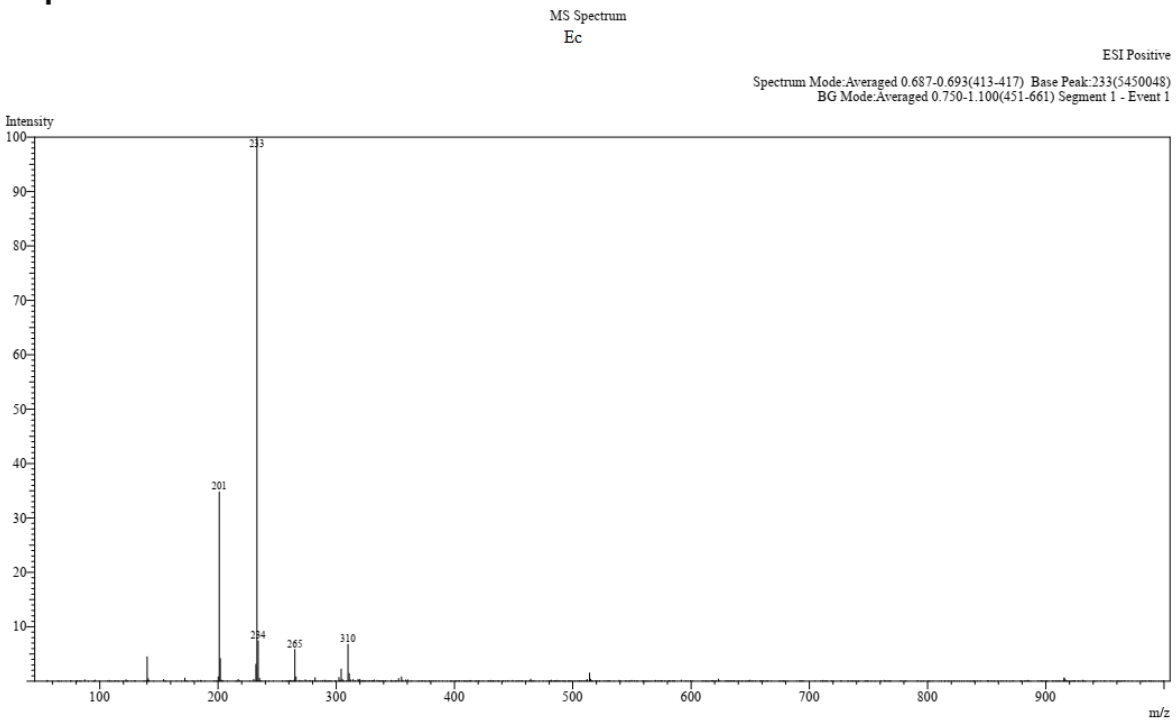

Figure S126: (E)-N-(2-fluorophenyl)-1-(pyridin-4-yl)methanimine E_c

==== Shimadzu LabSolutions Data Report ====

<Spectrum>

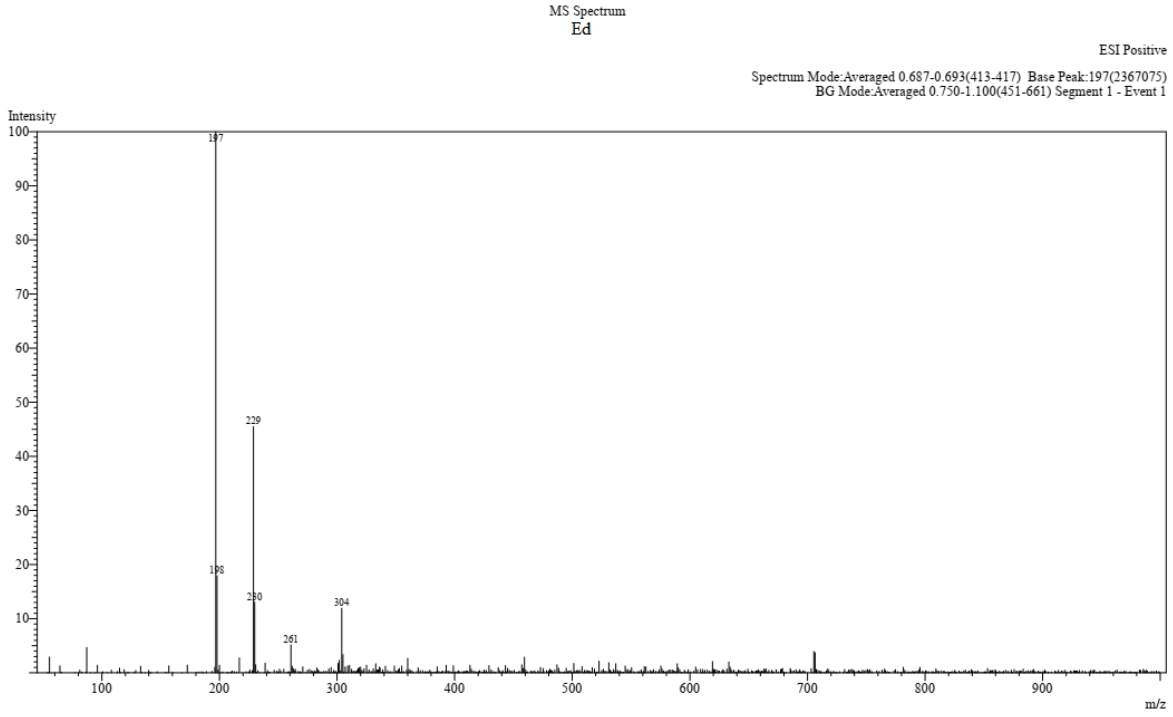

Figure S127: (E)-1-(pyridin-4-yl)-N-(p-tolyl)methanimine E_d

==== Shimadzu LabSolutions Data Report ====

<Spectrum>

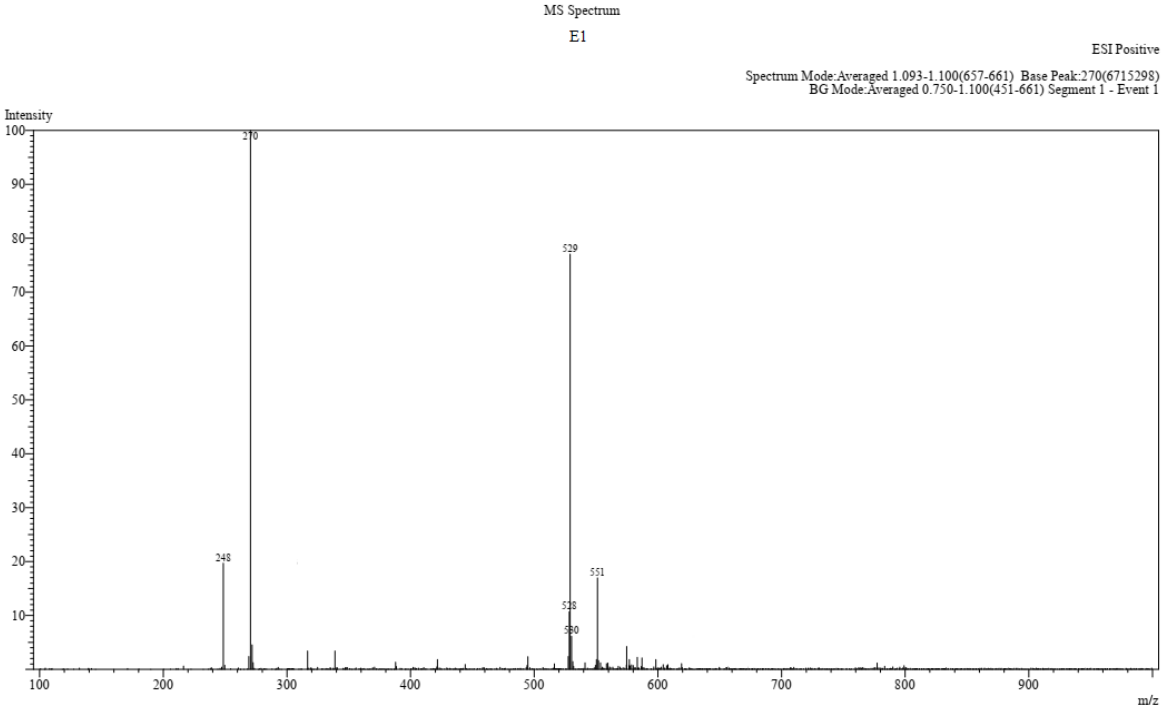

Figure S128: $[Ag(E_a)_2]NO_3$ 1

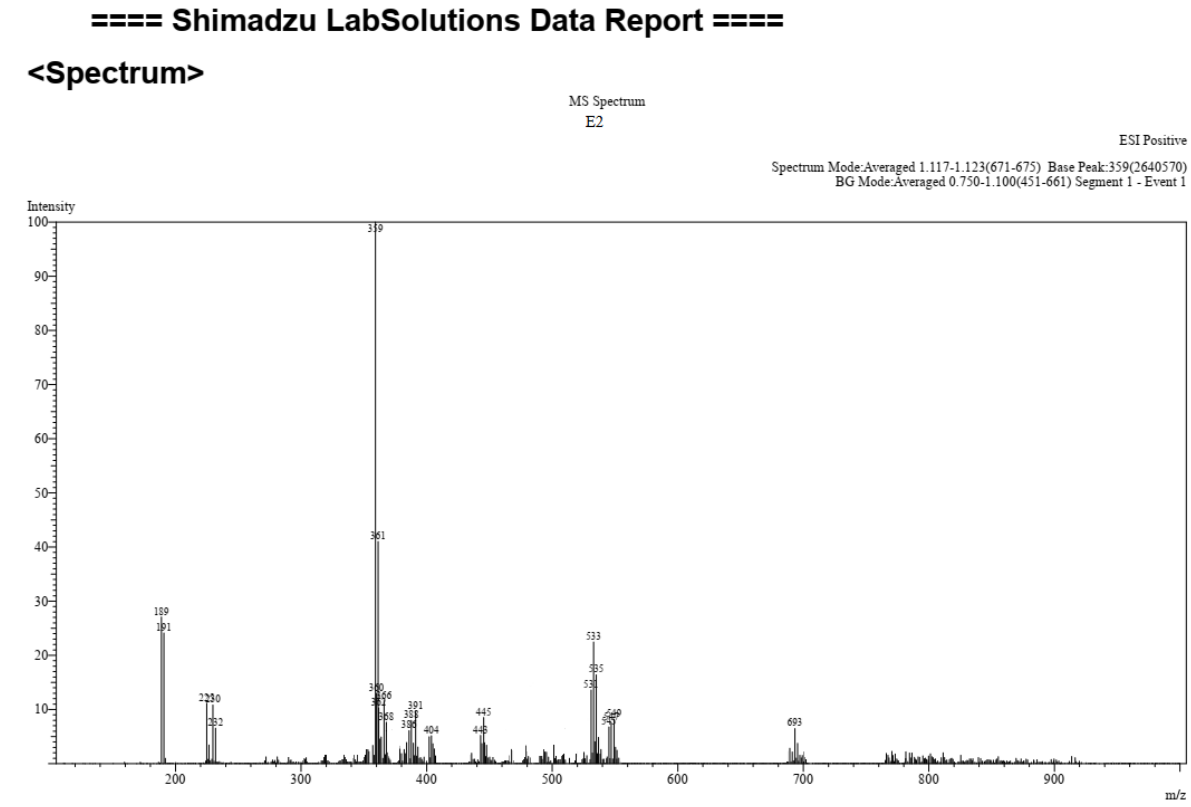

Figure S129: $[Ag(E_b)_2]NO_3$ 2

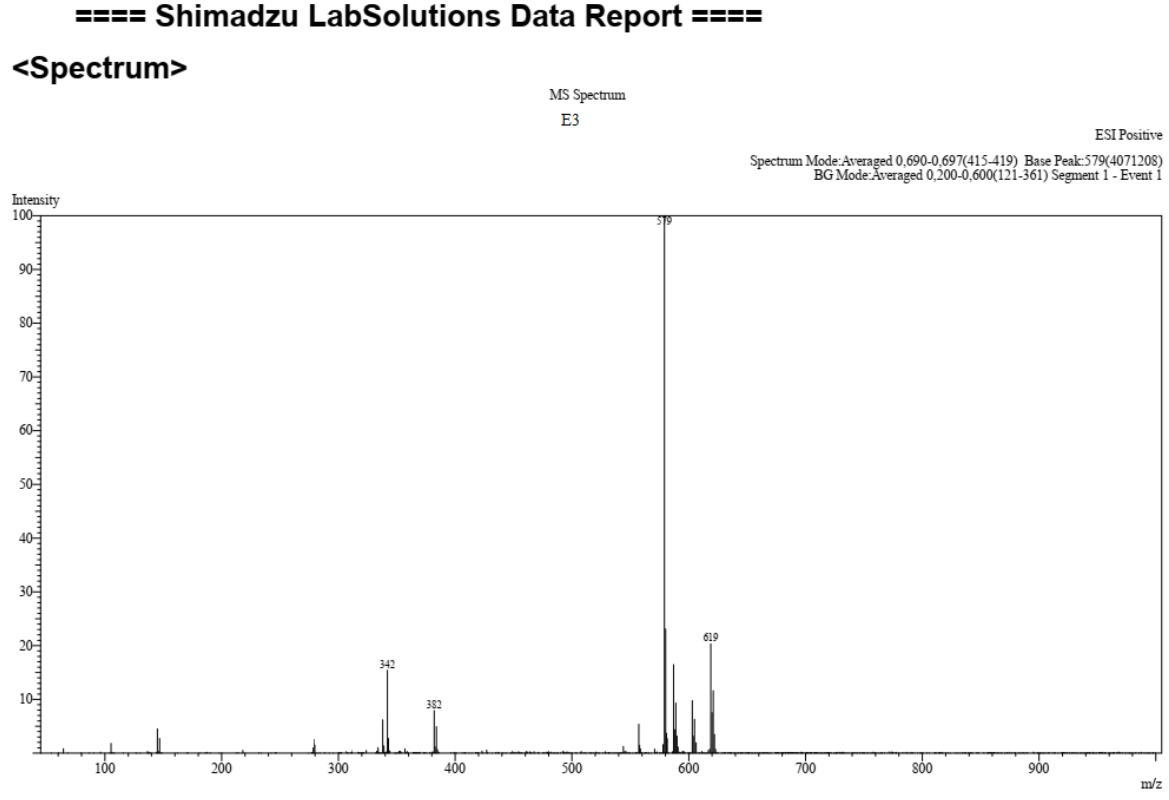

Figure S130: $[Ag(E_c)_2]NO_3$ 3

==== Shimadzu LabSolutions Data Report ====

<Spectrum>

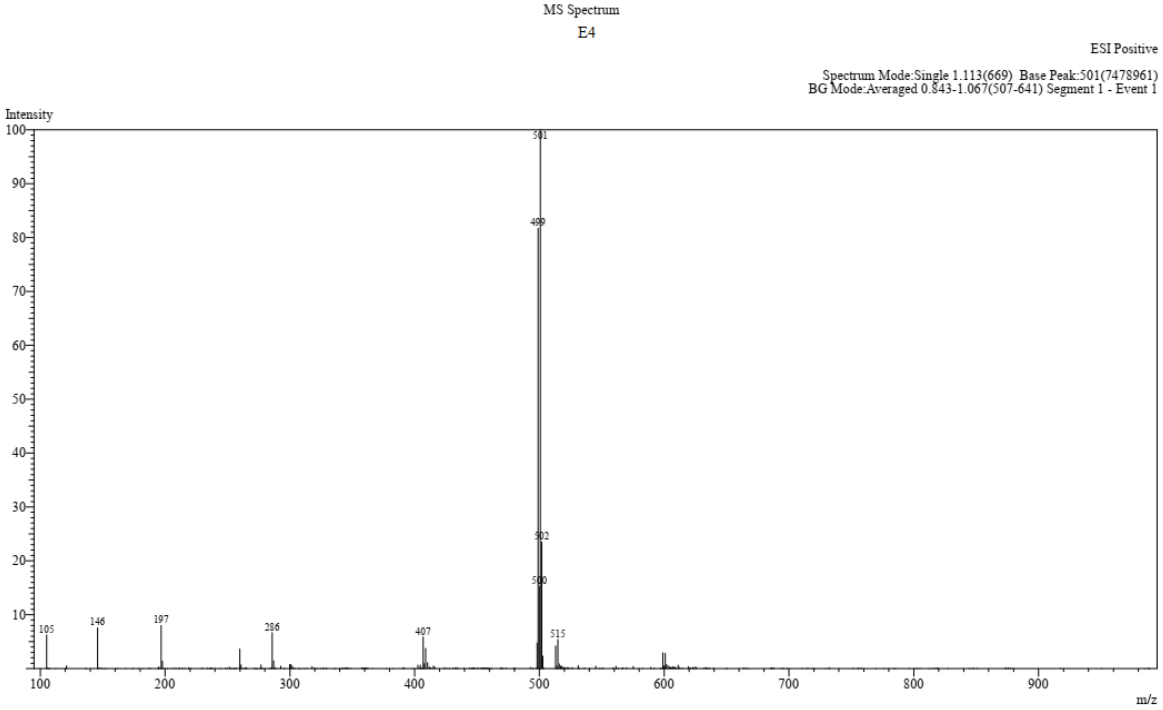

Figure S131: $[Ag(E_d)_2]NO_3$ 4

==== Shimadzu LabSolutions Data Report ====

<Spectrum>

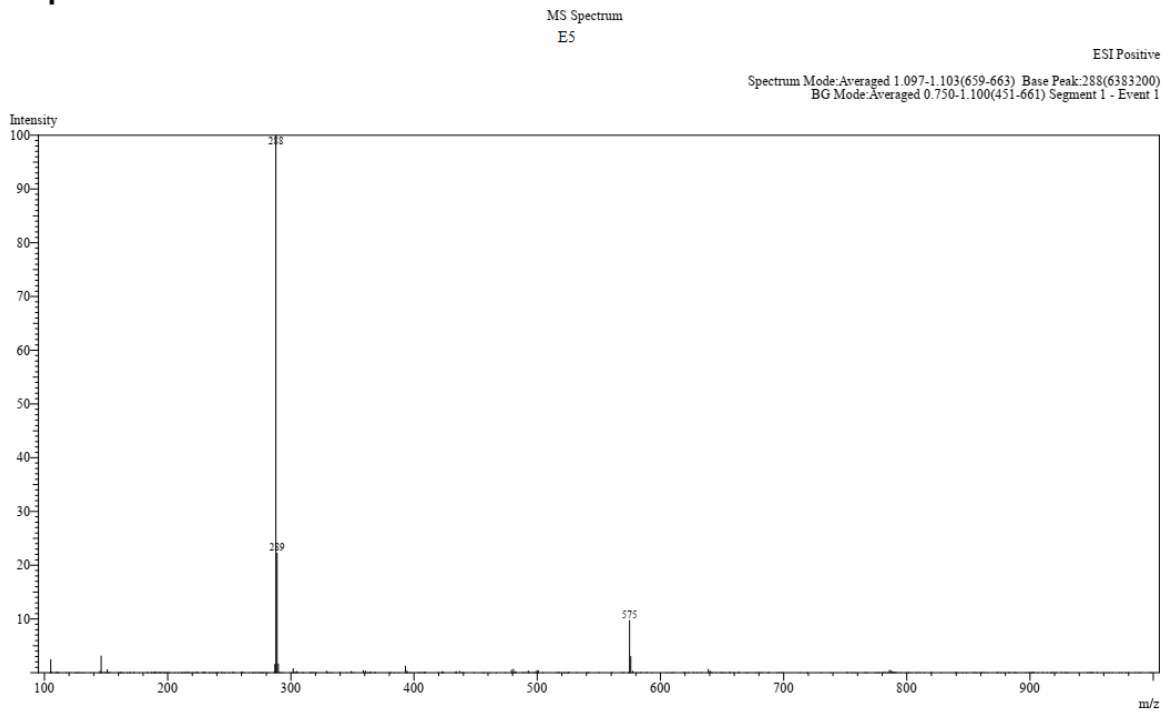

Figure S132: $[Ag(E_a)_2]ClO_4$ 5

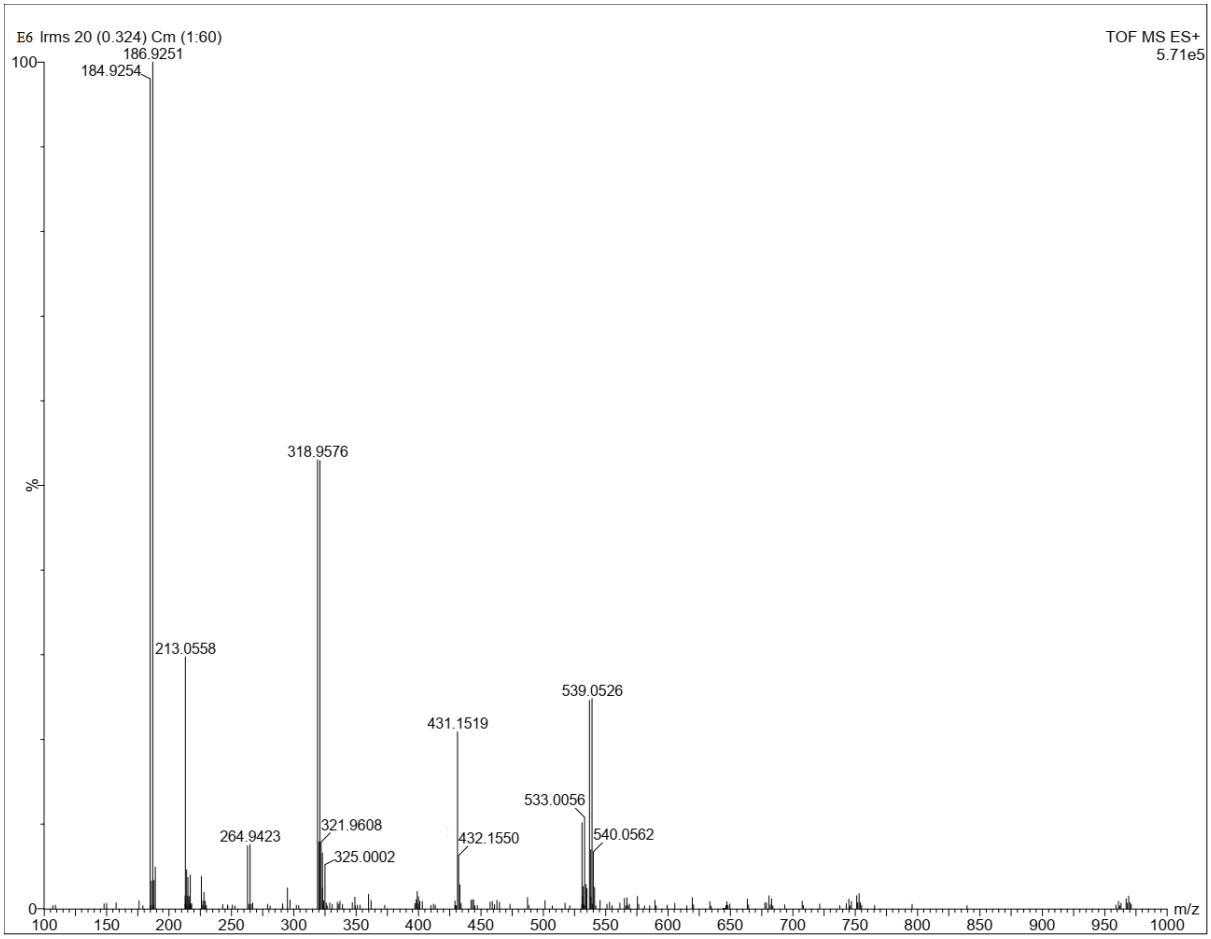

Figure S133: $[Ag(E_b)_2]ClO_4$ 6

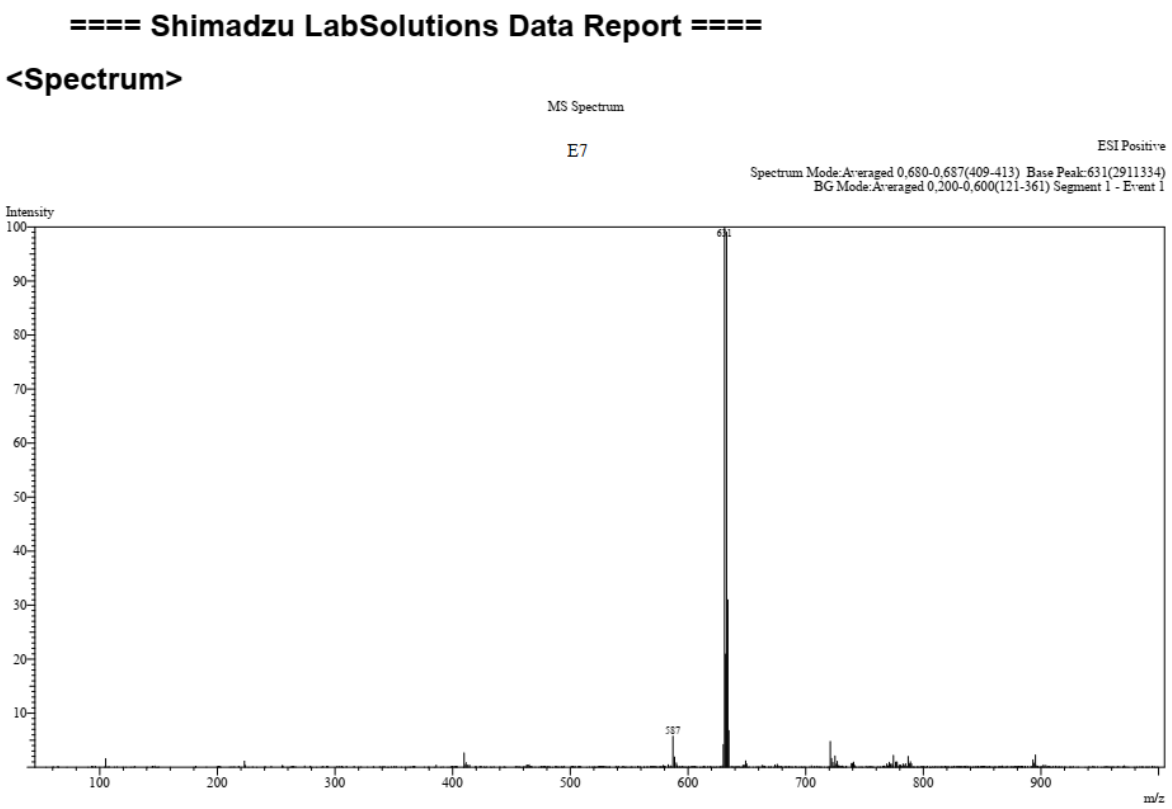

Figure S134: $[Ag(E_c)_2]ClO_4$ 7

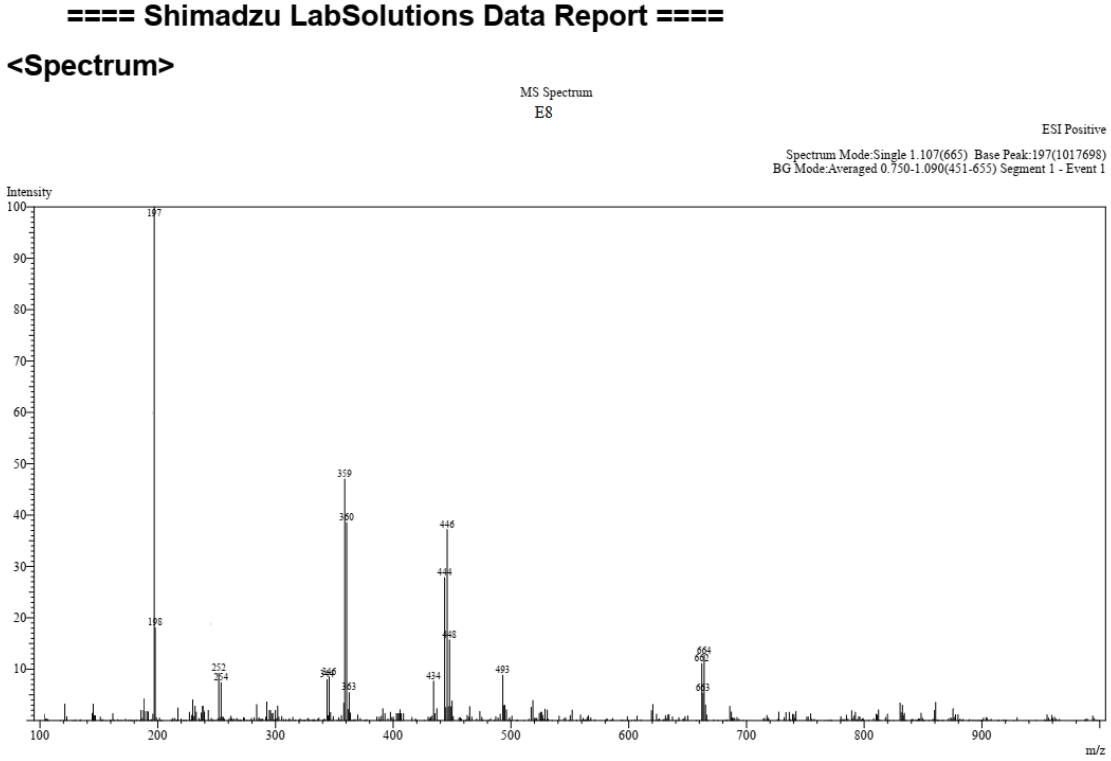

Figure S135: $[Ag(E_d)_2]ClO_4$ 8

==== Shimadzu LabSolutions Data Report ====

<Spectrum>

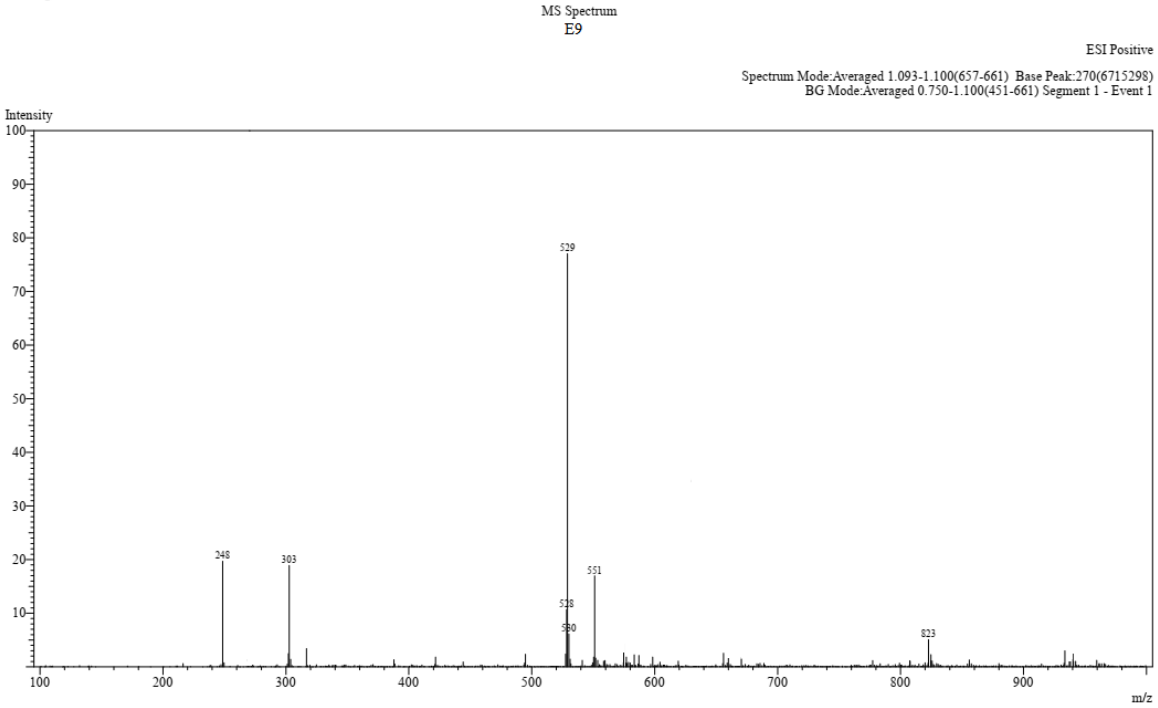

Figure S136: $[Ag(E_a)_2]CF_3SO_3$ 9

<Spectrum>

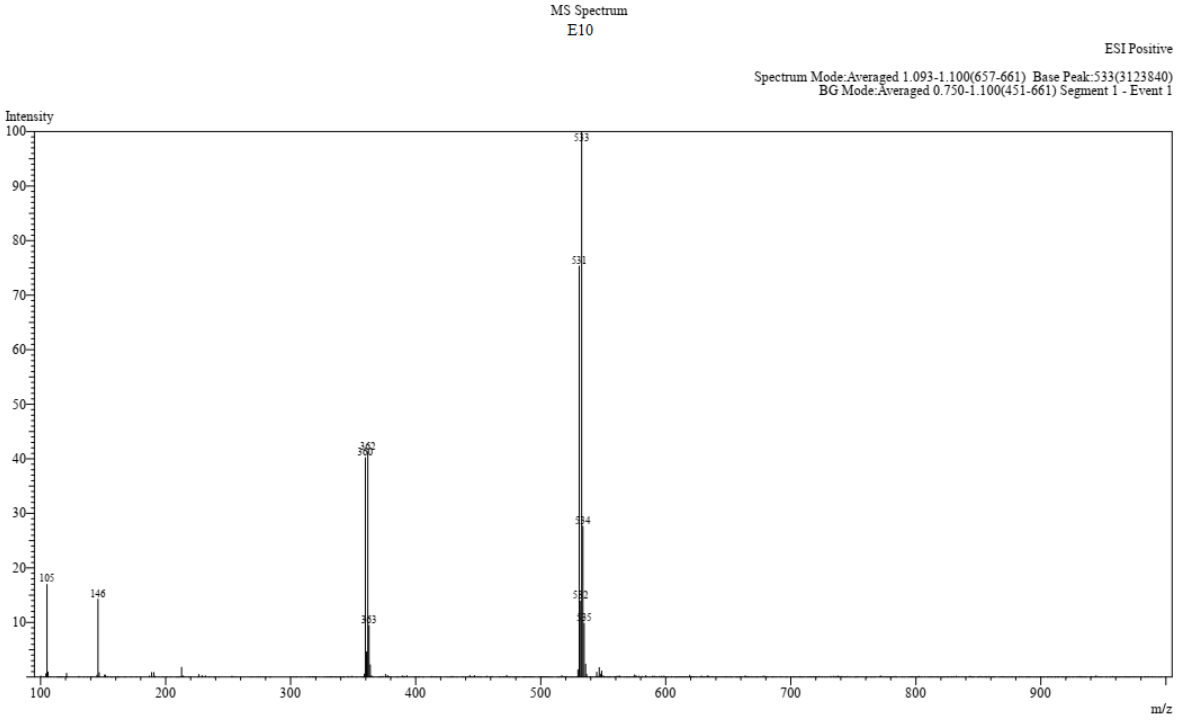

Figure S137: $[Ag(E_b)_2]CF_3SO_3$ 10

==== Shimadzu LabSolutions Data Report ====

<Spectrum>

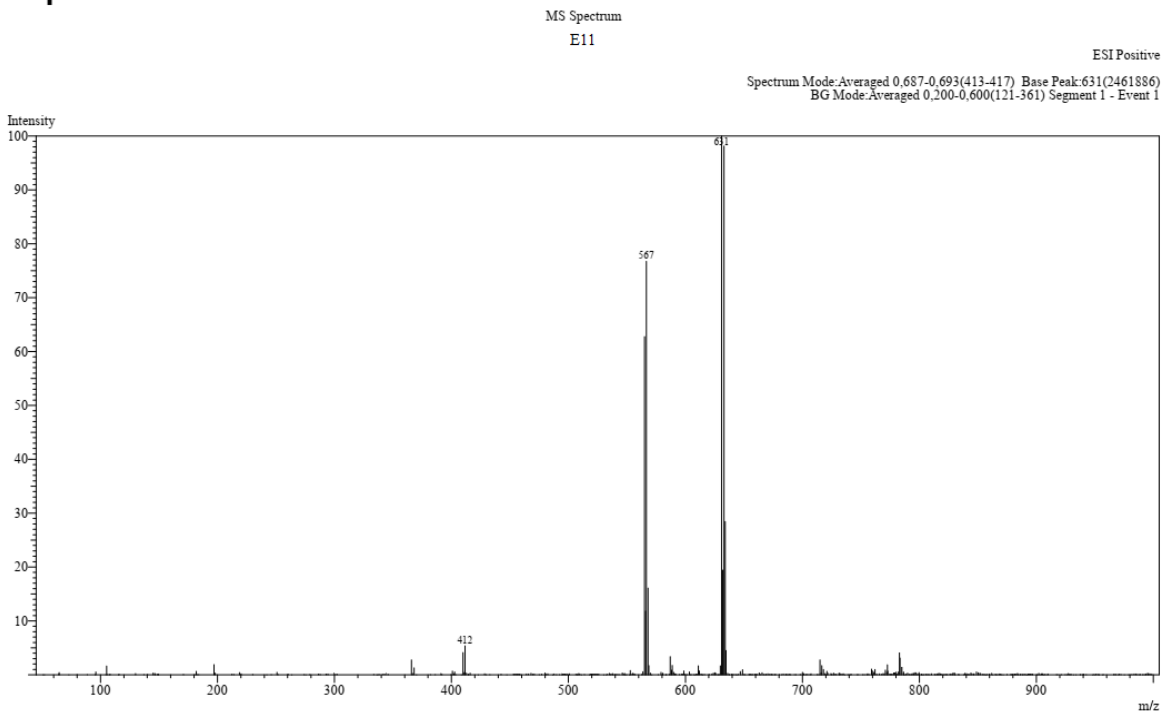

Figure S138: $[Ag(E_c)_2]CF_3SO_3$ 11

==== Shimadzu LabSolutions Data Report ====

<Spectrum>

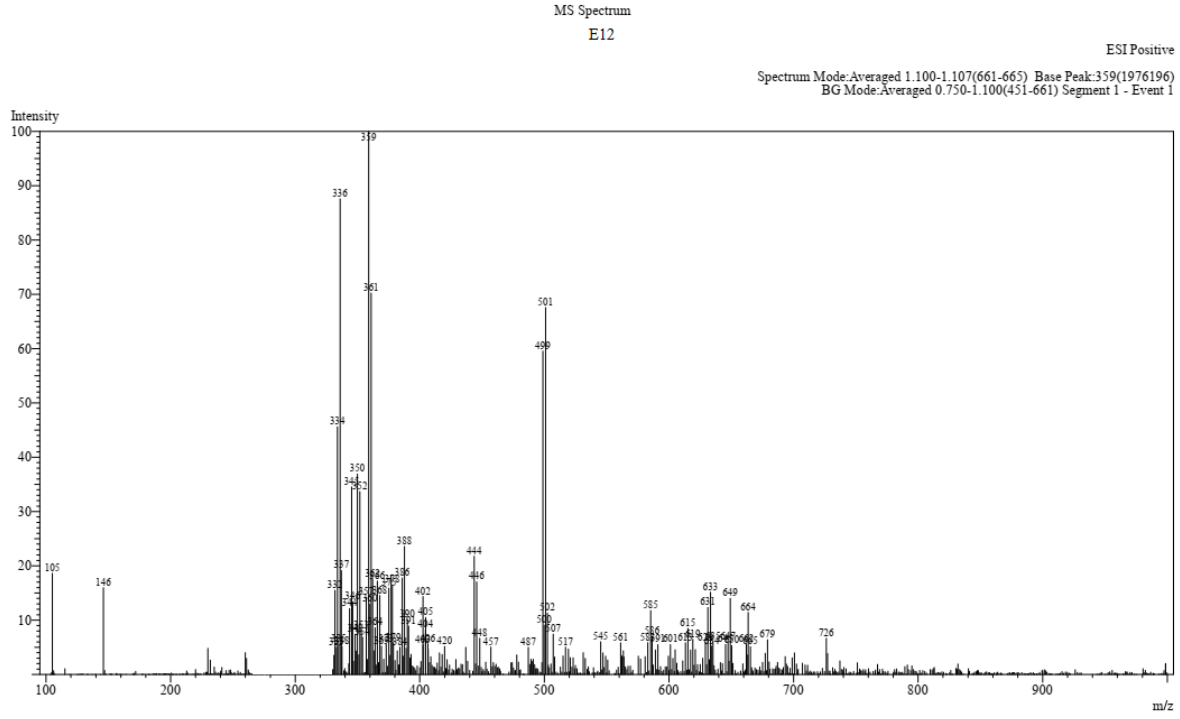

Figure S139: $[Ag(E_d)_2]CF_3SO_3$ 12